HYDRAULIC PROPERTIES OF FOUR SOILS FROM THE HERETAUNGA PLAINS AND PREDICTION OF THEIR SOIL WATER BEHAVIOUR DURING BORDER-DYKE IRRIGATION

A thesis submitted in partial fulfilment of the requirements for a Master of Philosophy in Soil Science at Massey University

Freeman John COOK,
1980

ABSTRACT

An irrigation scheme has been proposed for the Ngatarawa region of the Heretaunga Plains (Hawkes Bay). The method proposed for irrigation of these soils is the border-dyke method. It was felt that this method could be inefficient in the use of water and considerable amounts of water could be lost to drainage from some of the soils in this region. Thus experiments were performed on the four major soil types of this region - Poporangi sandy loam (Typic Durochrept), Ngatarawa sandy loam (Typic Ustorthent), Takapau sandy loam (Andri Ustochrept), and Pakowhai silt loam (Aquic Ustifluvent) - to determine their hydraulic properties.

The instantaneous profile method was used to measure the drainage, and water storage behaviour of these soils, and their hydraulic conductivity. Hydraulic conductivity could not be calculated for the Poporangi sandy loam, due to the duripan causing lateral flow. This invalidated the assumption that the movement of water was only vertical. For one other soil, Ngatarawa sandy loam, the hydraulic conductivity data obtained were considered to be unreliable. Reliable hydraulic conductivity data were obtained for Takapau sandy loam and Pakowhai silt loam. From data obtained from "undisturbed cores" and the field experiments, the drainage behaviour and water storage properties were determined for all four soils.

Using a numerical technique, vertical movement of water in Takapau sandy loam and Pakowhai silt loam, during and following ponded infiltration, was simulated using a CSMP computer model. These simulations indicate that the loss of water to through drainage from Takapau sandy loam would be at least 50% of that infiltrated, if the proposed residence time for ponding of water of 70 minutes is used. For Pakowhai silt loam the simulations indicate that little water is likely to

be lost to drainage if a residence time of 120 minutes is used. As hysteresis in the volumetric water content/pressure potential relationship is likely to affect the validity of these simulations, the extent of hysteresis on this relationship in these soils was investigated.

From all of these data it was concluded that only the Pakowhai silt loam would be suitable for irrigation by the border-dyke method. If this method was used on the other soils, large amounts of water could be lost to drainage. This would not only be a waste of a scarce resource, but as the Ngatarawa region lies over the unconfined part of the aquifer from which Napier and Hastings cities draw their water, it could also be a health hazard, as the drainage water from these soils could cause the nitrate level in the water in this aquifer to increase. Thus it would be better to irrigate the other three soils (Poporangi sandy loam, Ngatarawa sandy loam and Takapau sandy loam) using a sprinkler system. The application rate of the sprinkler system should be less than the saturated hydraulic conductivity of the A horizon of the soil, otherwise horizontal distribution of the amount of water infiltrating into the soil can be very uneven.

ACKNOWLEDGMENTS

The experimental work in the field was conducted jointly by Mr J.P.C.Watt and myself. Assistance, which was much appreciated was provided by Miss P. Guerin, Messrs G.W. Sayers, A.J. Unsworth, E. Griffiths, B.R. Purdie, J.P.C. Watt, and Dr R.J. Jackson. I would like to thank - Messrs D.R. Twigg, R. Sowersby, T.C. Thompson and especially J.B. Talbot who gave permission for these experiments to be performed on their properties; Mrs N. McLean for typing this thesis; the State Services Commission for providing a grant, and Dr R.B. Miller for allowing me study leave to do this degree. Useful discussions about this work were provided by Messrs E. Griffiths, J.P.C. Watt and Drs R.J. Jackson, K.G. McNaughton and D.R. Scotter. The friendly atmosphere of the Soils Department at Massey and especially the other inmates in TVL was appreciated. I would especially like to thank Dr D.R. Scotter for his advice and encouragement during this study, and my wife Polly for help with editing, English, and motivation.

TABLE OF CONTENTS

LIST OF TABLES

LIST OF FIGURES

INTRODUCTION

1.1 Aim of the Study

Water is essential for plants to survive and grow. If plants do not obtain sufficient water through their root system to meet the transpiration demand of the atmosphere, then they become stressed. Though the plant may still survive, its growth rate compared to when it is transpiring freely, will be less (Hsiao, 1973).

The Heretaunga Plains area of Hawkes Bay has warm dry summers and is a region where horticultural crops can be readily produced, so long as there is an adequate supply of water. However, it usually suffers a summer drought (MOW, 1975), during which water requirements of the crops have to be supplemented by irrigation.

An irrigation project (MOW, 1975) has been proposed for the Ngatarawa region of the Heretaunga Plains, in which the border-dyke system of surface irrigation would be used. Following a preliminary investigation of the soils in this area (Griffiths, 1975a), it was felt that some of the soils in the scheme would be more efficiently irrigated by other methods.

The four major soils of the area - Poporangi sandy loam (Typic Durochrept)*, Ngatarawa sandy loam (Typic Ustorthent), Takapau sandy loam (Andri Ustochrept), and Pakowhai silt loam (Aquic Ustifluvent) - have different hydraulic properties. The aim of this study was to measure some of these hydraulic properties, and to use the data to predict the infiltration and redistribution of water in these soils under border-dyke irrigation.

---

* Soil classification using Soil Taxonomy (Soil Survey Staff, 1975)

1.2 Describing Water Movement in Soil

The first recorded attempt to describe mathematically water movement in soil was Buckingham (1907), who proposed that Darcy's Law could be applied to describe one-dimensional movement of water in soils. That is:

$$q = -k(\Theta)\partial\psi_t/\partial x \qquad \text{--- (1)}$$

where q is the flux density of water (m s^{-1}) moving in direction x (m); $k(\Theta)$ is the hydraulic conductivity (m s^{-1}), which is a strong function of the volumetric water content, Θ; and ψ_t is the total potential (m),* which is the sum of the pressure potential, ψ_p (Θ) (m)*, (which is a function of Θ), and the gravitational potential, ψ_g (m). Little further progress was made until Richards (1931) combined the equation of continuity (conservation of mass) with Darcy's Law and obtained a partial differential equation describing transient water movement. In one-dimension this is:

$$\partial\Theta/\partial t = \partial[k(\Theta)\ \partial\psi_t/\partial x]/\partial x \qquad \text{---(2)}$$

where t is time (s).

Childs and George (1948) recognised that by use of the chain rule, equation (2) could be rearranged into a diffusion-type equation for horizontal flow as:**

$$\partial\Theta/\partial t = \partial[D(\Theta)\partial\Theta/\partial z]/\partial z \qquad \text{---(3)}$$

where $D(\Theta) = k(\Theta)\ d\psi_p/d\Theta$ and is called the soil water diffusivity ($m^2\ s^{-1}$).

---

* Soil water potential has length units if expressed in terms of energy per unit weight of water

** For horizontal flow $\partial\psi_g/\partial x = 0$, therefore $\partial\psi_t/\partial x = \partial\psi_p/\partial x$

The general equation describing transient water movement in unsaturated non-swelling soils was presented by Klute (1952), and is:

$$\partial\Theta/\partial t = \nabla(D(\Theta)\ \nabla\Theta) - \partial k(\Theta)/\partial z \qquad \text{--- (6)}$$

where z is the vertical co-ordinate (m). For one-dimensional vertical flow equation (6) reduces to

$$\partial\Theta/\partial t = \partial[D(\Theta)\ \partial\Theta/\partial z]/\partial z - \partial k(\Theta)/\partial z \qquad \text{--- (7)}$$

The second term on the right hand side of equations (6) and (7) arises from the gravitational potential, ψ_g, which equals minus z, if referenced to the surface and depth is taken as positive downwards. This term, and the dependence of the hydraulic conductivity on the volumetric water content, make analytical solution of equation (7) difficult. Equation (7) has been solved for various boundary conditions using two basic approaches, quasi-analytical and numerical. These will be described in more detail in Chapter 2.

1.3 Measuring Unsaturated Hydraulic Conductivity

In order to calculate water movement in soil, it is essential to know the relationship between the hydraulic conductivity and the volumetric water content. There are many different methods for measuring this relationship (Nielsen *et al.*, 1972), which can be divided into two main groups:

(a) Laboratory methods, where an "undisturbed" core of soil is taken and measurement of the relationship between the hydraulic conductivity and volumetric water content made in the laboratory.

(b) Field or *in situ* methods, where measurement of the hydraulic conductivity/volumetric water content relationship of the soil is made in the field.

Although very detailed measurements can be made on cores in the laboratory, the validity of such measurements is questionable (Davidson *et al.*, 1969), due in part to disturbance to soil structure during sampling, whereas in field methods disturbance to soil structure is minimised

(Hillel *et al.*, 1972).

A field method, the instantaneous profile method (Rose *et al.*, 1965; Watson, 1966; Hillel *et al.*, 1972) was used in this study, and although this method has some limitations (Baker *et al.*, 1974), which preclude its use on sloping or forest sites, it is adequate for some of the flat sites in this study. Fluhler *et al.*, (1976) in an analysis of errors likely to be generated by the instantaneous profile method found that errors were small in the wet region where water movement is important, and that other field methods would generate similar errors. The instantaneous profile method not only provides data for obtaining the relationship between the hydraulic conductivity and the volumetric water content, but also provides data on the water storage characteristics and drainage behaviour of the soil, which are important in determining the water requirements of a soil and the most efficient means of irrigating that soil.

CHAPTER 2

METHODS

2.1 PROCEDURE

2.1.1 Plot Layout

Two plots (2 x 2 m) were laid out on flat areas for each of the four soils in this study. These duplicate plots were within 20 m of each other. The plots were constructed by digging a trench into which planks with a bevelled edge were pushed (Fig.1). These planks were bolted together, and soil packed into the trench. Vegetation on the plots was ryegrass/white clover pasture, which was less than 50 mm long.

In order to minimise disturbance to the soil surface, duck-boards were used when installing and monitoring the instruments in the plots (Fig.2). A fence was constructed around the plots to keep stock out.

2.1.2 Instrumentation

An aluminium access tube for the neutron probe was installed in the centre of each plot 6 months prior to these experiments. The tubes were installed to a depth of 3 m (Pakowhai silt loam), or until an obstacle (gravel, stones) was reached.

Stainless steel access tubes were installed in an arc 0.5 m from the aluminium access tube; these were used for housing the tensiometer probes (Fig.2). Two tensiometers were installed at the bottom of each soil horizon. Also some tensiometers were placed within horizons, but not duplicated. Pressure potentials in the tensiometers were measured using mercury manometers.

Two infiltrometer rings were pushed into the surface of the plots prior to wetting (Fig.2). These were used to monitor the infiltration rate during wetting and were removed when ponding ceased.

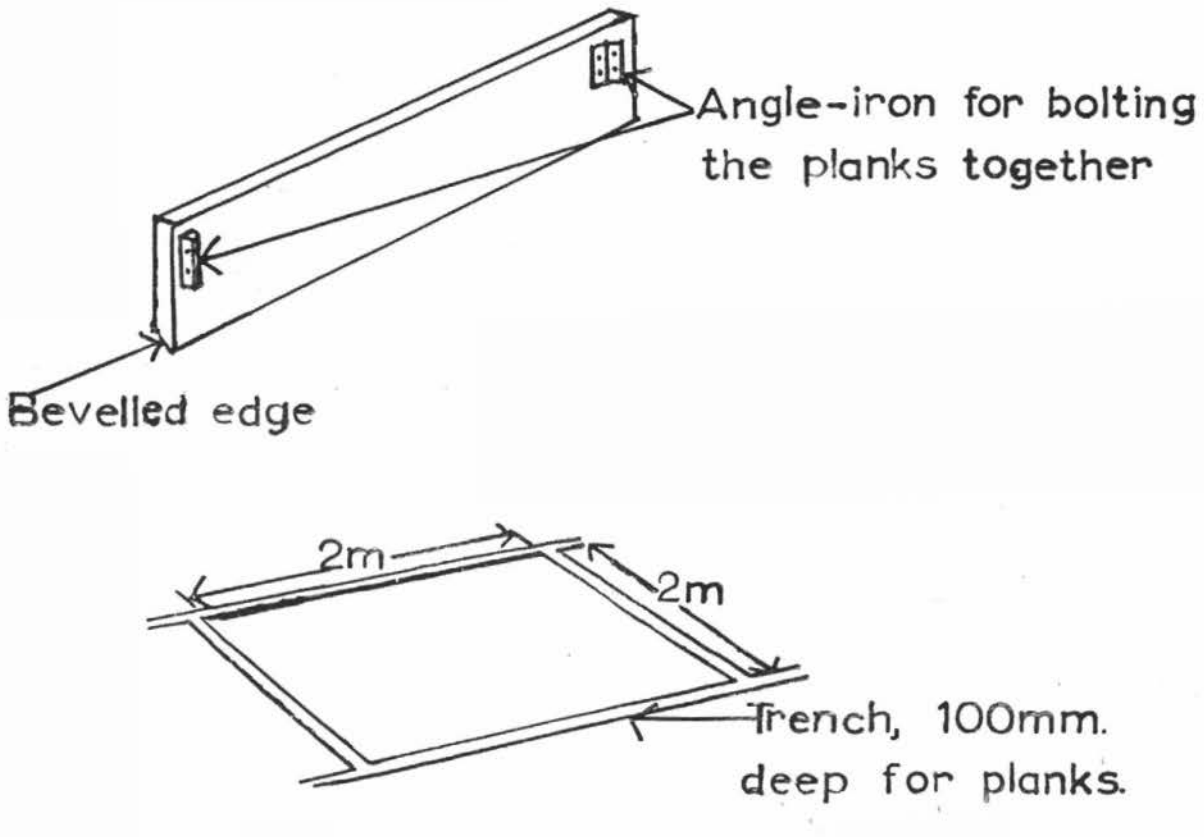

Fig.1 Sketch of a plank and the trenches used in constructing the plots. A cross-section of a plank in position is also sketched.

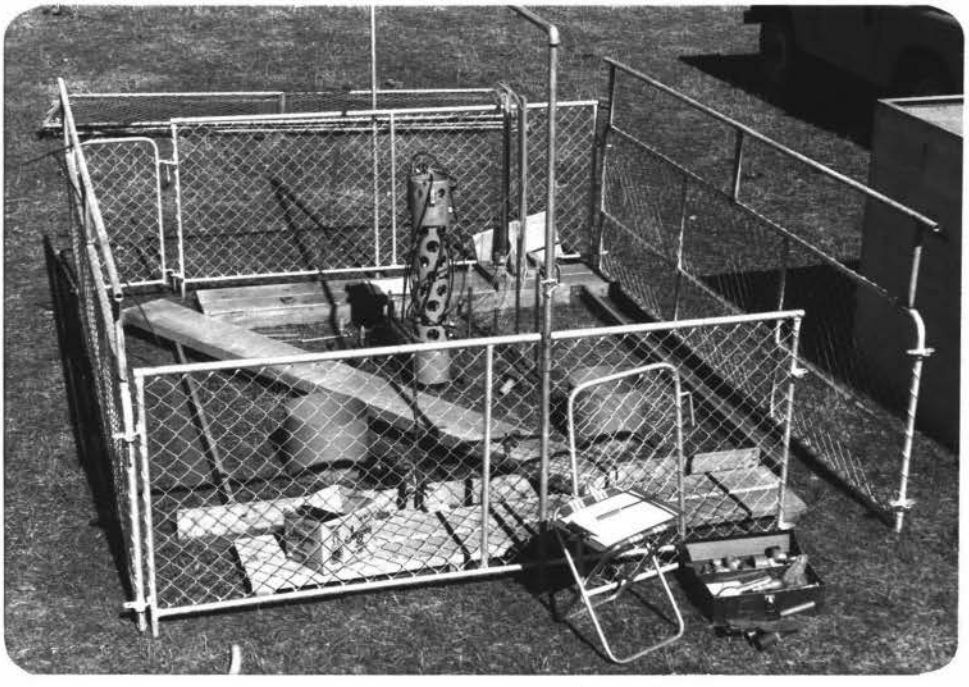

Fig.2 Photograph of a plot showing the neutron probe, tensiometers, infiltrometer rings, duck-boards and fences. (Photograph credit J.P.C.Watt).

2.1.3 Wetting

Water was ponded onto the plots, to an average depth of 0.03 m, and maintained at this depth until the pressure potential measured by the deepest tensiometer reached a constant value. In order to minimise subsequent lateral movement into the drier surrounding soil during drainage, large quantities of water were applied to the soil surrounding the plots during wetting. The soils in this study took up to approximately 24 hours of continuous ponding to wet.

2.1.4 Drainage

Drainage of the soil was taken as starting when no free-standing water was present on 90% of the plot's surface. During drainage the plot was covered with a plastic sheet to prevent evapotranspiration (Fig.3). A tent-like cover was placed over the plot and fenced surrounds (Fig.3). This prevented any rain entering the plot and rewetting the soil, and also shaded the plot, minimising soil temperature fluctuations which could induce moisture movement (Philip and de Vries, 1957). Panels were placed at the ends of this cover to provide further shading of the plot.

Frequent concurrent measurements of pressure potential and water content down the profile were made using the tensiometers and a neutron probe. The frequency of monitoring was reduced as drainage proceeded, and the rate of water movement through the soil decreased.

2.1.5 Sampling for "Undisturbed" Soil Cores

A pit was dug in each plot, except for the Pakowhai silt loam where one pit was dug between the two plots. The soil profiles were described (Appendix I), and "undisturbed" cores taken from each horizon in the manner described by Gradwell (1971). A further set of "undisturbed" cores of the Takapau sandy loam and Pakowhai silt loam were taken from

Fig.3 Photograph of a plot showing the plot cover and an end panel (Photograph credit J.P.C.Watt).

the same pits 15 months later for use in the experiment described in Appendix II.

The first set of cores were taken back to the laboratory and smaller cores hand carved from them and fitted into brass liners (Gradwell, 1971). These hand-carved cores were used for determining the relationship between volumetric water content and pressure potential for the 0 to -10 m range, using methods described by Gradwell (1971). Small crumbs of soil produced when carving the cores were used for determining the volumetric water content at a pressure potential of -154 m (-15 bars), following Gradwell's (1971) method.

The bulk density (ρ_b) could be measured using the hand-carved cores, as the brass liners were of a known volume.

The particle density (ρ_s) was determined using moist samples, as some volcanic material was present in these soils, using the method described by Gradwell (1971).

2.2 CALCULATIONS FOR HYDRAULIC CONDUCTIVITY

2.2.1 Theory

Vertical transient movement of water through a soil must obey the continuity equation, which may be written:

$$\partial\Theta/\partial t = -\partial q/\partial z \qquad \text{--- (8)}$$

Let $W = \int_0^{\zeta}\Theta.dz$

W is the equivalent depth of water (m) in the soil profile to a depth ζ. If there is no evapotranspiration from the soil, then the downward flux-density of water through a horizontal plane at depth ζ equals the rate of change in W with time. Thus integration of equation (8) with respect to z gives:

$$-q_{\zeta} = \int_0^{\zeta}\partial\Theta/\partial t.dz = \partial W/\partial t \qquad \text{--- (9)}$$

Darcy's Law describing vertical flow of water (equation 1) is:

$$q = -k(\Theta)\,\partial\psi_t/\partial z \qquad \text{--- (10)}$$

Equating equations (9) and (10) and rearranging to solve for the hydraulic conductivity gives:

$$k(\Theta) = (\partial W/\partial t)_\zeta/(\partial\psi_t/\partial z)_\zeta \qquad \text{--- (11)}$$

Thus if $\partial W/\partial t$, $\partial\psi_t/\partial z$, and Θ at ζ can be found, the relationship between the hydraulic conductivity and the volumetric water content can be calculated.

2.2.2 Flux Density

From the tensiometers, the pressure potential at various depths was calculated using:

$$\psi_p = (D-K) + \zeta - 12.6(X+K) - C \qquad \text{--- (12)}$$

where the symbols are defined in Figure 4. At the bottom of each horizon, where there were duplicate tensiometers, the mean value of X was used in calculating the pressure potential for that depth. The duplicated tensiometers gave quite close agreement with the difference in X usually being 1 mm and always less than 5 mm (0.06 m of water). To overcome problems due to air slowly appearing in the tensiometers, they were flushed every 3 days with de-aired water. Using the laboratory retentivity data obtained during drainage (i.e. the relationship between volumetric water content and pressure potential), volumetric water content of each soil horizon at the time of measurement could be obtained from the pressure potential and so W_ζ calculated.

It was initially intended to use the neutron probe data for calculating volumetric water content and W_ζ, but due to problems with calibration near the surface and the shallowness of some of the soils, these data were not used.

If W_ζ is plotted against the logarithm of time, the data often points fall approximately on a straight line (Fig.5). This behaviour was first described by Wilcox (1959), and indicates that the relationship between W_ζ

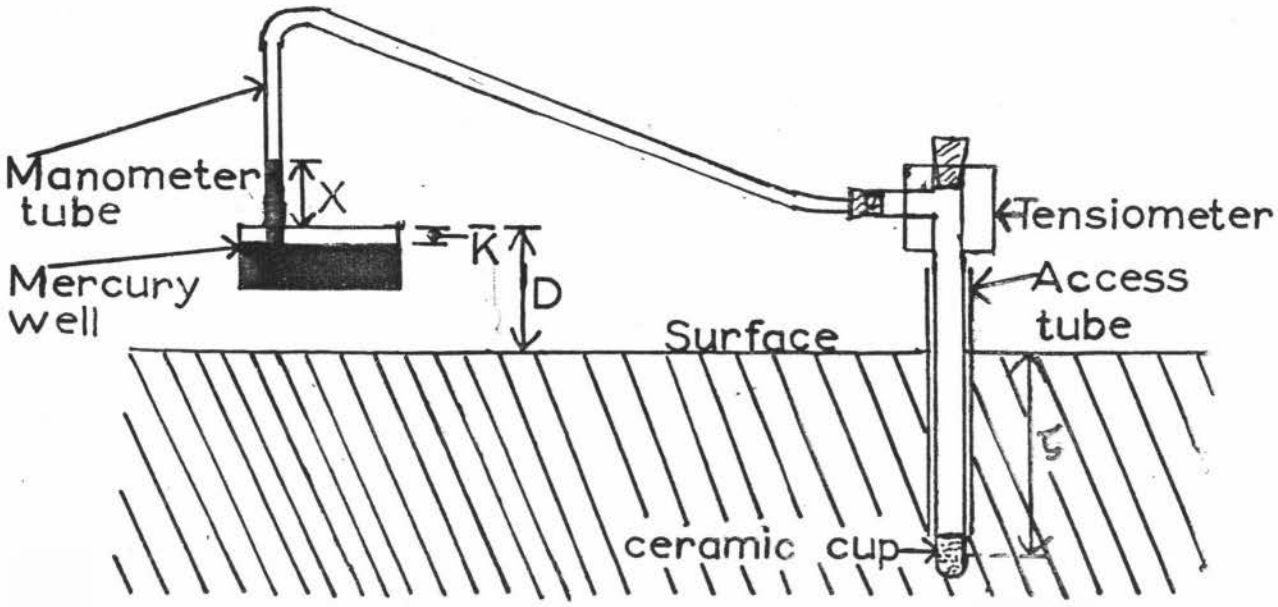

ζ is the mean depth from the datum (ground surface) to the ceramic cup (m).

D is the height of the top of the mercury well above datum (m).

K is the distance between the top of the mercury well and the level of mercury in the well (m)

X is the height of mercury in the manometer tube above the top of the mercury well (m)

C is the capillary depression, which for these manometer tubes is 0.175 m of water.

Fig. 4 Cross-sectional sketch of the manometer, tensiometer system, used to measure pressure potential.

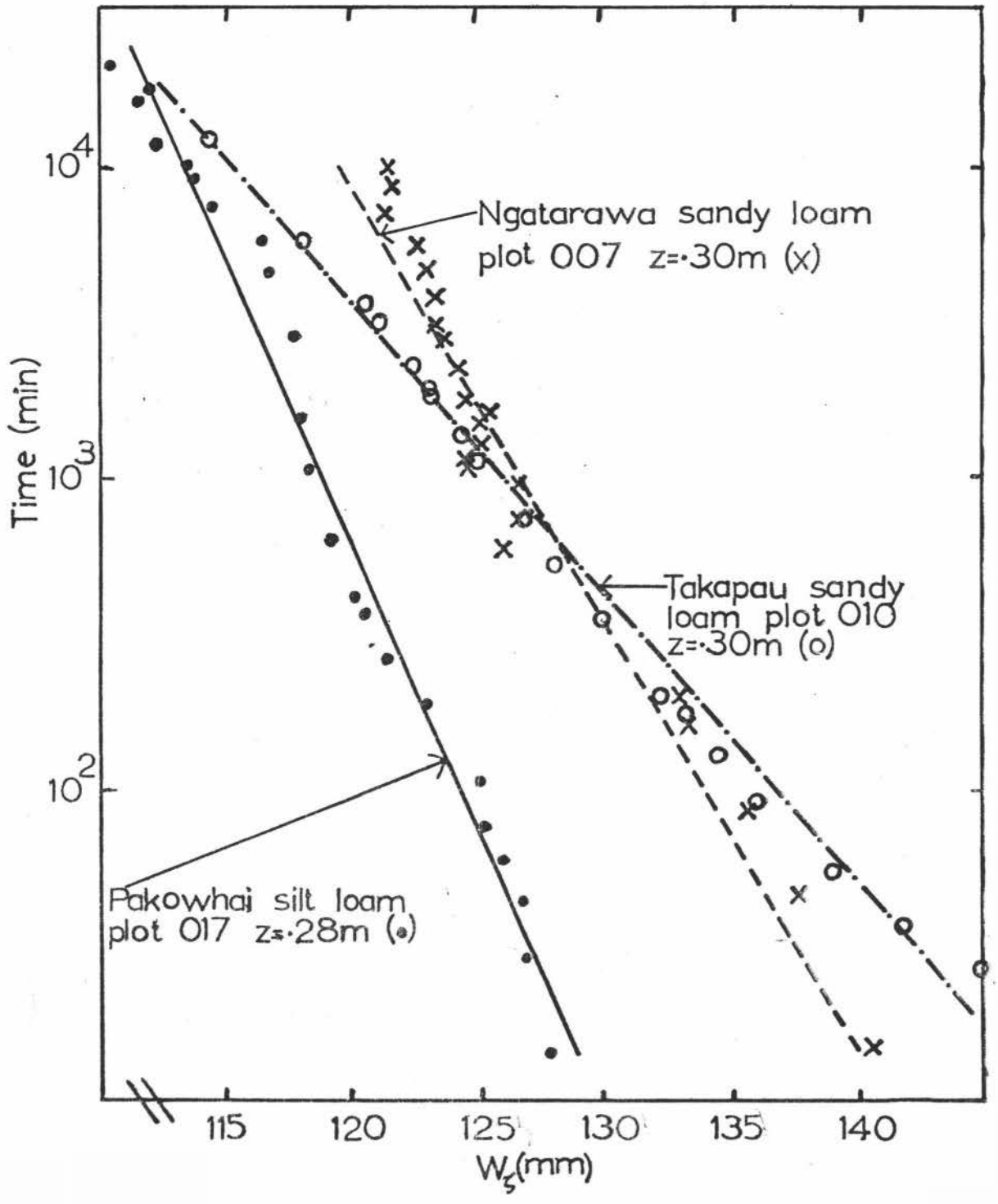

Fig.5 Typical W_ζ against $\log_{10}$ time data, the lines drawn are linear regressions obtained from these data.

and time (t) can be described by:

$$W_\zeta = \alpha \ln t + \beta \qquad \text{--- (13)}$$

where α and β are empirical constants. Differentiating equation (13) with respect to time gives:

$$(dW/dt)_\zeta = \alpha/t \qquad \text{--- (14)}$$

α can be obtained as the slope of a linear regression of W_ζ on ln t. The flux density at ζ can thus be calculated at any time t, by using equation (14), so long as t lies within the regressed range. For the regressions obtained in this study the correlation coefficient was never less than 0.90.

2.2.3 Hydraulic Gradient

Using the symbols Z(i) and $\psi_p(i)$ to denote the depth and pressure potential of the tensiometer at the bottom of the ith horizon, then $\psi_t(i)$, the total potential at this depth, is given by:

$$\psi_t(i) = \psi_p(i) - Z(i) \qquad \text{--- (15)}$$

The hydraulic gradient in the ith horizon may then be approximated by a finite difference:

$$(\partial\psi_t/\partial z)_{Z(i)} = (\Delta\psi_t/\Delta z) = [\psi_p(i) - \psi_p(i-1)] / [Z(i)-Z(i-1)]-1 \qquad \text{--- (17)}$$

Depths Z(i-1) and Z(i) are known, and at the time of measurement so are pressure potentials $\psi_p(i-1)$ and $\psi_p(i)$. Thus using equation (17) the hydraulic gradient across the horizon at this time can be calculated.

For water to flow downwards the total potential gradient $(\partial\psi_t/\partial z)$ must be negative. Water may also flow laterally in response to a horizontal total potential gradient. In calculating the hydraulic conductivity it is assumed that all water movement is vertical i.e. the horizontal total potential gradient is negligible or zero. To minimise any possible horizontal total potential gradient, water was applied to the soil surrounding the plots and measurements were made only on a cylinder of soil 0.5 m in radius in the centre of each plot. Also, as

errors due to lateral flow are likely to be most significant when $|\partial\psi_t/\partial z|$ is small, the hydraulic conductivity was only calculated when $|\partial\psi_t/\partial z|$ was greater than or equal to 0.3.

2.2.4 Hydraulic Conductivity

For each horizon, the total potential gradient across it, and the flux density of water out of the horizon are known. Thus the hydraulic conductivity can be calculated using equations (9) and (11). Due to the hydraulic conductivity (k) changing many orders of magnitude for small changes in volumetric water content (Θ), data are presented graphically as $\log_{10}k$ against Θ. Depending on the appearance of the data, a linear or quadratic regression of $\log_{10}k$ on Θ was obtained and plotted.

In these calculations, it has been assumed that each of the pedologically distinct horizons or layers identified, has constant physical properties and a uniform total potential gradient. Comparison of the relationship between pressure potential and volumetric water content for each horizon of the duplicate plots is possible for three of the soils, giving some indication of the degree of uniformity. Also, comparison of the relationship between hydraulic conductivity and volumetric water content within a horizon or layer, where tensiometers were located within a layer, and between duplicate plots is possible.

2.2.5 Available-water Holding Capacity

The available-water holding capacity (AWC) is defined as the volume of water held in the rooting zone of a soil between "field capacity" (FC) and the "permanent wilting point" (PWP) (Gradwell, 1971). The PWP is usually taken as the volumetric water content when the pressure potential is -154 m (-15 bar). The AWC is thus given by:

$$AWC = \int_0^{z_r} (\Theta_{FC} - \Theta_{PWP})\,dz = \sum_{i=1}^{n} (\Theta_{FC}(i) - \Theta_{PWP}(i))T(i) \qquad \text{--- (18)}$$

where Z_r is the rooting depth (m) (equal to $\sum_{i=1}^{n} T(i)$), Θ_{FC} is the volumetric water content at "field capacity", Θ_{PWP} is the volumetric water content at the PWP, i is an index interger referring to finite depth increments T(i), and n is the number of increments. The AWC was calculated using various values of "field capacity" from the field experiments, and estimates obtained from the retentivity data, and these values of AWC compared.

Although Θ_{PWP} may approximate the lower limit of available water for pasture, production is reduced when the soil pressure potential decreases to approximately -10 m (Hagan and Stewart, 1972). The water held at the root zone between "field capacity" and the volumetric water content at which the pressure potential is -10 m, will be called the readily available-water holding capacity (RAWC). In an irrigated moisture regime where it is hoped plant production can be maximised, irrigation should commence as soon as the readily available water in the soil has been used up.

2.2.6 Macro-porosity

The macro-porosity is defined as the difference between the total porosity and the volumetric water content at a pressure potential of -0.5 m ($\Theta(0.5)$) (Gradwell, 1971). The total porosity (TP) and macro-porosity (MP) are calculated as:

$$TP = 1-\rho_b/\rho_s \qquad \text{--- (19)}$$

where ρ_b is the bulk density and ρ_s is the particle density, and:

$$MP = TP - \Theta(0.5) \qquad \text{--- (20)}$$

2.3 PREDICTION OF WATER MOVEMENT IN SOIL

Prediction of water movement in soil was investigated using a quasi-analytical method (the flux-concentration relation) and a numerical simulation method. The quasi-analytical method is limited to infiltration, as the relationship between volumetric water content and pressure potential

must be monotonic. Also, the prediction of infiltration is restricted to the A horizon, as in layered situations a discontinuity in the diffusivity/volumetric water content relationship occurs at the interface of the layers, and this means that the quasi-analytical solution is no longer valid. The numerical simulation method can, however, be used for all soil water dynamic processes.

2.3.1 Quasi-analytical Solutions

Philip (1957a) was the first to provide a quasi-analytical solution to equation (7) for certain boundary and initial conditions related to infiltration (Philip, 1957a,b,d). This is a series solution i.e.

$$z = \nu t^{\frac{1}{2}} + \beta t + \gamma t^{\frac{3}{2}} + \ldots + f_m(\Theta) t^{\frac{m}{2}} + \ldots \qquad \text{--- (21)}$$

where ν, β, γ and $f_m(\Theta)$ are functions of the volumetric water content and are solutions of ordinary differential equations.

A simplified approximation of the above solution proposed by Philip (1957c) is:

$$I = St^{\frac{1}{2}} + At \qquad \text{--- (22)}$$

where I is the cumulative infiltration (m), S is the sorptivity ($m\ s^{-\frac{1}{2}}$) and A is a parameter ($m\ s^{-1}$). Solutions obtained using equation (22) were compared with those obtained using earlier infiltration equations by Philip (1957c). Other quasi-analytical solutions published before 1969 are reviewed by Philip (1969).

Further advances in quasi-analytical solutions were provided by Parlange (1971a,b,c, 1972a,b,c), with the introduction of the flux-concentration relation F(H). F is the dimensionless ratio of the flux at any depth to that at the source (surface) i.e. for vertical infiltration

$$F = (q-k_n)/(q_o-k_n) \qquad \text{--- (23)}$$

and H in the dimensionless water content given by

$$H = (\Theta-\Theta_n)/(\Theta_o-\Theta_n) \qquad \text{--- (24)}$$

In these equations Θ_n is the initial volumetric water content, Θ_o and q_o are the volumetric water content and flux density respectively at the source (surface), q is the flux density of water at some depth z, where the volumetric water content is Θ, and k_n is the hydraulic conductivity corresponding to Θ_n. Philip (1973) gives a clear explanation of the flux-concentration relation. Knight and Philip (1974) criticised Parlange's earlier work on the grounds of its failure to meet continuity requirements, the failure of his iterative solution to converge, and for his erroneous claim that this method was generally applicable to two and three dimensional systems.

Philip and Knight (1974) demonstrated the usefulness of the flux-concentration concept, however, by showing that F(H) is a conservative relation, and for constant-concentration (ponded) infiltration a good approximation of F is:

$$F = H = (\Theta-\Theta_n)/(\Theta_o-\Theta_n) \qquad \text{--- (25).}$$

White et al. (pers. comm. via D. Scotter) found for constant flux adsorption that measured F was only slightly above the F = H line and errors in determining $D(\Theta)$ were more critical than any error introduced by assuming F = H. For constant-concentration vertical infiltration the necessary equations are (Philip and Knight 1974):

$$t = \int_{\Theta_n}^{\Theta_o} \frac{(\Theta-\Theta_n)\,DF}{(k-k_n)^2} \left[\frac{(k-k_n)}{(q-k_n)F-(k-k_n)} - \ln \frac{(q-k_n)F}{(q-k_n)F-(k-k_n)} \right] d\Theta \qquad \text{---(26)}$$

and

$$z = \int_{\Theta}^{\Theta_o} \frac{D}{(q-k_n)F-(k-k_n)}\, d\Theta \qquad \text{--- (27)}$$

In this study the above integrals were evaluated using trapezodial numerical integration, with 0.01 increments of Θ. To use these equations the following procedure was followed. Values of q were chosen and substituted into equation (26) to give the required time range. Substituting a value of q in equation (27), various values of Θ were chosen and z calculated.

Thus the soil water content profile at any time during wetting can be calculated.

Similarly, for constant-flux infiltration the equations needed are (White *et al.* : pers. comm. via D. Scotter):

$$(q_o-k_n)^2 t = \int_{\Theta_n}^{\Theta_o} (\Theta-\Theta_n) \left[\frac{D}{F} + \frac{\eta D}{F(F-\eta)}\right] d\Theta \qquad \text{--- (28)}$$

and

$$(q_o-k_n) z = \int_{\Theta_o}^{\Theta} \left[\frac{D}{F} + \frac{\eta D}{F(F-\eta)}\right] d\Theta \qquad \text{--- (29)}$$

where $\eta = (k-k_n)/(q_o-k_n)$, and q_o is the constant flux density at the source. To solve these equations a value of Θ_o is chosen and the time and water content profile for this value of Θ_o calculated.

These equations can only be used for homogeneous soils or for infiltration into the homogeneous A horizon. Equations (26) and (27) were used in this study to calculate infiltration into the A horizon of the Takapau sandy loam for comparison with the numerical result.

2.3.2 Numerical Solutions

For situations where quasi-analytical methods cannot be used to solve equation (6), a solution can usually be obtained using a numerical method. Hanks and Bowers (1962) first solved equation (6) numerically using the finite-difference method for one-dimensional vertical flow. Rubin (1968) solved equation (6) for two-dimensional flow, using numerical methods. Many other workers have since used finite-difference methods to solve the flow equation for various boundary and initial conditions e.g. Brandt *et al.* (1971), van Keulen and van Beek (1971), Bhuiyan *et al.* (1971), Stroosnijder *et al.* (1972), Nimah and Hanks (1973), and Selim and Kirkham (1973). The finite-element method has been used also, (Neuman *et al.*, 1975, Guymon, 1974) to solve the flow equation.

Significant progress with numerical methods was made by de Wit and van Keulen (1972), when they recognised that the Continuous System Modelling Program (CSMP) computer language (IBM, 1969) made numerical methods easy to use. This computer language was designed to solve boundary-value differential equations, thus it is "tailor-made" for solving equation (6). The numerical method used in this study is based on that presented by Hillel (1977), using CSMP as the programming language.

Vertical movement of water in bare soil can be described by equation (7). To allow for root uptake of water a sink term $S[m^3$ of water consumed $(m^3$ of soil$)^{-1}.s^{-1}]$ must be included in equation (7), which can then be written:

$$\partial\Theta/\partial t = \partial(k(\Theta)\partial\psi_t/\partial z)/\partial z - S \qquad \text{--- (30)}$$

This can be integrated to give:

$$\Theta-\Theta_n = \int_o^t [\partial(k(\Theta)\,\partial\psi_t/\partial z)/\partial z - S]d\beta \qquad \text{--- (31)}$$

where Θ_n is the volumetric water content when $t = 0$. The computer simulation model outlined below essentially solves equation (31) using finite differences for the differentials.

2.3.3 The Computer Simulation Model

The soil is considered to be a vertical column with a unit cross-sectional area (Fig.6) which is made up of a number of compartments. Using the index variable I these compartments are numbered I = 1,2, ...n. These compartments have finite difference thickness (TCOM(I)), and using finite-difference time steps (DELT) equation (31) is solved using a semi-parallel procedure. Explanation of the model will be given using the terms and expressions (Fortran notation) used in the computer program (Appendix III).

The procedure for simulation of water movement by this model can be described by considering three adjacent compartments, the (I-1)th, the

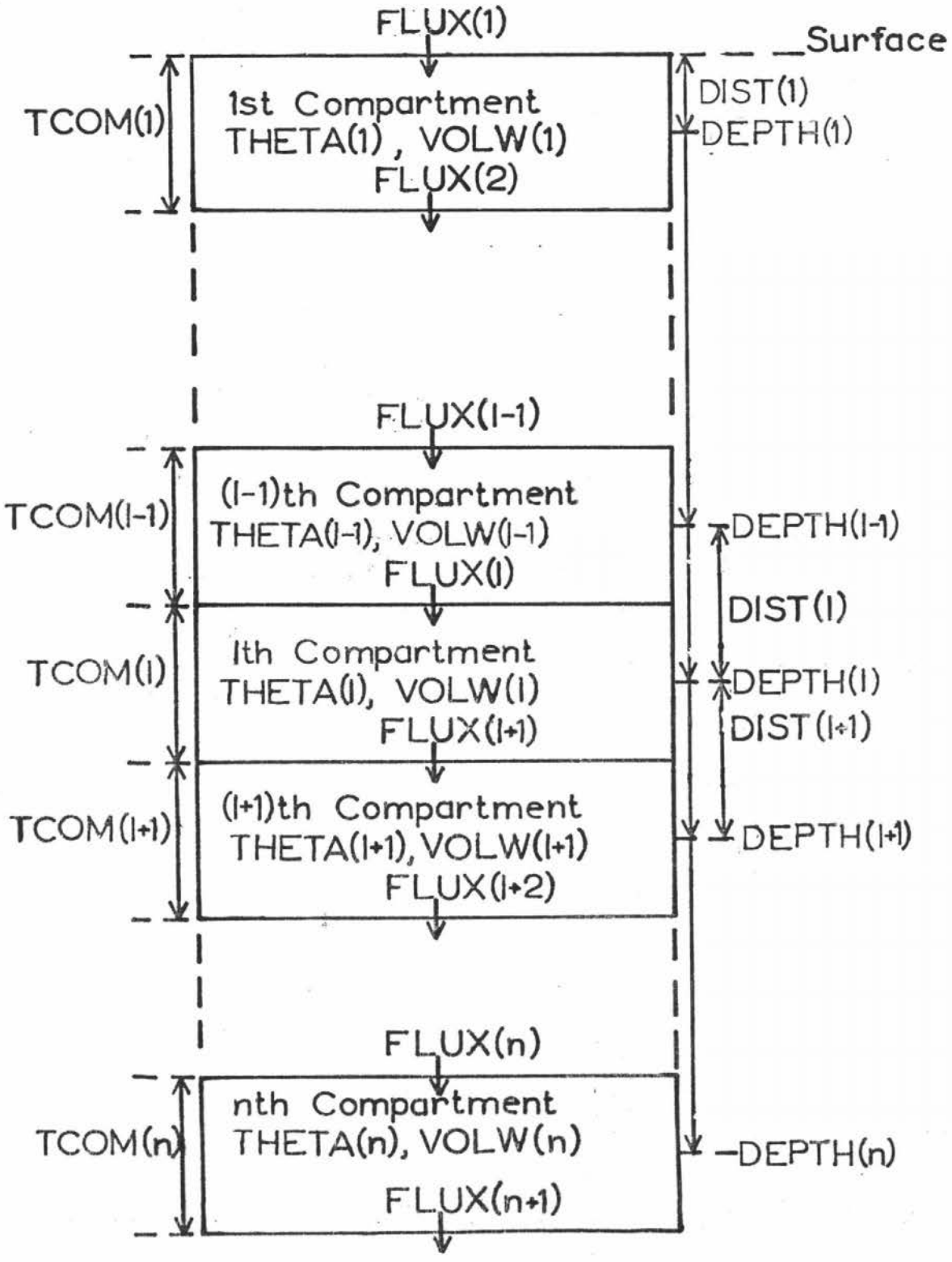

Fig. 6 The scheme used in the computer model to simulate vertical water movement in a soil profile.

Ith and the (I+1)th, each with unit cross-sectional area. These compartments have volumetric water contents of THETA(I-1), THETA(I) and THETA(I+1) respectively. The volume of water in each compartment is VOLW(I) = THETA(I)*TCOM(I). The pressure potential in each compartment (MPOT(I)) is obtained from THETA(I) using a function table for the relationship between volumetric water content and pressure potential. A linear function generator (AFGEN) was used to interpolate between the data points in the function table. The total potential (HPOT(I)) is calculated as:

HPOT(I) = MPOT(I) - DEPTH(I)

where DEPTH(I) is the depth from the surface to the midpoint of the Ith compartment.

The hydraulic conductivity (COND(I)) is calculated as COND(I) = EXP(a*THETA(I)**2+b*THETA(I)+c) where a,b, and c are arbitrary constants obtained from the regressions of ln k on Θ. Water is considered to flow linearly from the midpoint of one compartment (I-1) to the midpoint of the adjacent compartment (Ith). As these compartments may have different hydraulic conductivity values, an average conductivity relating to the flow between these compartments must be calculated. Various averaging techniques have been used by other workers. De Wit and van Keulen (1972) weighted the average in favour of the hydraulic conductivity of the wettest compartment. They argued that this was better than an arithmetic mean, as when a wetting front is moving into a dry soil most of the energy must be dissipated on the wet side of the wetting front. Van Keulen and van Beek (1971) used four different averaging techniques and found that the simulated wetting fronts differed only slightly. They concluded that use of an arithmetic average of the hydraulic conductivities does not lead to large errors. The method used in this study to calculate the average hydraulic conductivity is that

proposed by Hillel (1977). It is an arithmetic average weighted to take account of the respective length of the flow path in each compartment i.e.

AVCOND(I)=[COND(I)*TCOM(I)+COND(I-1)*TCOM(I-1)]/(TCOM(I)+TCOM(I-1)).

Using Darcy's Law the flux density (FLUX(I)) of water moving between the (I-1)th and Ith compartments can be calculated as:

FLUX(I)=(HPOT(I-1) - HPOT(I))*AVCOND(I)/DIST(I)

where (DIST(I) is the distance between the midpoints of the (I-1)th and Ith compartments. The flux densities at the boundaries, FLUX(1) and FLUX(n+1) are calculated as follows. The flux density out of the bottom compartment (FLUX(n+1) is assumed to be equal to the hydraulic conductivity of the nth compartment i.e. gravity drainage is assumed to occur.

The flux density across the surface is simulated as follows: during drainage FLUX(1) = 0. For ponded infiltration FLUX(1) = INCAP where:

INCAP = (0-HPOT(1))*(SATCON+COND(1))*0.5/DIST(1)

where SATCON is the saturated hydraulic conductivity of the surface. For sprinkler irrigation or rainfall FLUX(1) = RAIN if RAIN $\leq$ INCAP otherwise FLUX(1) = INCAP, where RAIN is the flux density of water applied at the surface.

Evapotranspiration was simulated as follows: two extremes were used in this study, zero, and 5 mm day^{-1}. The evapotranspiration rate (SINK) was assumed to follow a sine curve during the day and to be zero at night, i.e.:

SINK = A*SIN(B*TIME) if SINK>0, otherwise SINK=0, where B = $\pi/43200$ (s^{-1}) and A is calculated as follows:

$$\int_0^{43200} (A \sin Bt)dt = E \qquad \text{--- (32)}$$

where E is amount of water evaporated daily (0 or 0.005 m).

Evaluating the integral in equation (32) and rearranging to solve for A gives:

$$A = BE/2 \qquad \text{--- (33)}$$

The rooting depth over which water was extracted by the pasture was assumed to be 0.4 m. The rate of extraction was assumed uniform with depth so that the amount extracted from each compartment was given by SINK*TCOM(I)/0.4.

Thus the net flux density of water to or from each compartment is calculated as:

NFLUX(I) = FLUX(I) - FLUX (I+1) - SINK*TCOM(I)/0.4

if DEPTH(I) + TCOM(I)/2 $\leq$0.4 otherwise NFLUX(I) = FLUX(I)-FLUX(I+1).

It is assumed during a short time interval (DELT) that flux densities are constant. The change in the volume of water in the Ith compartment VOLW(I) during DELT is then NFLUX(I)*DELT. If the Ith compartment contained an initial volume of water, IVOLW(I), then at time t,

$$VOLW(I) = IVOLW(I) + \int_0^t NFLUX(I)\,d\beta \qquad \text{--- (34).}$$

Equation (34) is essentially the same as equation (31).

A number of different integration methods are available with CSMP73(Fugazi, 1973). The most commonly used methods are the Runga-Kutta fourth order method (de Wit and van Keulen, 1972; Hillel, 1977) and the Milne fifth order predictor-corrector method (de Wit and van Keulen, 1972). These two methods are explained fully by Milne (1960), although a brief description is given by Fugazi (1973). With these methods the time steps (DELT) used for the integration are calculated according to error criteria. These methods use considerable computing time, but as the DELT used for each integration step is maximised the overall computing costs compared to simple rectangular integration with a fixed time step are similar. With CSMP73 the DELT used with rectangular integration can be varied by use of a CONTIN

statement in the terminal section. (For a full explanation of this see Appendix III.) In this study rectangular integration was used, with DELT being adjusted during the simulation to reduce computation cost while maintaining stability. The method used to calculate DELT is explained in Appendix III.

The choice of compartment size was a compromise between sensitivity and cost. The smaller the compartments, the more sensitive the model, but smaller DELTs are then needed to maintain stability, hence the cost increases. The flux density near the surface is greatest during infiltration, so to maintain sensitivity small compartments are used there (Appendix III). The effect of compartment size on sensitivity has been investigated by van Keulen and van Beek (1971), and will not be discussed further here.

3 RESULTS AND DISCUSSION

The four soils in this study have different layering, textures, and rooting depths (Appendix I). These differences affect the movement and storage of water in these soils. For two of the soils, Poporangi sandy loam and Ngatarawa sandy loam, data on the relationship between the hydraulic conductivity and the volumetric water content were unobtainable, or were considered unreliable. Thus simulation of water movement in these soils using the computer model (Chapter 2) was not attempted. However, their behaviour during drainage, following thorough wetting of the soil, can still be predicted from the data obtained in this study.

3.1 Poporangi Sandy Loam

Poporangi sandy loam has a dense, cemented layer (duripan) (Appendix I) at a depth of approximately 0.5 m. This layer is only very slowly permeable to water, so lateral flow in the soil above this layer is probably greater than vertical flow through the duripan. This meant that no data on the relationships between hydraulic conductivity, and volumetric water content were obtained for this soil using the instantaneous profile method.

During the experiment, after the soil in the plots had been draining for one day, a storm occurred which deposited 80 mm of precipitation on the soil surrounding the plots. As the plots were covered, no water fell onto them directly, but lateral water movement from the surrounding soil caused rewetting. The drainage phase for the plots was taken as starting after this rewetting rather than after ponding. As the surrounding soil was as wet as the soil in the plots, drainage of the plots was not affected by any edge effects.

One tensiometer in the duripan (at a depth of 0.52 m) in one plot

gave negative pressure potentials for 3-4 days (Fig.8). The other tensiometers above the duripan showed positive pressure potentials. This indicates that it took a considerable time for the duripan to wet up. The other tensiometers in the duripan did not indicate negative pressure potentials, probably due to water moving down either the sides of the tensiometer access tube or a soil fissure, to the tensiometer tip.

If the hydraulic conductivity of the soil above the duripan is much greater than that of the duripan, then during drainage a perched water-table will occur. The pressure potential profile (pressure potential related to depth) expected in the soil above the perched water-table would have a slope approaching 1 and could be described by:

$$\psi_p(z) = z - Z_w \qquad \text{--- (35)}$$

where Z_w is the depth of the perched water-table. The pressure potential profiles measured during drainage have slopes that are equal to 1 (Figs. 7,8). This indicates that the pressure potential profile that develops during drainage in this soil can be described by equation (35).

The perched water-table, as indicated by tensiometers showing zero or positive pressure potentials, lowers with time, indicating that drainage of water from this soil does occur. This drainage is thought to occur through small areas where the duripan has not formed (E. Griffiths, pers. comm.). Thus drainage of this soil is mainly via lateral flow in the saturated soil below the perched water-table to those areas. When the perched water-table ceases to exist drainage will become minimal and the soil is then at "field capacity". This occurred after 10 days of drainage.

"Field capacity" is often defined as the volumetric water content

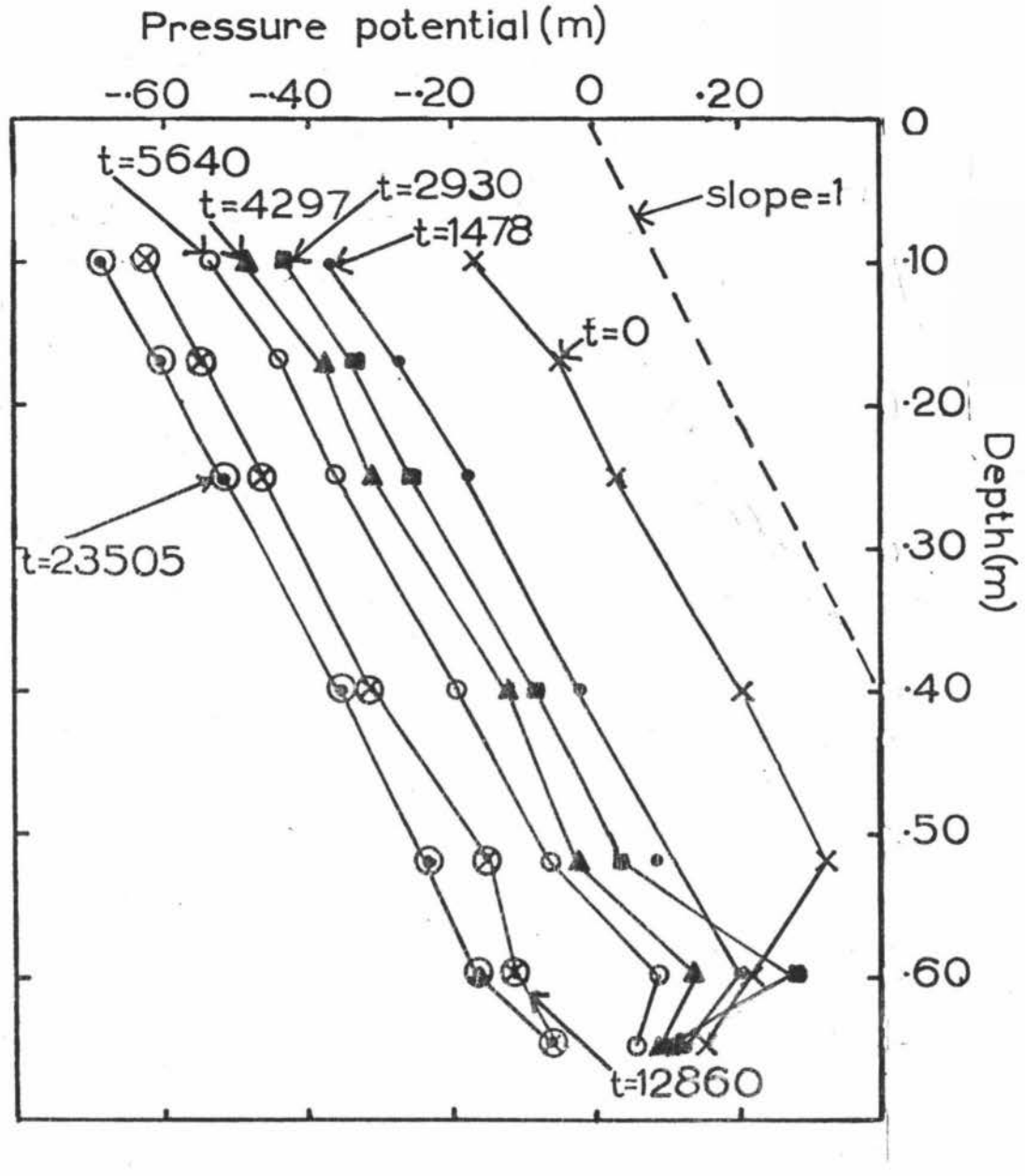

Fig.7 Pressure potential profiles (pressure potential against depth) at various times, t (minutes) during drainage of plot 011 of Poporangi sandy loam. The dashed line has a slope of 1 and is for comparison with the slope of the experimental pressure potential profiles.

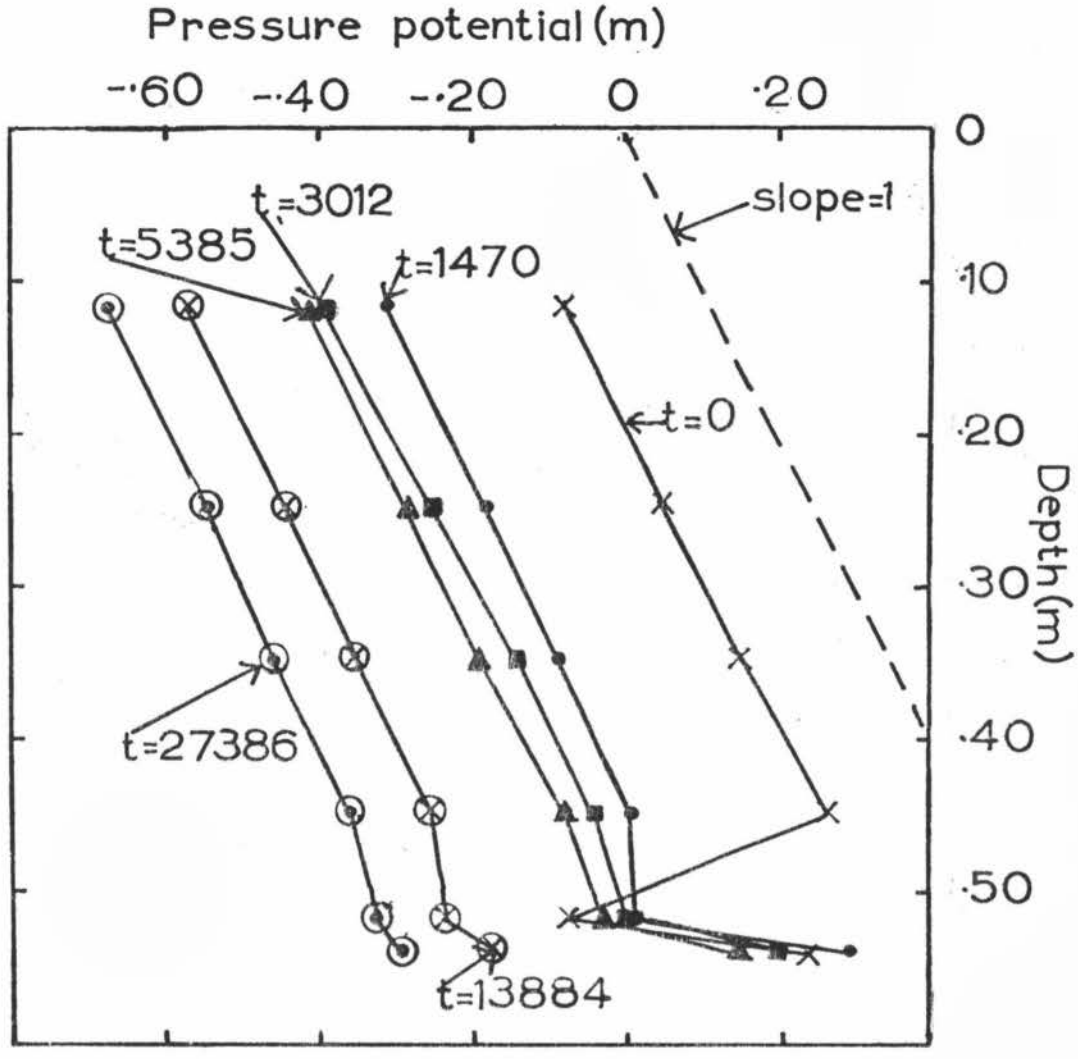

Fig.8 Pressure potential profiles at various times, t (minutes) during drainage of plot 020 of Poporangi sandy loam. The dashed line has a slope of 1 and can be compared with the slope of the experimental pressure potential profiles.

of the soil after 2 to 3 days of drainage, following a thorough wetting of the soil (Rich, 1971). Also, "field capacity" is often estimated by the volumetric water content at specific pressure potentials (Gradwell, 1971; Maclean and Yager, 1972), using the water retentivity data (volumetric water content/pressure potential relationship) (Figs. 9,10). The AWC was calculated using these various values of "field capacity" and is compared with AWC_E (the AWC calculated using the experimentally determined "field capacity" after 10 days of drainage) in Table 1. If "field capacity" had been assumed to occur after 2 to 3 days of drainage, the AWC would have been over-estimated. However, if "field capacity" had been estimated using the volumetric water content at a pressure potential of -1 m or -2 m the AWC would have been under-estimated. For this soil the best estimate of AWC compared to AWC_E was obtained using "field capacity" estimated by the volumetric water content when the pressure potential was -0.5 m.

During the 10 days taken to reach "field capacity", the top 0.3 m of the soil, where most of the roots are situated, was at a pressure potential of greater than, or equal to, -0.5 m. This, coupled with the presence of a perched water-table during drainage, indicates that oxygen deficiency problems may arise in this soil, which is supported by the presence of iron manganese concretions (Appendix I). Though the macro-porosity would appear to be adequate (15-20% by volume), a proportion of this is in "blind pores"* (Figs. 11,12), so that the "available" macro-porosity might be about 10% by volume in the soil above the duripan. Thus, as long as the

---

* Blind pores are taken here as the difference between the total porosity calculated using the bulk and particle densities and the porosity measured at saturation. This difference may, however, be due to other factors as well.

Table 1: Comparison of available water capacity (AWC) calculated using experimental and laboratory estimates of "field capacity", for Poporangi sandy loam. Also the equivalent depth of water held between pressure potentials of -10 m and -154 m.

AWC (mm) calculated using "field capacity" as:	Plot	
	011*	020*
3 days of drainage	102	99
10 days of drainage AWC_E	91	85
Θ at a pressure potential of -0.5 m	97	81
Θ at a pressure potential of -1.0 m	75	72
Θ at a pressure potential of -2.0 m	60	59
Equivalent depth of water held between pressure potentials of -10 m and -154 m (mm)	32	28

* Rooting depth taken as 0.45 m

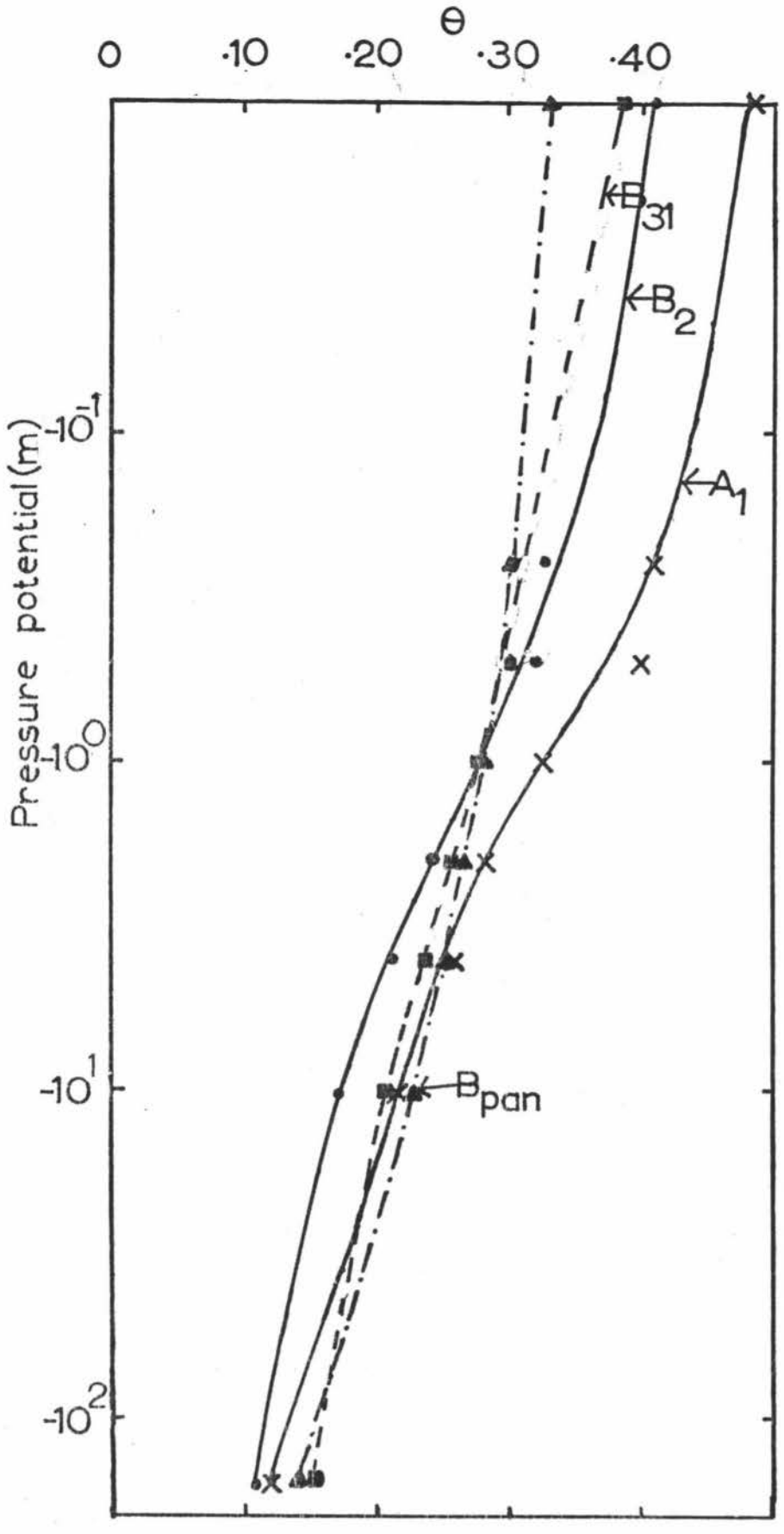

Fig.9 Volumetric water content (θ) against pressure potential for A_1 (X), B_2 (●), B_{31} (■), and B_{pan} (▲) horizons of plot 011 of Poporangi sandy loam. The lines are fitted by eye.

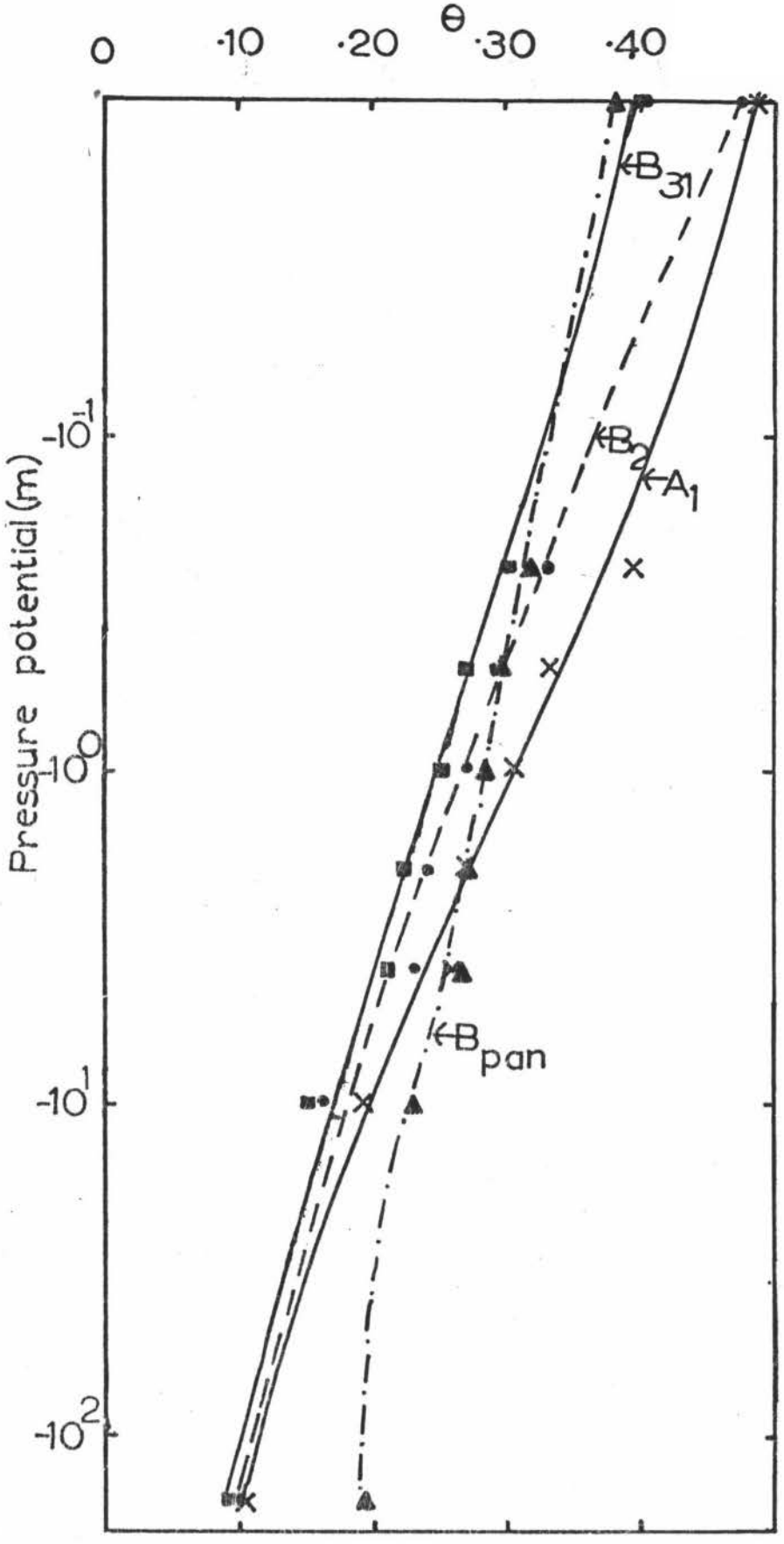

Fig.10 Volumetric water content (θ) against pressure potential for A_1 (×), B_2 (●), B_{31} (■), and B_{pan} (▲) horizons of plot 020 of Poporangi sandy loam. The lines are fitted by eye.

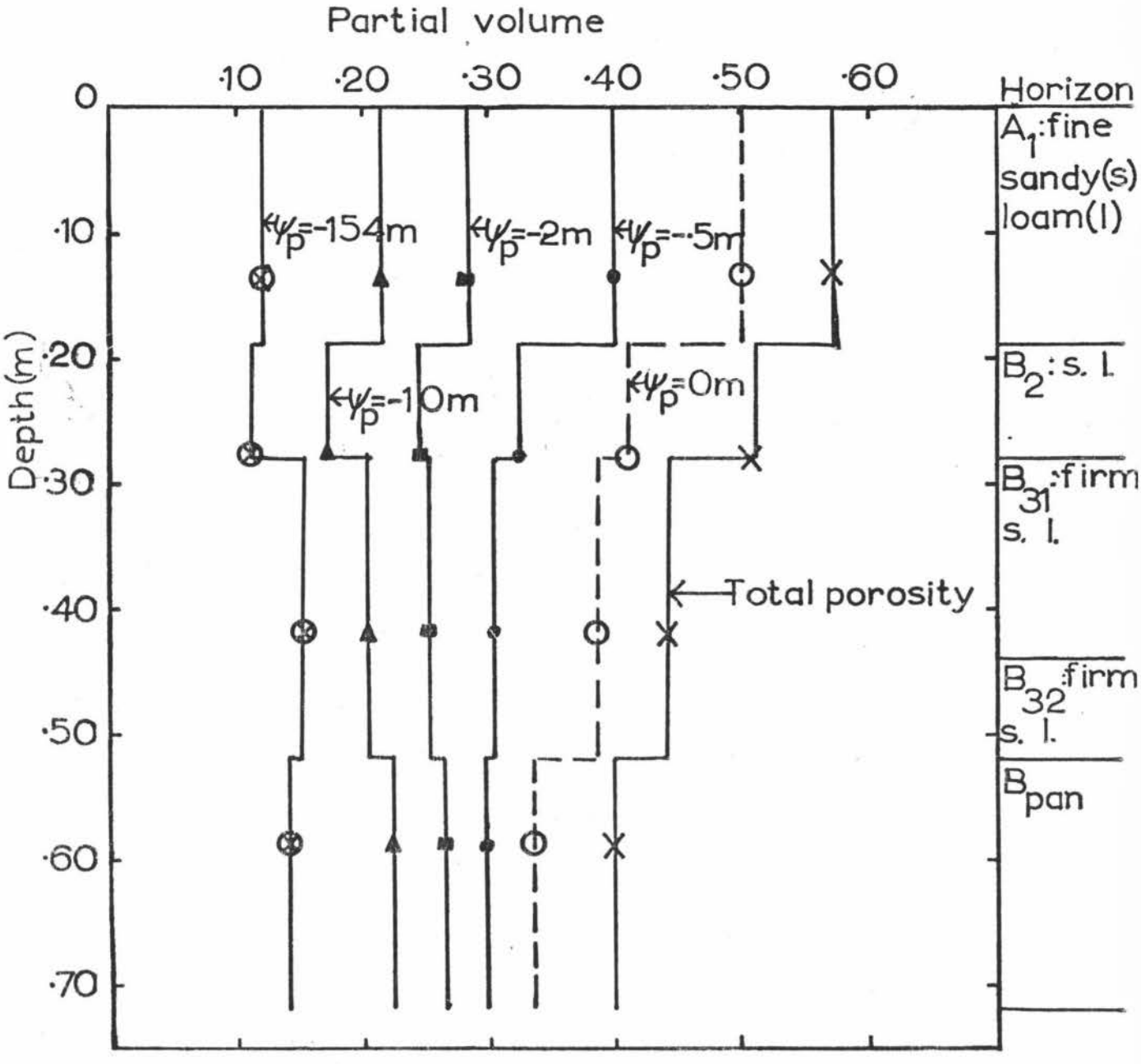

Fig.11 Partial volume of the soil occupied by water at various pressure potentials, the total porosity, depth and texture of each soil horizon of plot 011 of Poporangi sandy loam.

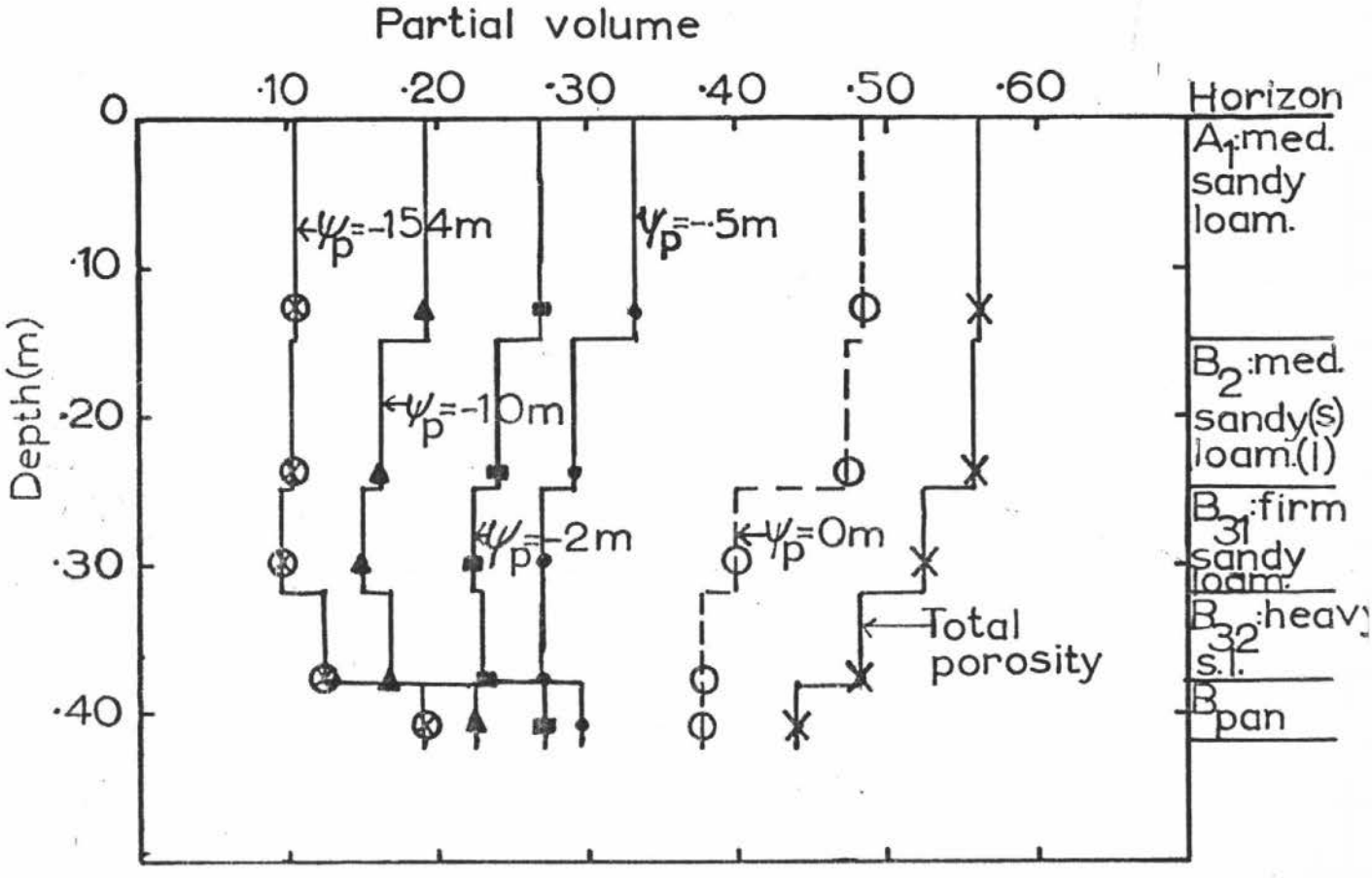

Fig.12 Partial volume of the soil occupied by water at various pressure potentials, the total porosity, depth and texture of each soil horizon of plot 020 of Poporangi sandy loam.

perched water-table does not persist for long periods, oxygen deficiency problems should not be severe. The proportion of "blind pores" (which are possibly non-conducting) in the duripan (Figs.11,12) is high, greater than 50%, which explains why the duripan appears to have reasonable macro-porosity (10-15%) whilst being in fact impermeable.

Draining this soil by a mole and tile system would speed up the lowering of the perched water-table, which would ensure that severe oxygen deficiency problems did not occur. If a drainage system was used the pressure potential profile at "field capacity" would be similar to that found now (Scotter, 1976; Cook, 1976). Thus equation (35) would still hold, but Z_w would be the depth of the mole and tile system. Also the value of AWC_E given in Table 1 would still be pertinent.

The amount of the AWC_E which was held between pressure potentials of -10 m and -154 m was about 30 mm. Thus the RAWC is about 58 mm, and would be the amount of water required at each irrigation to prevent pasture becoming stressed. This is not a large amount of water, and to apply 58 mm using a border-dyke method would be difficult, unless the lengths of the borders were short. Short borders are costly, and a sprinkler irrigation system would be a better method for irrigating this soil.

Although simulation of infiltration and drainage could not be attempted for this soil, the available water data presented could be used in a water balance equation to determine when irrigation of pasture was necessary. The likely depth that the perched water-table may rise to if excess water is applied, could also be predicted using these data, and the likely benefit of a drainage system predicted.

3.2 Ngatarawa Sandy Loam

Ngatarawa sandy loam has a gravelly sandy loam layer* which occurs at depths varying from about 0.4 m to 0.65 m (Appendix I). Clothier *et al.* (1977) found that a coarse layer in the Manawatu sandy loam, caused the water storage of that soil to be greater than that if the soil consisted of a homogeneous texture. Whether this behaviour occurs in the Ngatarawa sandy loam is of interest, as well as any data on the relationship between the hydraulic conductivity and volumetric water content of the soil layers.

Due perhaps to a surface crust, the infiltration rate at the surface is less than the saturated hydraulic conductivity of the lower layers, so the soil profile did not become saturated when water was continuously ponded on the surface of the plots (Figs.13, 14). Thus measurement of the relationship between the hydraulic conductivity and the volumetric water content near saturation could not be made. During infiltration, the tensiometer in the A layer at a depth of 0.10 m recorded a pressure potential of -0.12 m. Assuming that the A layer was not saturated due to a surface crust, the final infiltration rate was plotted corresponding to the volumetric water content (Fig.15) at this pressure potential. The pressure potential profiles at the start of drainage of the duplicate plots were very similar (Figs.13,14).

Data on the relationship between the hydraulic conductivity and the volumetric water content for the B and C layers of the duplicate plots compared well, but for the A layer the comparison is poor (Fig.15). The slope of $\log_{10}k$ against θ relationships for the A layers is similar, as the slope of W_ζ against ln t for the A layers

---

* Layers are referred to instead of horizons, as no horizon designation is given in the profile description (Appendix I).

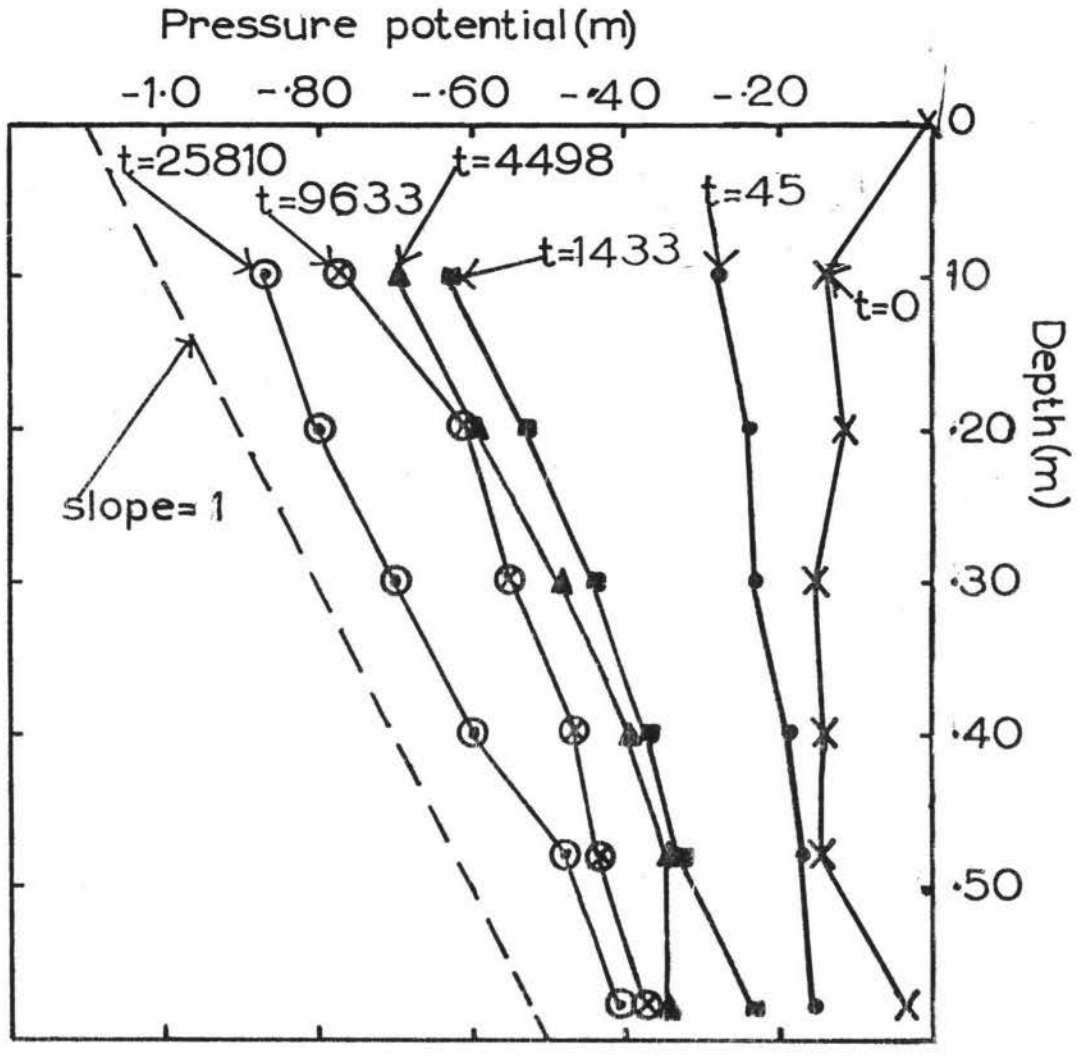

Fig.13 Pressure potential profiles at various times t, (minutes) during drainage of plot 007 of Ngatarawa sandy loam. The dashed line has a slope of 1 and can be compared with the slope of the experimental pressure potential profiles.

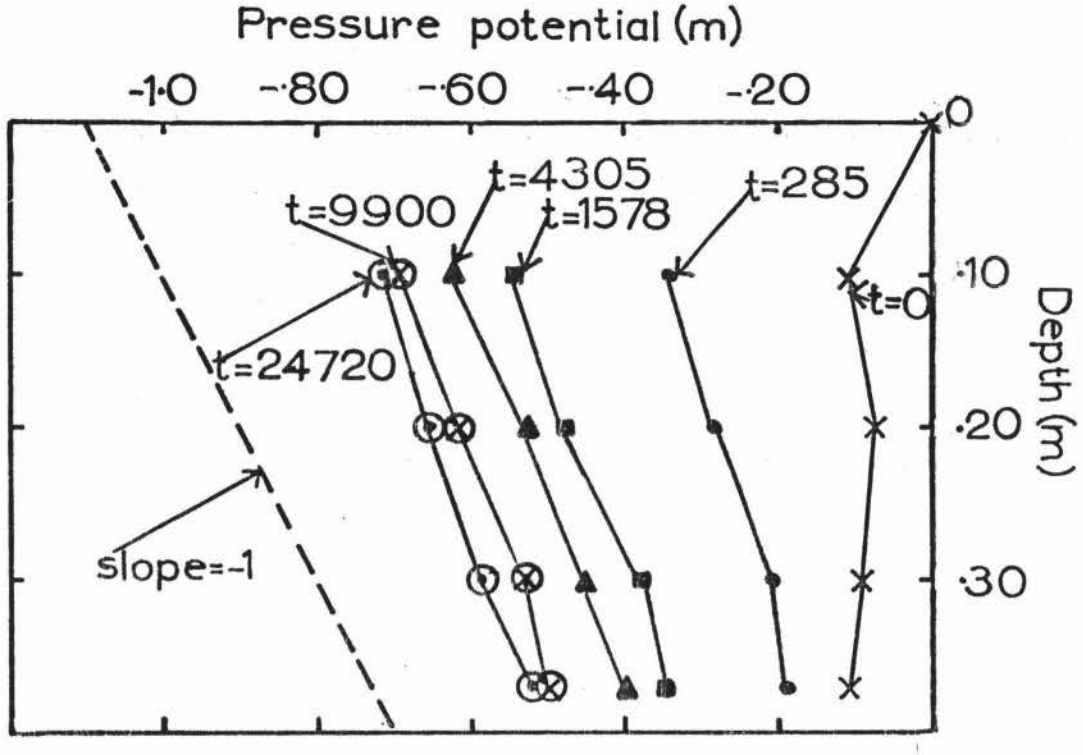

Fig.14 Pressure potential profiles at various times t, (minutes) during drainage of plot 008 of Ngatarawa sandy loam. The dashed line has a slope of 1 and can be compared with the slope of the experimental pressure potential profiles.

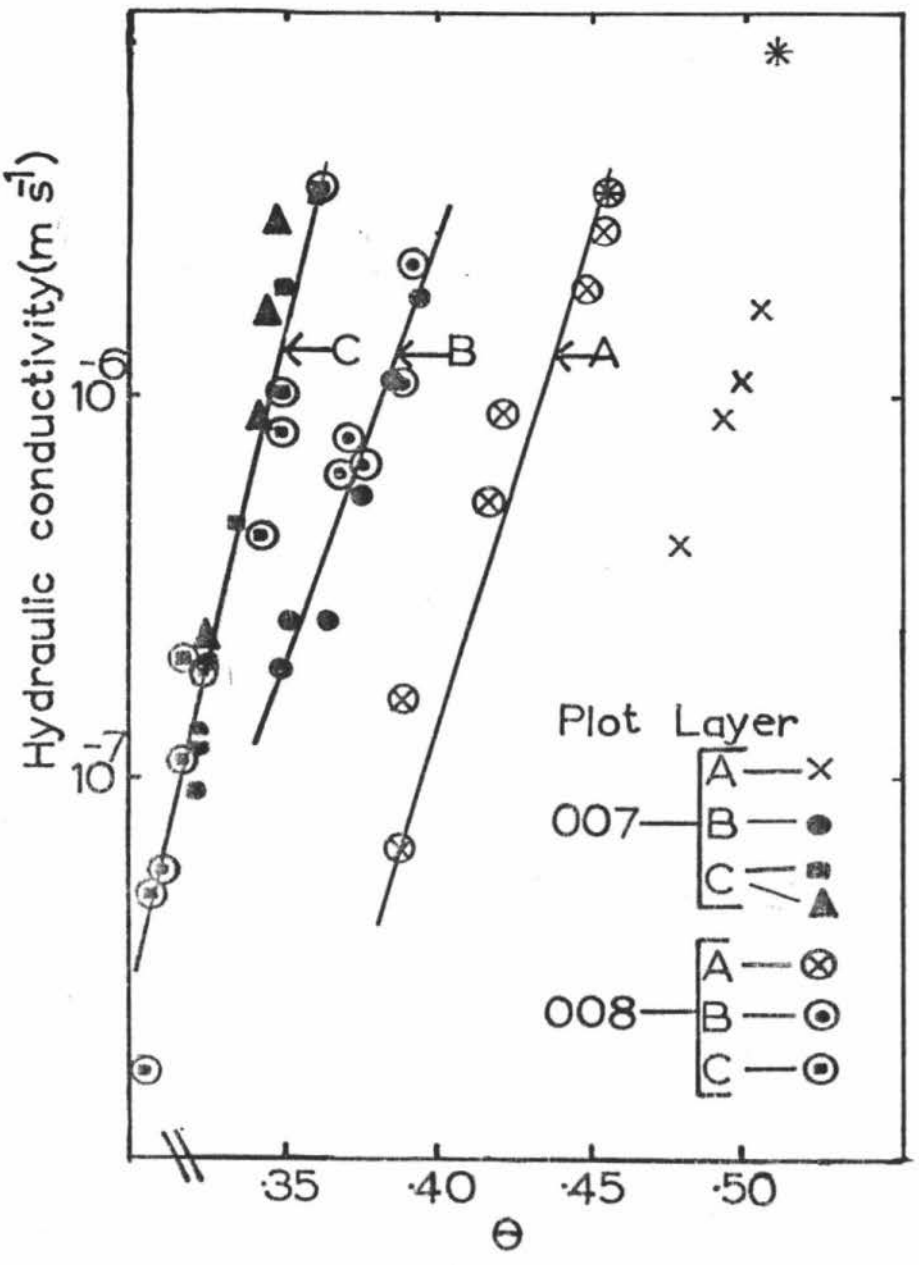

Fig.15 Hydraulic conductivity (k) against volumetric water content (θ), for A, B and C layers of Ngatarawa sandy loam. The final infiltration rates (✱⊛) are also plotted. The lines plotted are linear regressions of $\log_{10} k$ on θ.

of the two plots was similar, but the $\log_{10}k$ against θ curves are offset from one another (Fig.15). This is due to the difference in relationships between the volumetric water content and the pressure potential of the A layers of the two plots (Figs. 16,17). This indicates that the assumption of constant physical properties for pedological layers may not be valid. (This will be discussed in more detail later.) Most data on the relationship between hydraulic conductivity and volumetric water content for the A layer came from plot 008, so that only these data were used to obtain the regressed line shown in Figure 15. The regression lines shown for the B and C layers were obtained using data from both plots. These regressions, and the relationships between volumetric water content and pressure potential, were used to obtain the relationships between hydraulic conductivity and pressure potential shown in Figure 18.

Although no data on the hydraulic conductivity of the gravelly sandy loam layer were obtained, the tensiometers at the bottom of the layer, overlying the gravelly layer, give an indication of the drainage behaviour of this layer. After only six hours of drainage the pressure potential at the boundary between the gravelly sandy loam and the overlying soil had decreased to approximately -0.3 m. It decreased further only very slowly, reaching -0.5 m after 17 days. This indicates that the hydraulic conductivity of the gravelly sandy loam layer becomes small at a pressure potential of -0.4 m and drainage of water from the soil above then becomes minimal. Similar drainage behaviour to this was described for the Manawatu sandy loam by Clothier *et al.* (1977). They found that the pressure potential profile at "field capacity" could be described by:

$$\psi_p(z) = \psi_c - z_c + z \qquad \text{--- (36)}$$

for $z \leq z_c$

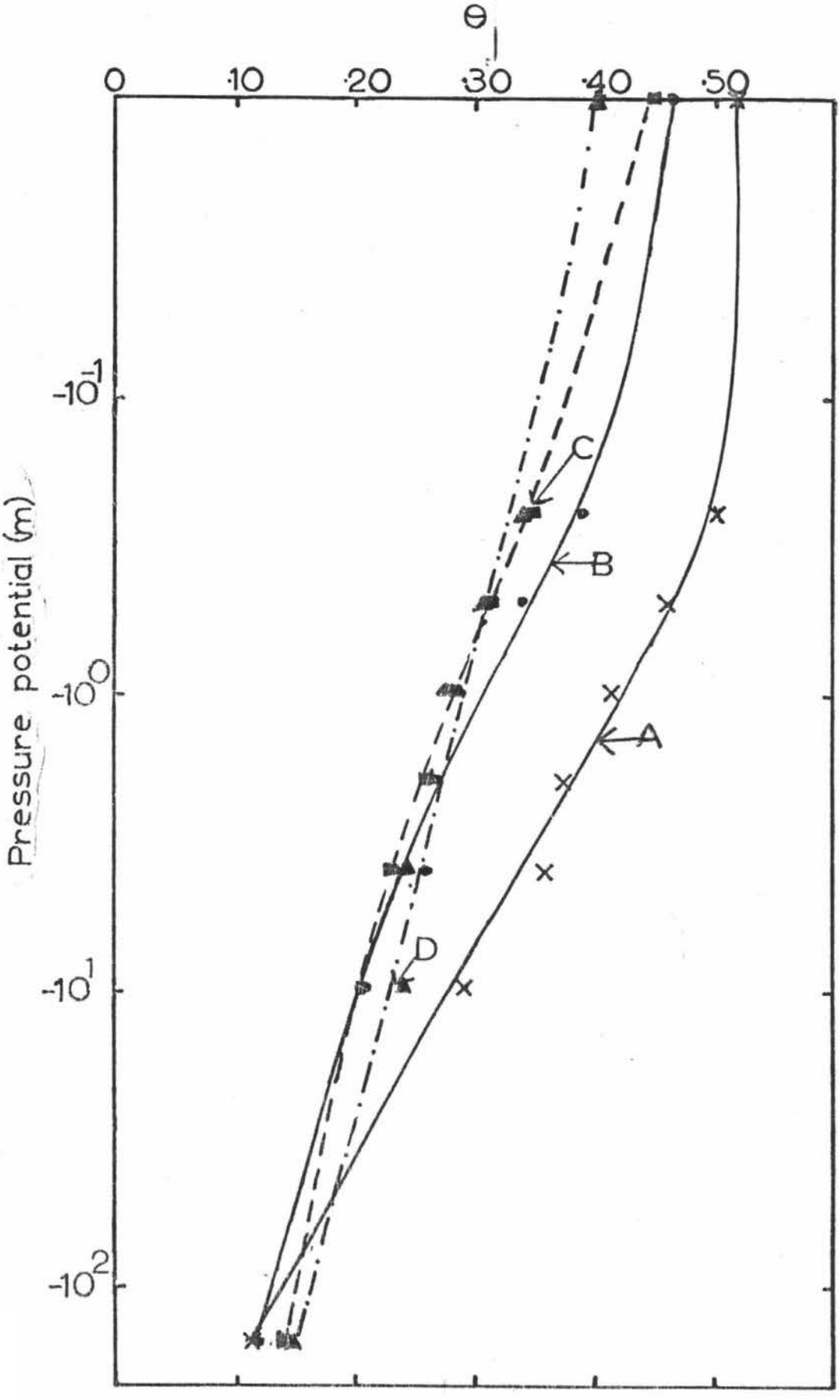

Fig. 16 Volumetric water content (θ) against pressure potential for the A(×), B(●), C(■), and D(▲) layers of plot 007 of Ngatarawa sandy loam. The lines are fitted by eye.

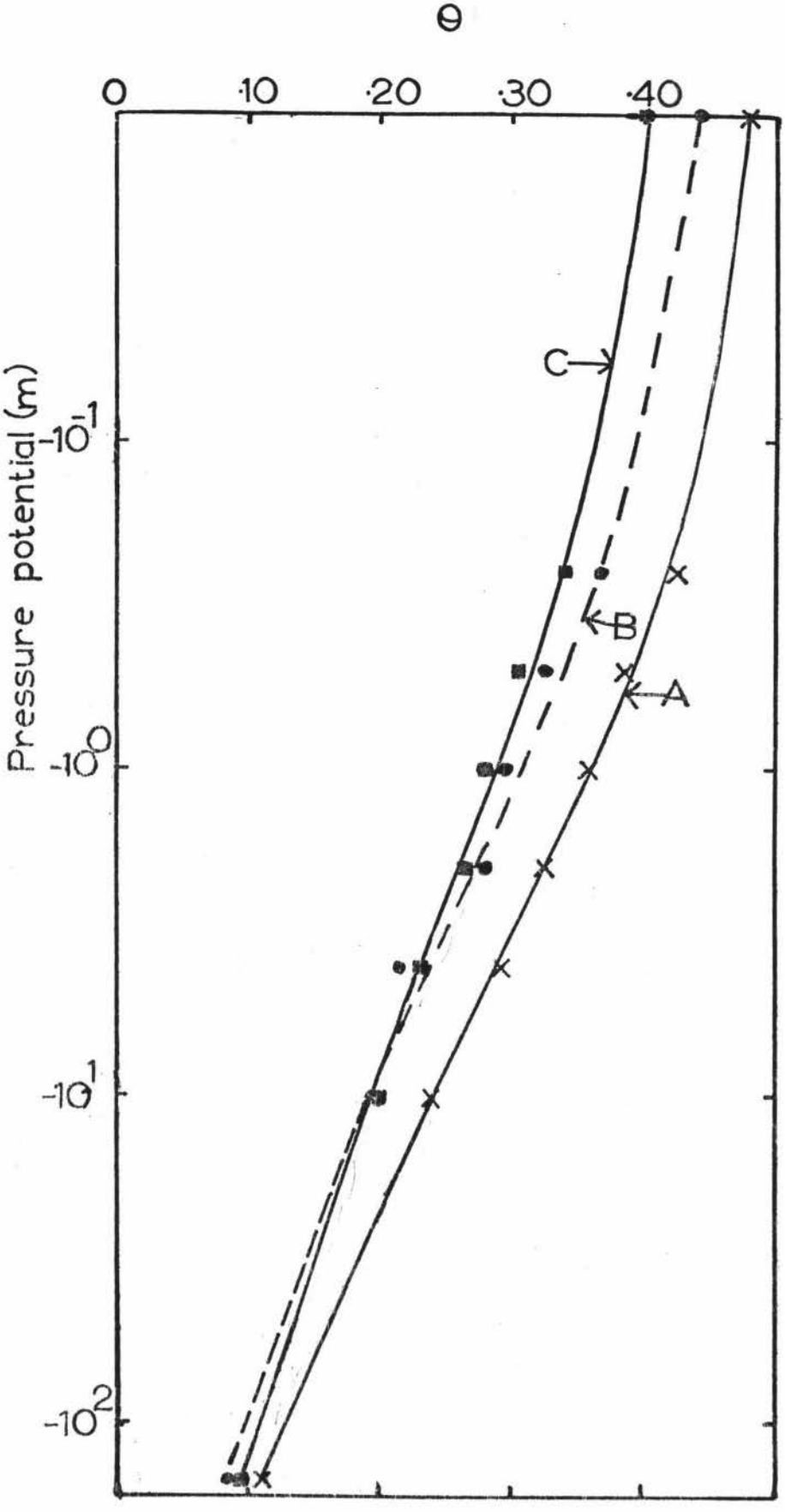

Fig.17 Volumetric water content (Θ) against pressure potential for the A(X), B(●), and C(■) layers of plot 008 of Ngatarawa sandy loam. The lines are fitted by eye.

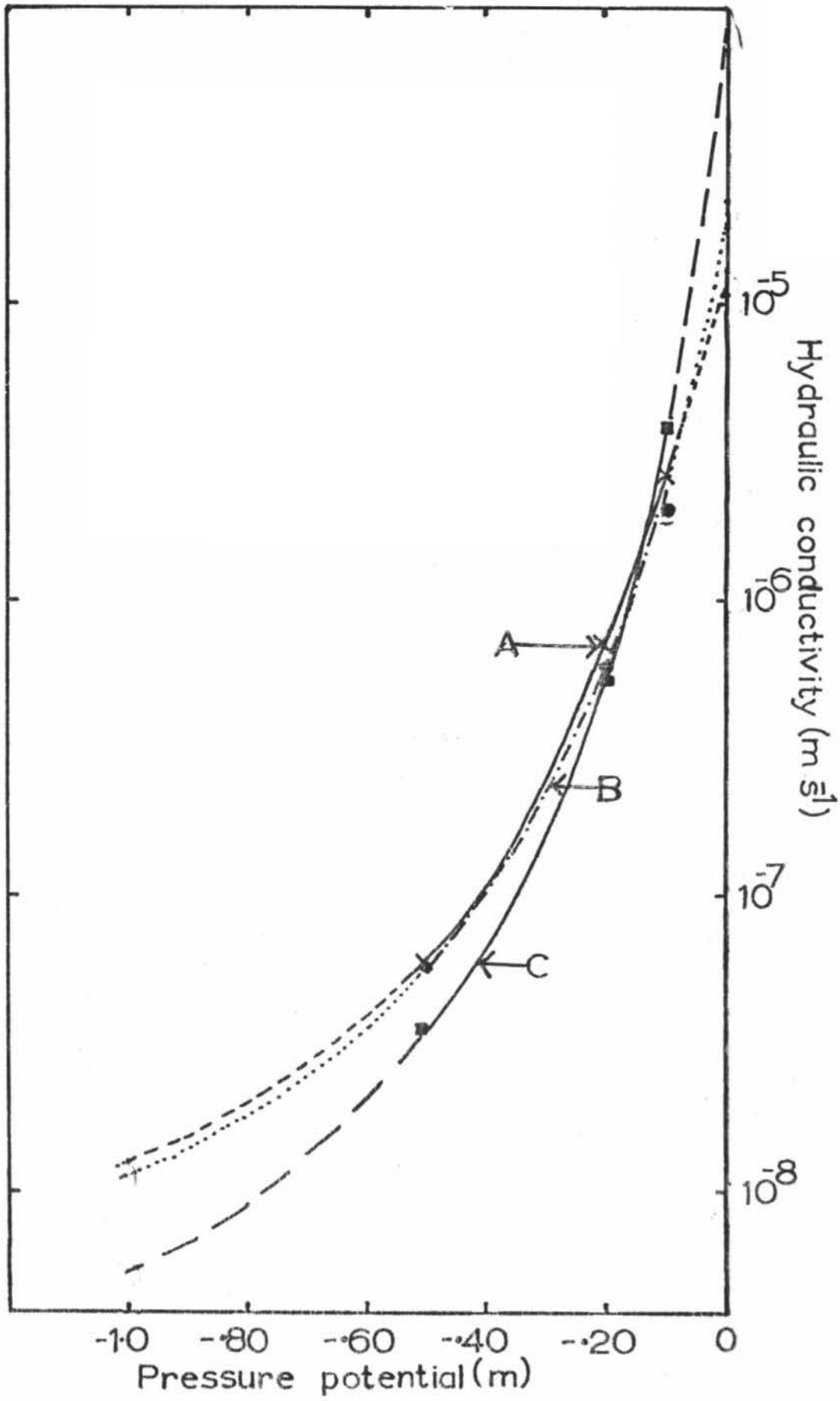

Fig.18 Hydraulic conductivity against pressure potential for the A(X), B(●), and C(■) layers of Ngatarawa sandy loam. The dashed or dotted sections of lines indicate where the line is extrapolated beyond the experimental data.

where z_c is the depth to the layer controlling the drainage rate, and ψ_c is the pressure potential at which the hydraulic conductivity of the controlling layer becomes negligible (-0.4 m). The near zero total potential gradient is due to the hydraulic conductivity of the soil above the controlling layer being greater than the hydraulic conductivity of the controlling layer at the prevailing values of pressure potential (a zero total potential gradient corresponds to a pressure potential gradient of 1). The pressure potential profiles (Figs.12,13) are approximately parallel to a line with a slope of 1, indicating that equation (15) describes the pressure potential profile developed in this soil during drainage.

Though drainage ceases at pressure potentials of more than -0.5 m no oxygen deficiency problems are envisaged, as the volume of macropores is 15-20% (Figs. 19,20). Approximately half of the macroporosity are in "blind pores", but as most of the drainage has occurred in the first 6 hours, there should be sufficient air space in the soil for no oxygen deficiency problems to arise.

The available water capacity, calculated using a pressure potential of -0.5 m, compares most favourably to that calculated using the experimental "field capacity" (AWC_E) (Table 2). The values of AWC_E given in Table 2 are possibly under-estimated, as the rooting depth was taken as the depth of measurement, whereas roots were observed down to between 0.65 m and 0.70 m (Appendix I). Thus the AWC of this soil would be approximately 160 mm, for a rooting depth of 0.7 m. Approximately 75 mm of this water is held between pressure potentials of -10 m to -154 m, so that the RAWC would be approximately 85 mm.

If the soil was irrigated to prevent moisture stress in pasture, the amount of water at each irrigation would need to be 85 mm. If the border-dyke irrigation method was used for this soil, application

Table 2: Comparison of available water capacity (AWC) calculated using experimental and laboratory estimates of "field capacity", for Ngatarawa sandy loam. Also the equivalent depth of water held between pressure potentials of -10 m and -154 m

AWC (mm) calculated using "field capacity" as:	Plot	
	007*	008**
1 day of drainage	141	95
8 days of drainage AWC_E	135	90
Θ at a pressure potential of -0.5 m	141	93
Θ at a pressure potential of -1.0 m	122	82
Θ at a pressure potential of -2.0 m	103	74
Equivalent depth of water held between pressure potentials of -10 m and -154 m (mm)	66	43

* Rooting depth taken as 0.58 m

** Rooting depth taken as 0.37 m

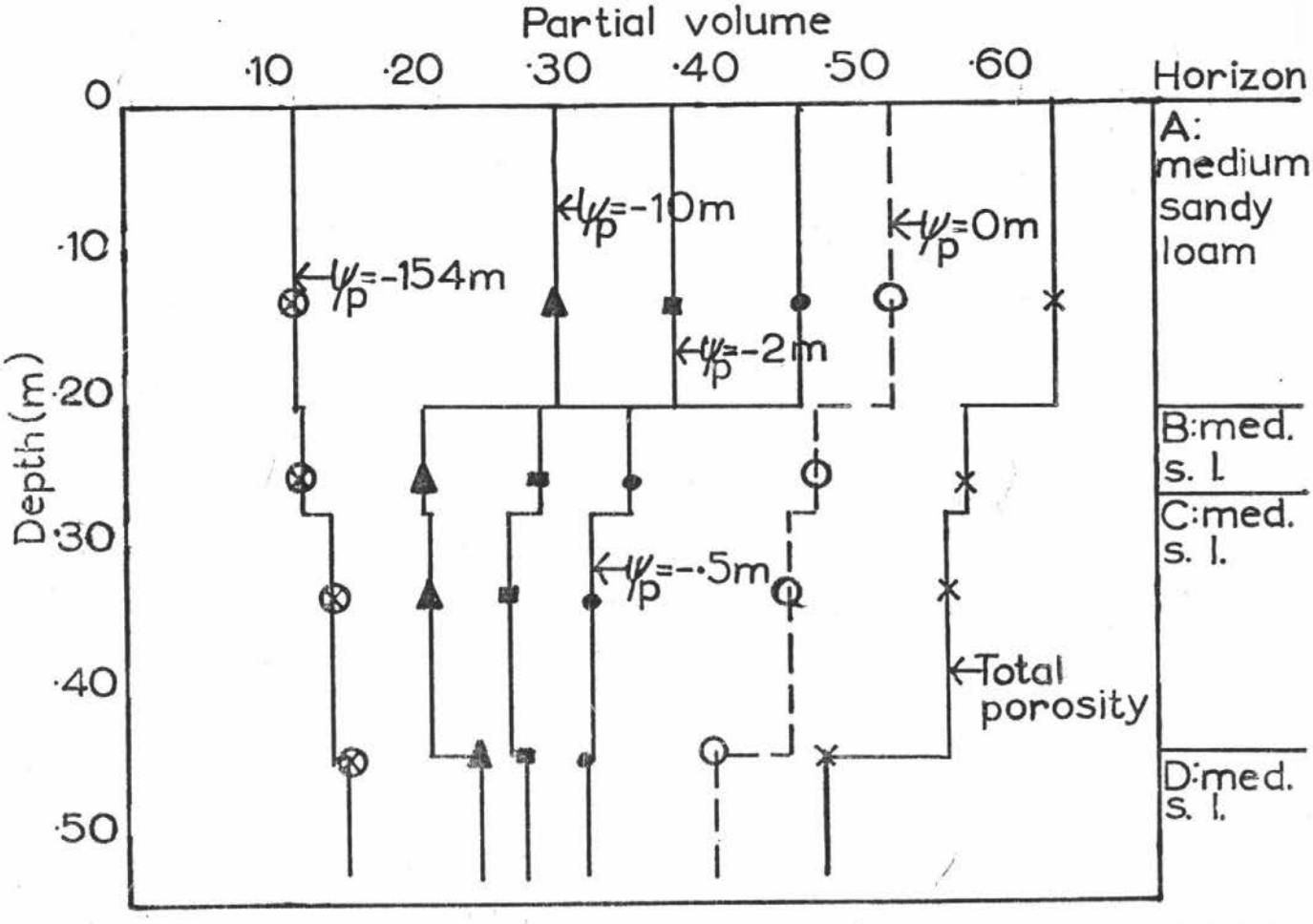

Fig.19 Partial volume of the soil occupied by water at various pressure potentials, the total porosity, depth and texture of each soil layer of plot 007 of Ngatarawa sandy loam.

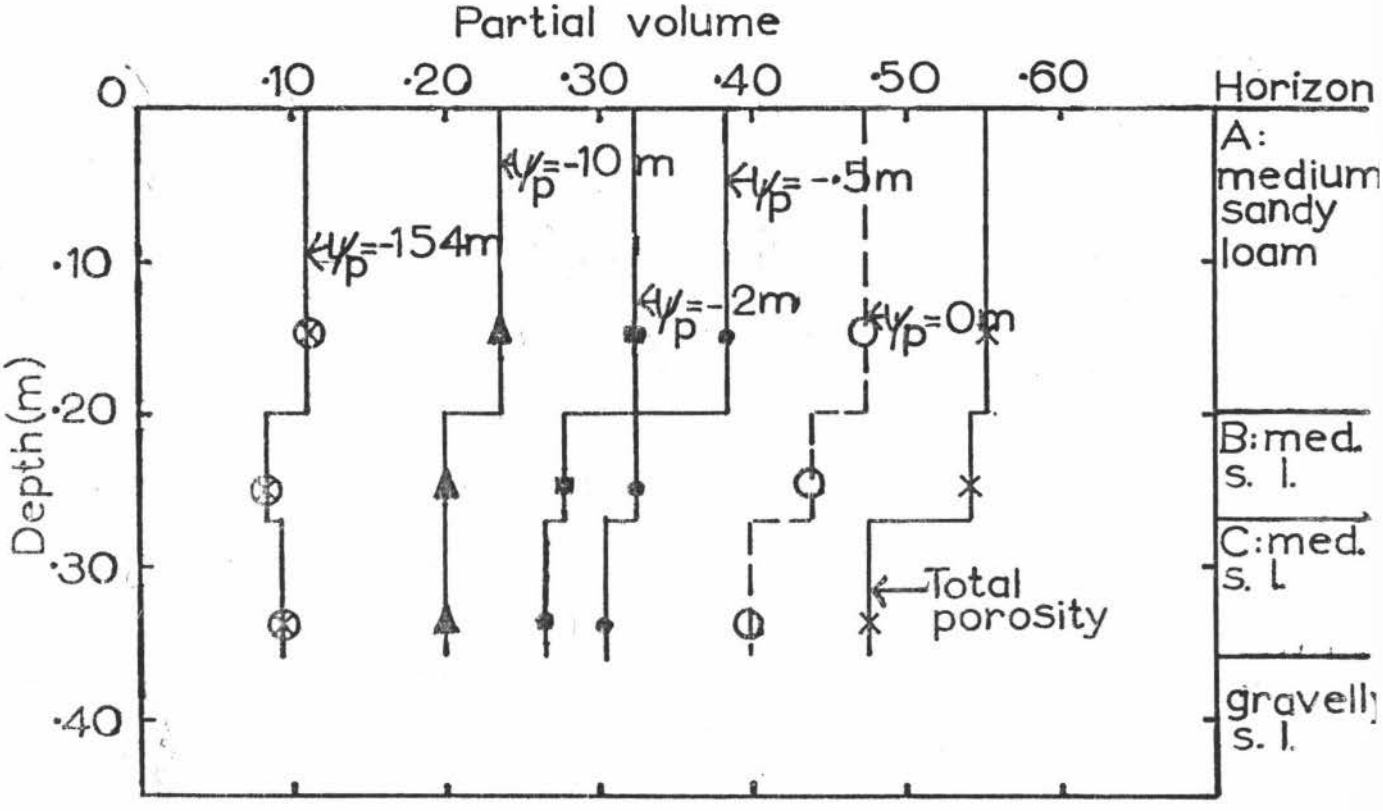

Fig.20 Partial volume of the soil occupied by water at various pressure potentials, the total porosity, depth and texture of each soil layer of plot 008 of Ngatarawa sandy loam.

of this amount to all parts of the border would be difficult without over-irrigation at the end of the border nearest the inlet. Any excess water would be rapidly lost to drainage, making the border-dyke method less efficient for this soil than a sprinkler method, where the amount of water applied per unit area of soil can be better controlled.

3.3 Takapau Sandy Loam

Takapau sandy loam, like Ngatarawa sandy loam, has a coarse layer (gravelly loamy sand) at 0.45 m to 0.65 m depth (Figs. 21,22) and the effect of this coarse layer on the drainage behaviour of the soil, compared to the Ngatarawa sandy loam, was of interest.

This soil was unable to be saturated (Figs. 23,24) even though the infiltration rate was rapid (Table 10). Tensiometers at 0.4 m and 0.5 m in plot 021 indicated pressure potentials greater than zero i.e. saturated, but this was possibly due to water moving down the sides of the tensiometer access tube, or a soil fissure (caused during installation) to the tensiometer tip, as the tensiometers above and below these depths indicated negative pressure potentials.

For plot 010 the pressure potential gradient in the B_{21} and B_{22} horizons quickly attained a value near 1 (Fig.23) i.e. zero total potential. Thus only limited hydraulic conductivity data for these horizons of this plot could be calculated (Fig.25). In plot 021 the pressure potential gradient in the A horizon rapidly attained a value near 1 (Fig.24) so that no hydraulic conductivity data for this horizon of this plot were calculated (Fig.25). The reasons for this behaviour are not clear.

Agreement between the hydraulic conductivity data obtained from both plots for the B_{21} and B_{22} horizons is quite good (Fig.25).

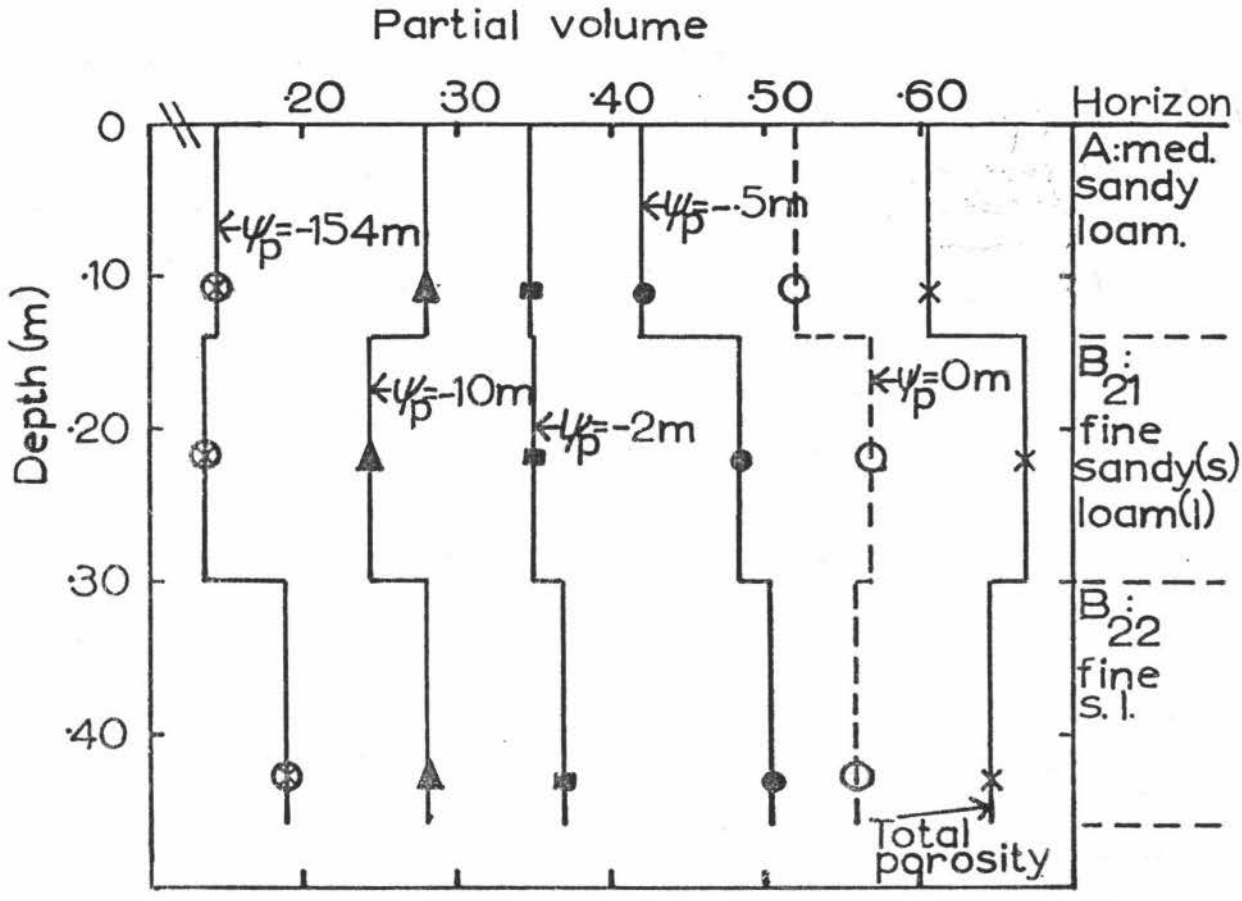

Fig.21 Partial volume of the soil occupied by water at various pressure potentials, the total porosity, depth and texture of each soil horizon of plot 010 of Takapau sandy loam.

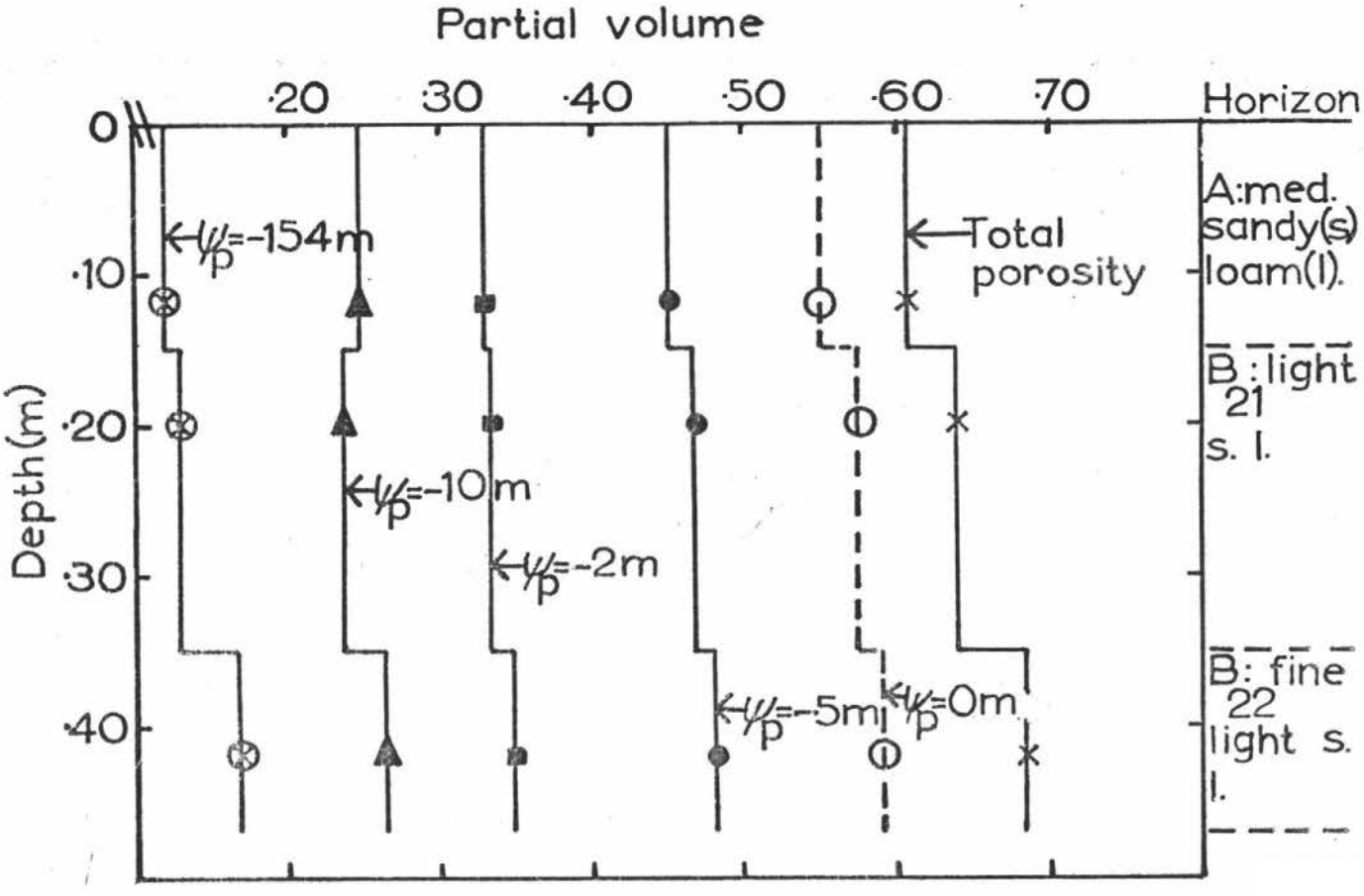

Fig.22 Partial volume of the soil occupied by water at various pressure potentials, the total porosity, depth and texture of each soil horizon of plot 021 of Takapau sandy loam.

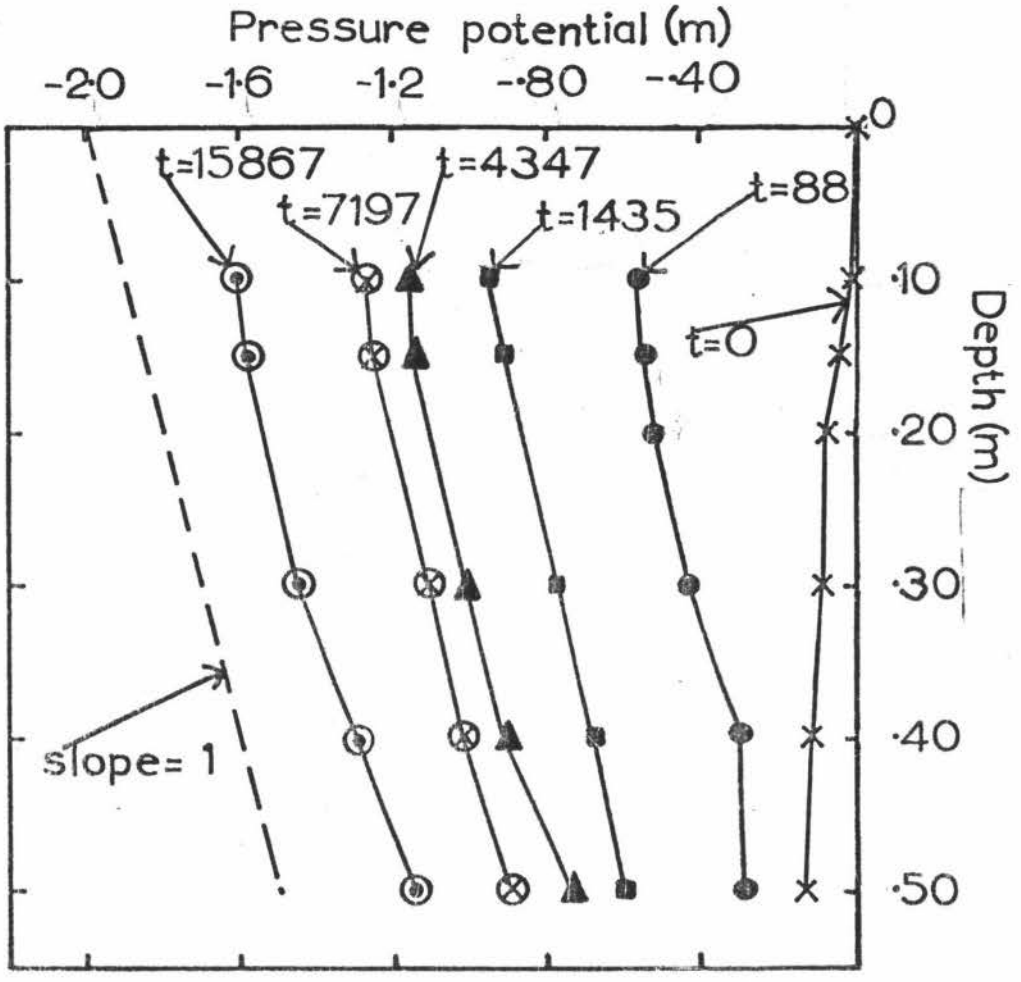

Fig.23 Pressure potential profiles at various times, t (minutes) during drainage of plot 010 of Takapau sandy loam. The dashed line has a slope of 1 and can be compared with the slope of the experimental pressure potential profiles.

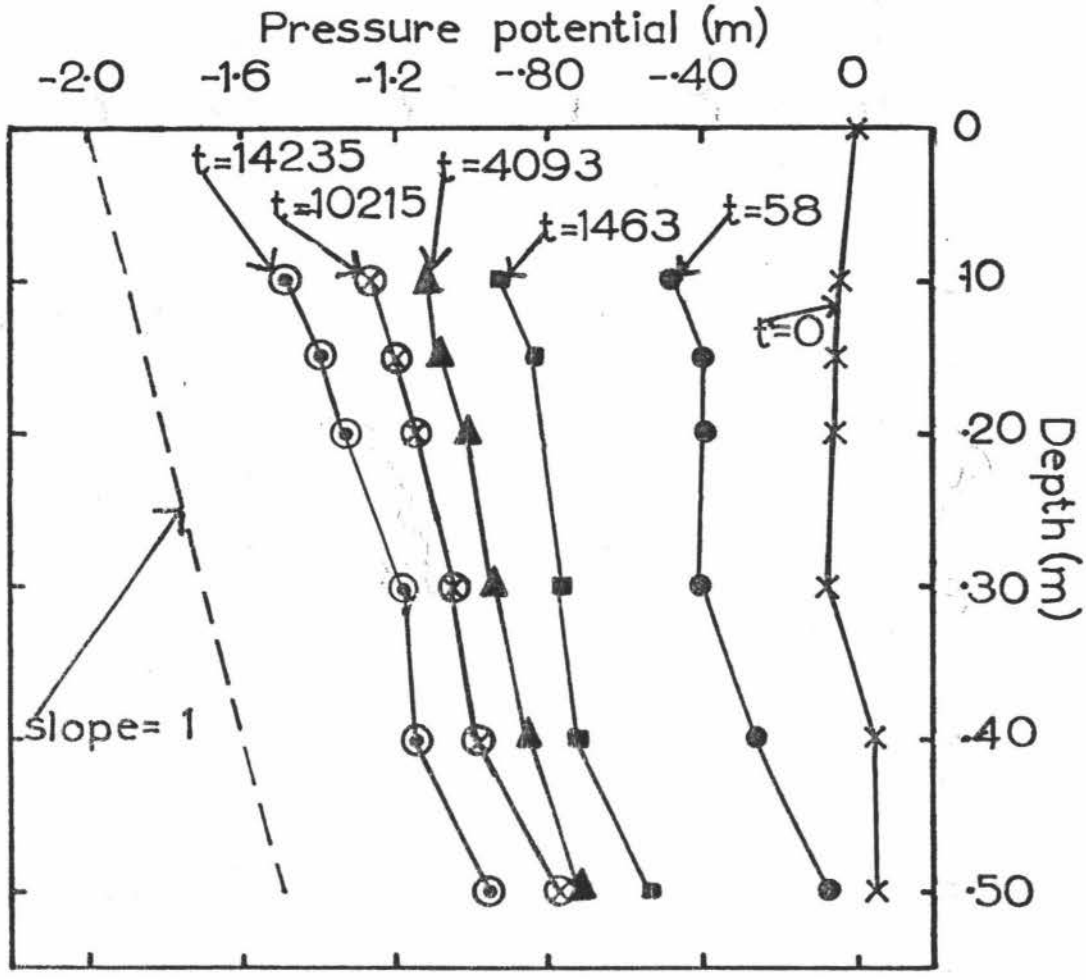

Fig.24 Pressure potential profiles at various times, t (minutes) during drainage of plot 021 of Takapau sandy loam. The dashed line has a slope of 1 and can be compared with the slope of the experimental pressure potential profiles.

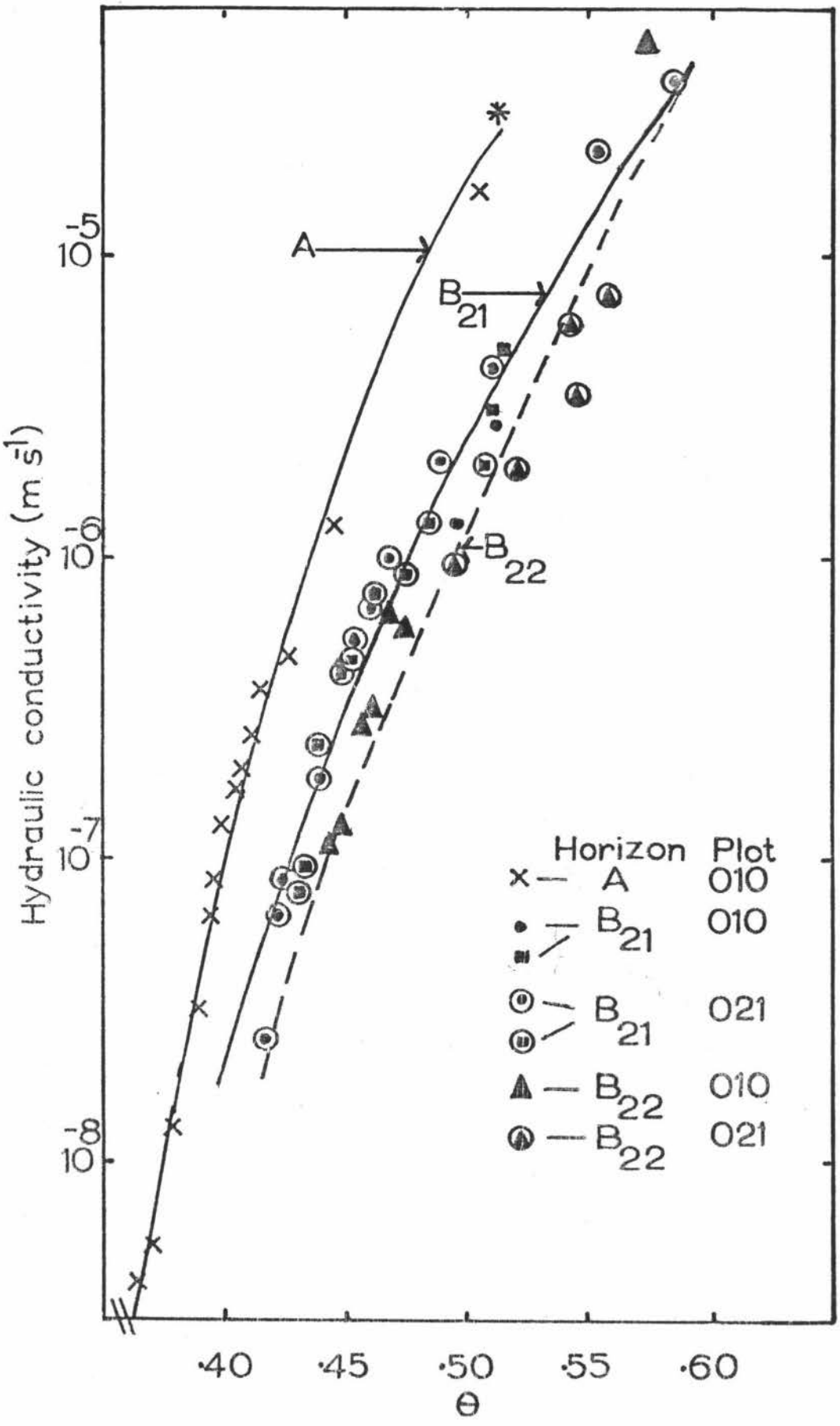

Fig. 25 Hydraulic conductivity (k) against volumetric water content (Θ), for A, B_{21}, and B_{22} horizons of Takapau sandy loam. The final infiltration rate (*) is also plotted. The lines shown are quadratic regressions of $\log_{10}k$ on Θ.

Quadratic regressions of the relationship between $\log_{10}k$ and Θ were obtained for these data and are also plotted in Figure 25. These regression equations were used in the computer simulation model.

The relationship between $\log_{10}k$ and pressure potential (Fig.26) was obtained using the relationship between $\log_{10}k$ and Θ (Fig.25) via the volumetric water content/pressure potential curves (Figs.27,28). As the hydraulic conductivity data for the A horizon came from plot 010, the volumetric water content/pressure potential relationship for this horizon (Fig.27) was used in obtaining the $\log_{10}k$/pressure potential relationship plotted in Figure 26. However as most of the hydraulic conductivity data for the B_{21} and B_{22} horizons came from plot 021 the volumetric water content/pressure potential relationships shown for these horizons in Figure 28 were used in obtaining the $\log_{10}k/\Theta$ relationships plotted in Figure 25. The relationship between $\log_{10}k$ and pressure potential (Fig.26) were similar for the A, B_{21}, and B_{22} horizons for pressure potentials greater than -0.8 m, but diverge for lower values of pressure potential.

The drainage behaviour of Takapau sandy loam, with its long drainage tail (Table 3), is different from Ngatarawa sandy loam, which has a fairly abrupt end to drainage after 1 day (Table 2). Both of these soils have a coarse layer underlying them but the gravelly loamy sand in Takapau sandy loam continues to conduct water at pressure potentials down to -1.2 m. However, the gravelly sandy loam in Ngatarawa sandy loam becomes only very slowly conducting below a pressure potential of -0.4 m. This indicates that the matrix (fine) material in these coarse layers have different hydraulic conductivity/pressure potential relationships. Particle size gradings for the matrix material of these two soils show Ngatarawa sandy loam having more clay sized material (J.P.C.Watt, pers. comm.) than Takapau sandy loam. Also the matrix material of

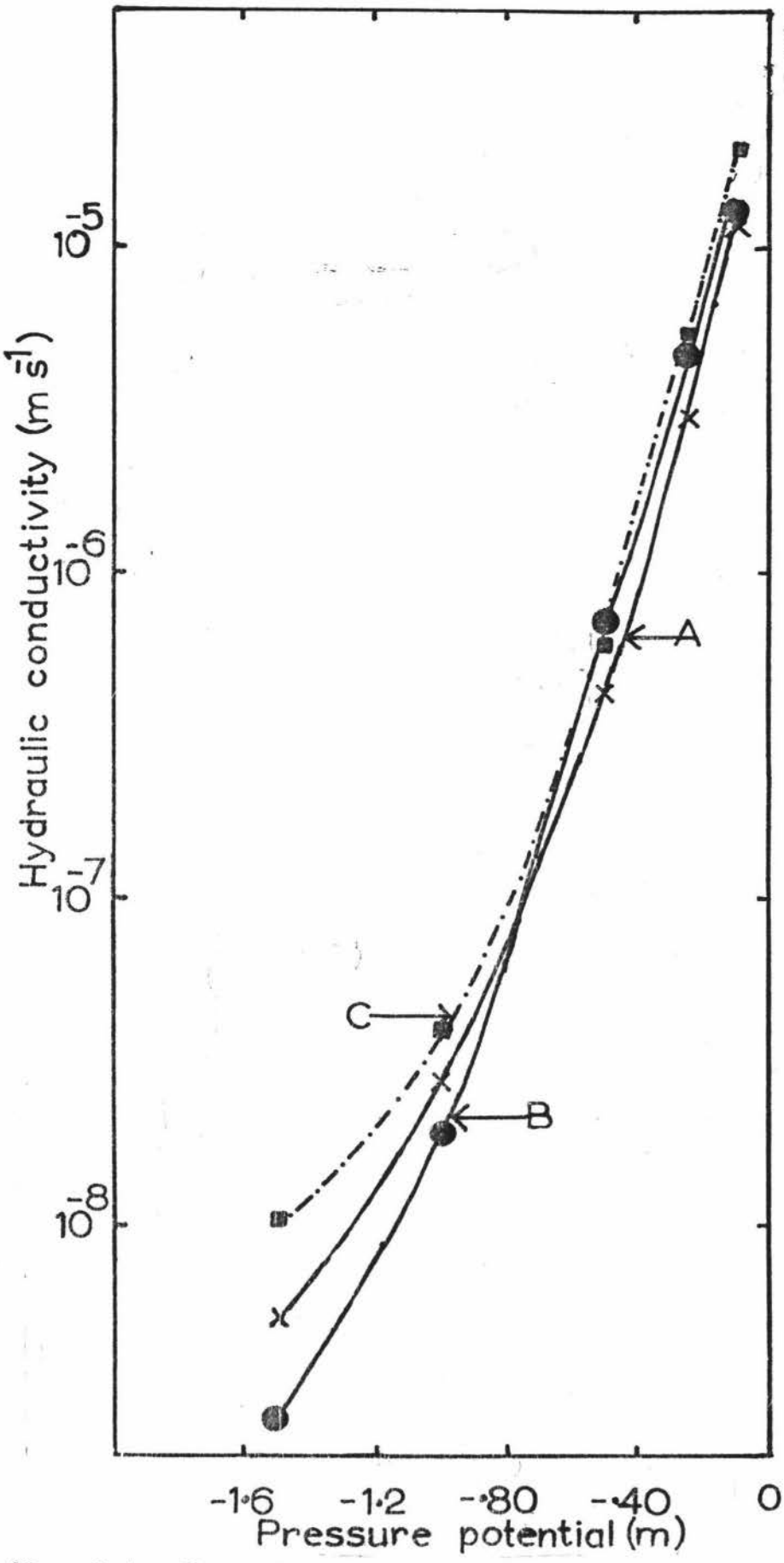

Fig.26 Hydraulic conductivity against pressure potential for the A(✕), B_{21}(●), and B_{22}(■) horizons of Takapau sandy loam. The dashed sections of the lines indicate where the line is extrapolated beyond the experimental data.

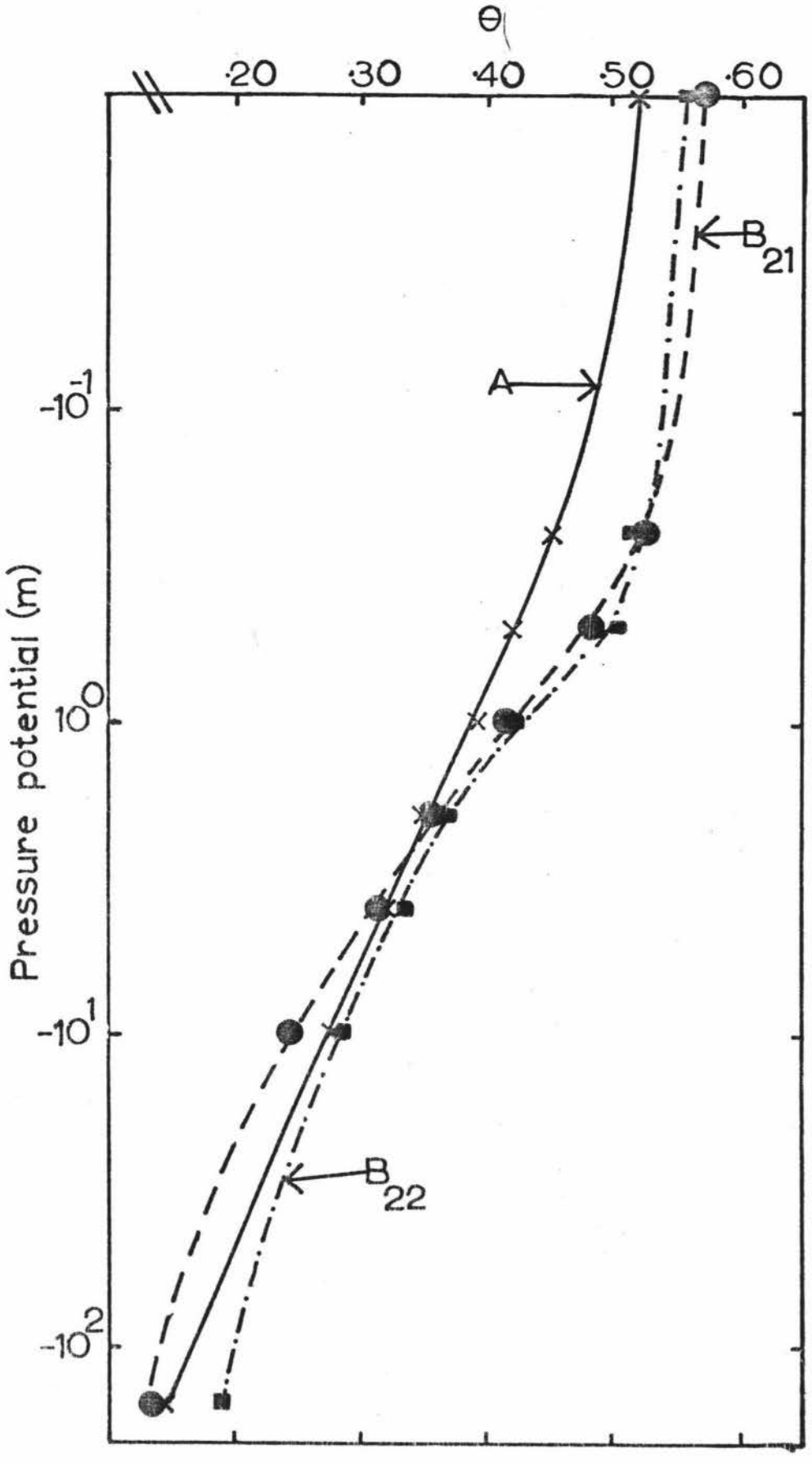

Fig.27 Volumetric water content (θ) against pressure potential for A(×), B_{21}(●), and B_{22}(■) horizons of plot 010 of Takapau sandy loam. The lines are fitted by eye.

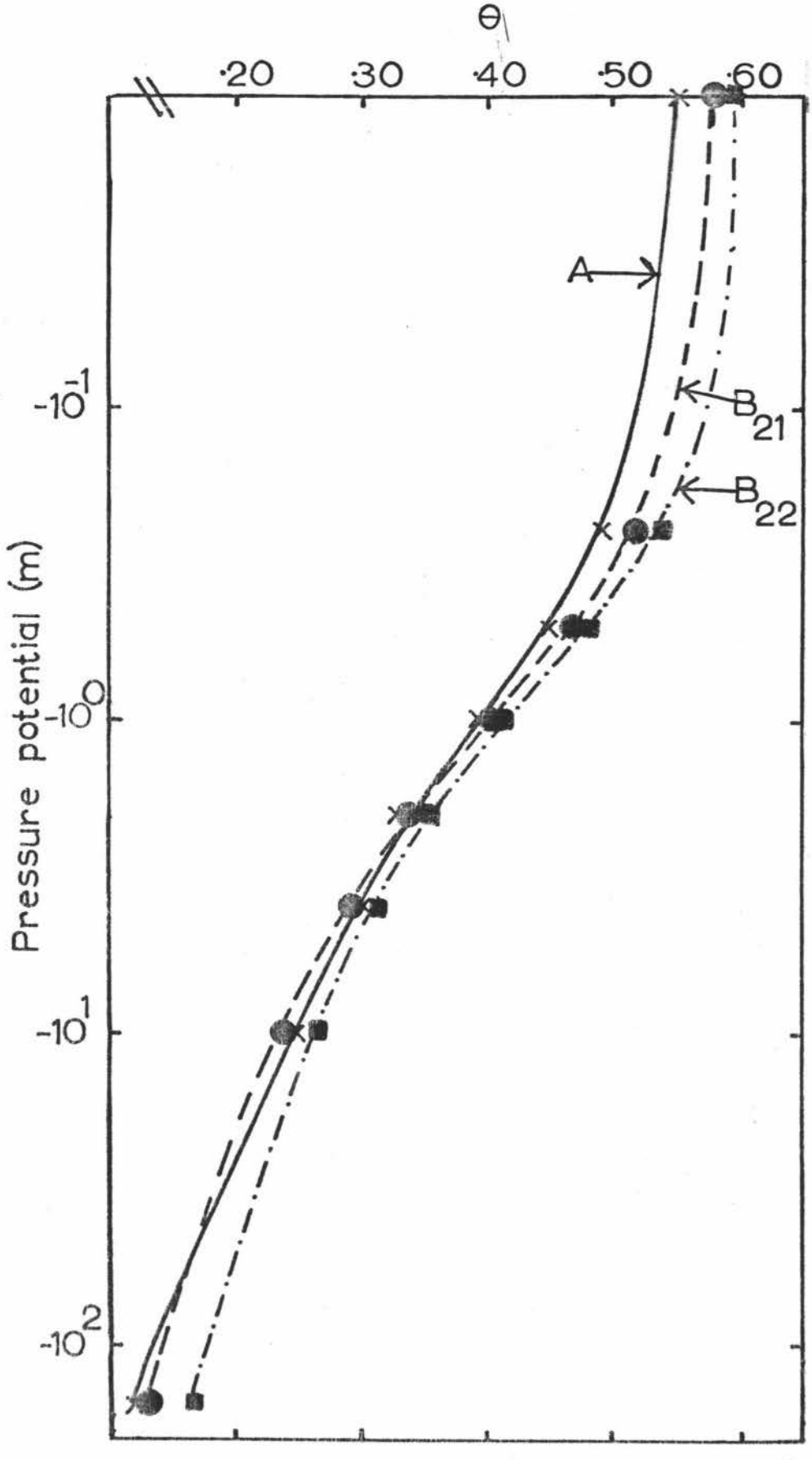

Fig.28 Volumetric water content (θ) against pressure potential for A(×), B_{21}(●), and B_{22}(■) horizons of plot 021 of Takapau sandy loam. The lines are fitted by eye.

the Ngatarawa sandy loam coarse layer has less total pore space than the matrix material of the Takapau sandy loam coarse layer (J.P.C. Watt, pers. comm.). This lesser pore space and possibly greater proportion of the pore space in fine pores (as more clay) of the matrix material in the coarse layer of Ngatarawa sandy loam, is a possible explanation for the different drainage behaviour exhibited by these two soils.

The AWC of the Takapau sandy loam would have been overestimated by approximately 20 mm if "field capacity" had been measured after 3 days of drainage, instead of when the drainage rate from the soil had become small (less than 1 mm day^{-1}) (Table 3). It took 10 days of drainage for the drainage rate beyond 0.50 m to become small (1 mm day^{-1}) for this soil. The best estimate of AWC, calculated using "field capacity" estimated by the volumetric water content at a specific pressure potential, compared to AWC_E, was when the pressure potential was -1.0 m (Table 3). This value of AWC does overestimate AWC_E slightly, but not by as much as when "field capacity" is taken as the volumetric water content at a pressure potential of -0.5 m (Table 3). The amount of water held between pressure potentials of -10 m and -154 m is approximately 75 mm. Thus the RAWC for Takapau sandy loam is approximately 95 mm. This is a similar amount to RAWC of the Ngatarawa sandy loam, but the pressure potential at "field capacity" is quite different for these two soils.

In irrigating this soil, because of the rapid infiltration rate (Table 10), it would probably be difficult to apply 95 mm of water uniformly using a border dyke system, and the rapid drainage of this soil (50 mm in the first 10 hours, after thorough wetting) would also mean that any over-irrigation could contribute considerably to the amount of water entering the groundwater.

Table 3: Comparison of available water capacity (AWC) calculated using experimental and laboratory estimates of "field capacity", for Takapau sandy loam. Also the equivalent depth of water held between pressure potentials of -10 m and -154 m

AWC (mm) calculated using "field capacity" as:	Plot	
	010*	021**
3 days of drainage	183	197
10 days of drainage AWC_E	158	182
Θ at a pressure potential of -0.5 m	240	236
Θ at a pressure potential of -1.0 m	175	188
Θ at a pressure potential of -2.0 m	137	141
Equivalent depth of water held between pressure potentials of -10 m and -154 m (mm)	71	78

* Rooting depth taken as 0.68 m

** Rooting depth taken as 0.74 m

3.3.1 Computer Simulations

To investigate the above predictions, the computer simulation model was used to simulate water movement in this soil. Following a preliminary investigation of hysteresis (Appendix II), the draining volumetric water content/pressure potential relationships were used for drainage and the wetting volumetric water content/pressure potential relationships used for infiltration.. The soil was considered to consist of three horizons A, B_{21} and B_{22} each of 0.15 m thickness, and any water passing out of the B_{22} horizon was considered to be lost to drainage.

Drainage from a similar initial state to that of the experimental plots was simulated. Agreement between the simulated and experimental pressure potential profiles at various times during drainage is good (Fig. 29), as is agreement between cumulative drainage (Fig.30).

Ponded infiltration (constant-concentration) was simulated using the computer model and the flux-concentration relation (equations (26) and (27)). The wetting fronts at various times compared quite well (Fig.31), as did cumulative infiltration (Fig.32). This comparison could only be performed until the wetting front reached the bottom of the A horizon, as the solution involving the flux-concentration relation can only be used for homogeneous soils. These comparisons indicate that the model is able to satisfactorily simulate the hydraulic behaviour of this soil.

An experiment to measure the depth of the wetting front and the water content behind the wetting front during an irrigation using a "Big Gun" irrigator was performed (Appendix IV). It was hoped that data from this experiment could also be used to check the model but as described in Appendix IV this was not possible due to the application rate from the "Big Gun" and subsequent non-uniform infiltration.

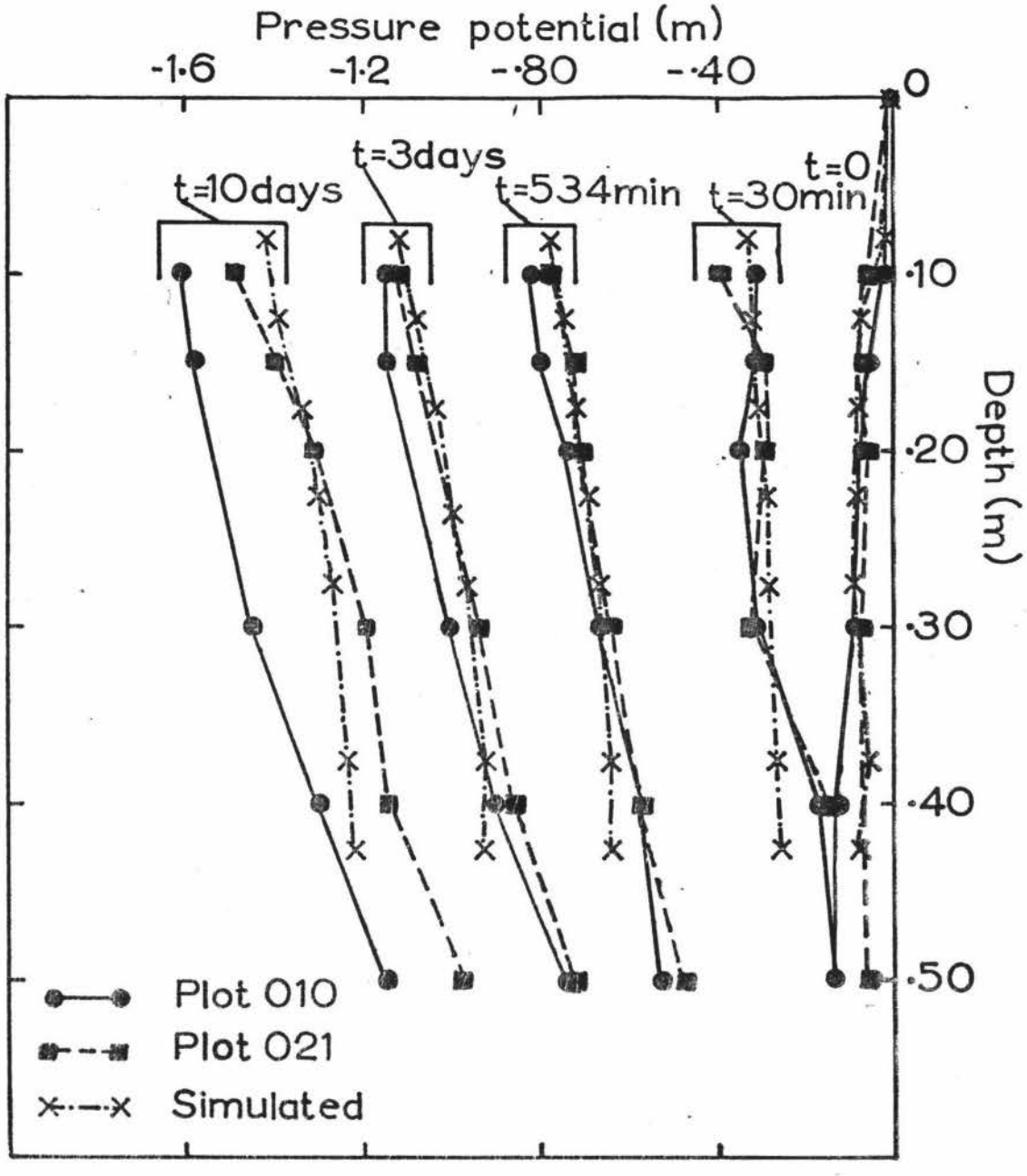

Fig.29 Simulated and experimental pressure potential profiles at various times, t, during drainage from a thoroughly wetted state, for Takapau sandy loam.

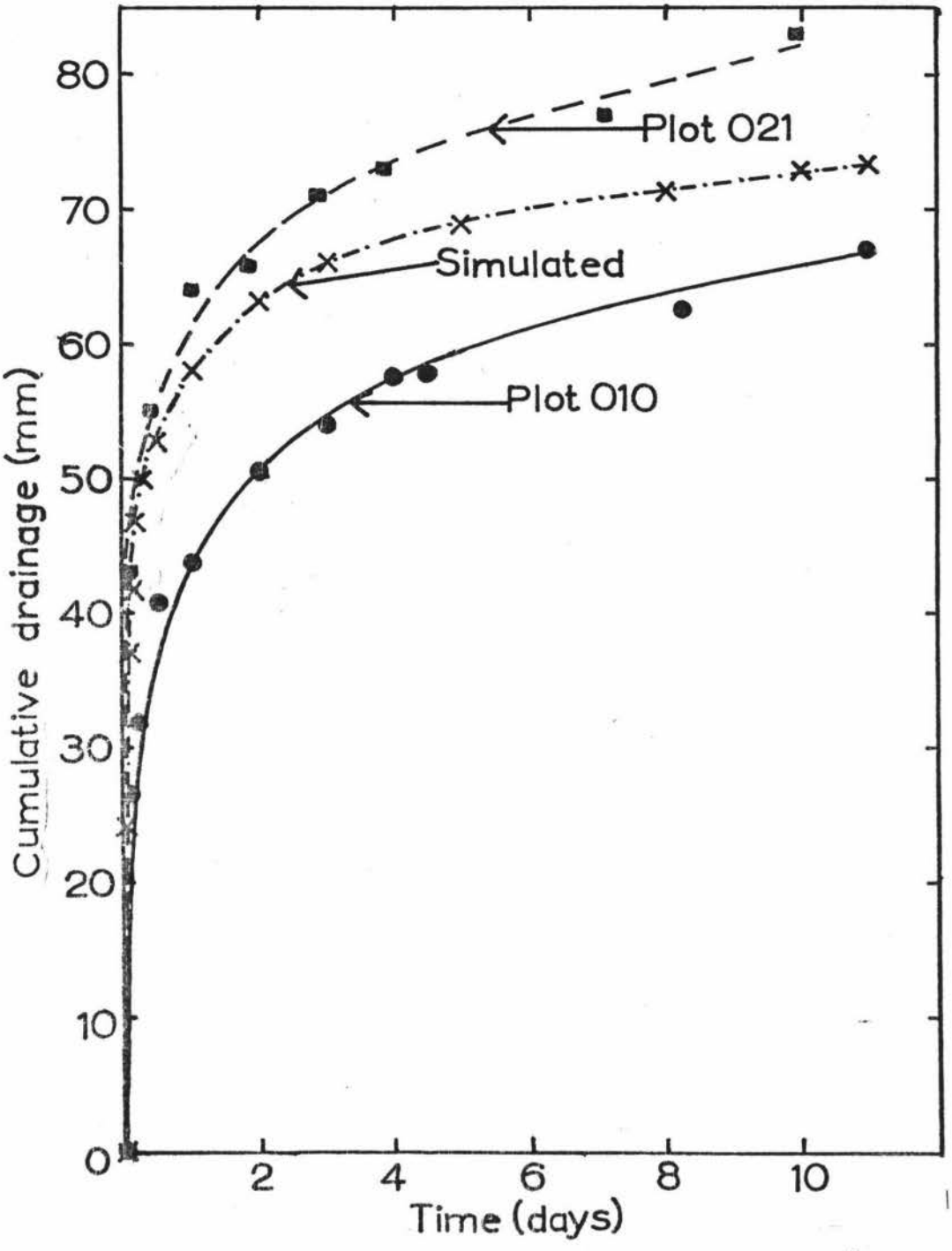

Fig.30 Simulated and experimental cumulative drainage (beyond 0.45 m) against time, for Takapau sandy loam.

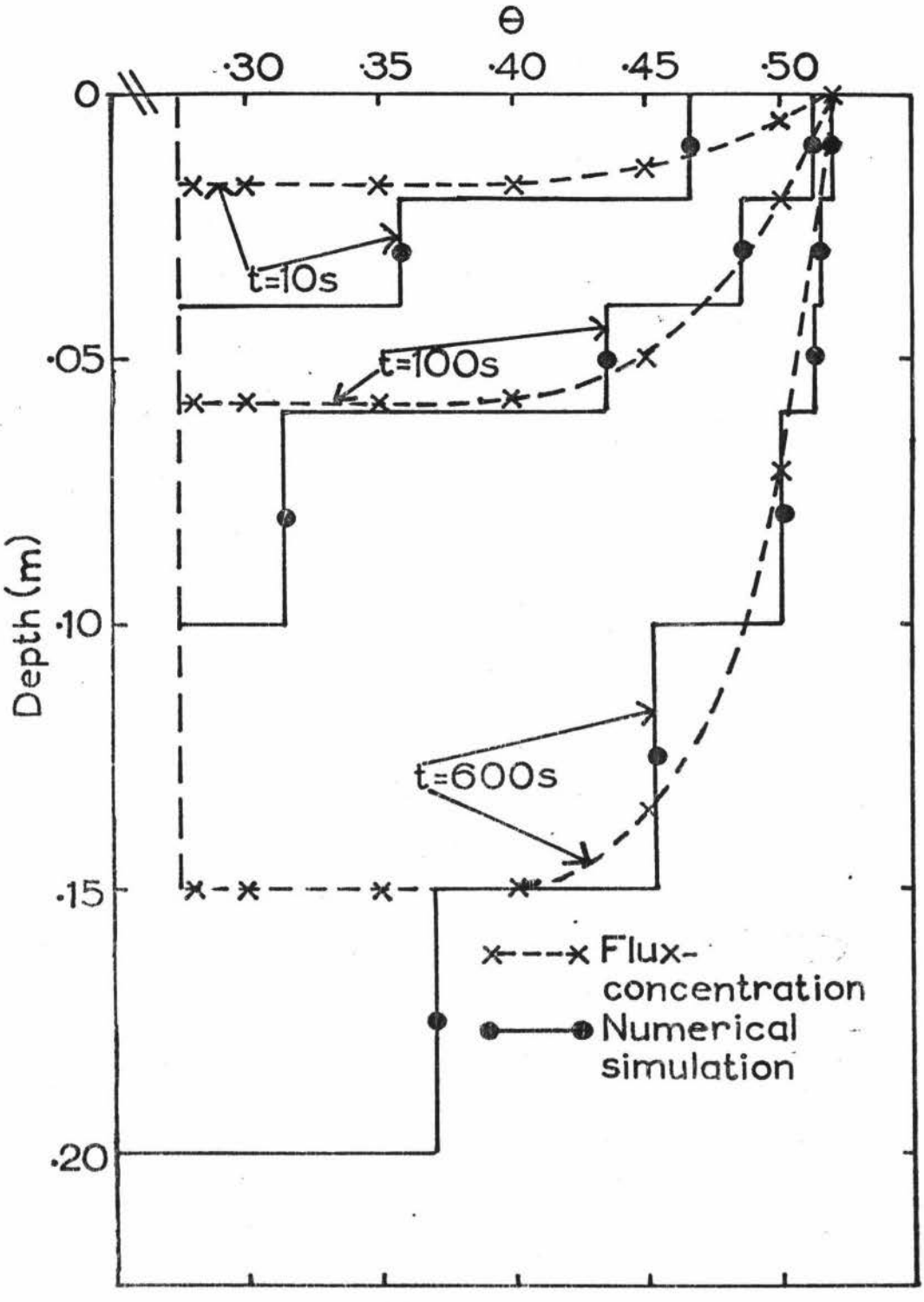

Fig.31 Simulated wetting fronts (θ against depth) calculated using flux-concentration and numerical methods at various times, t, during ponded (constant concentration) infiltration into Takapau sandy loam A horizon, which was at an initial pressure potential of -10 m.

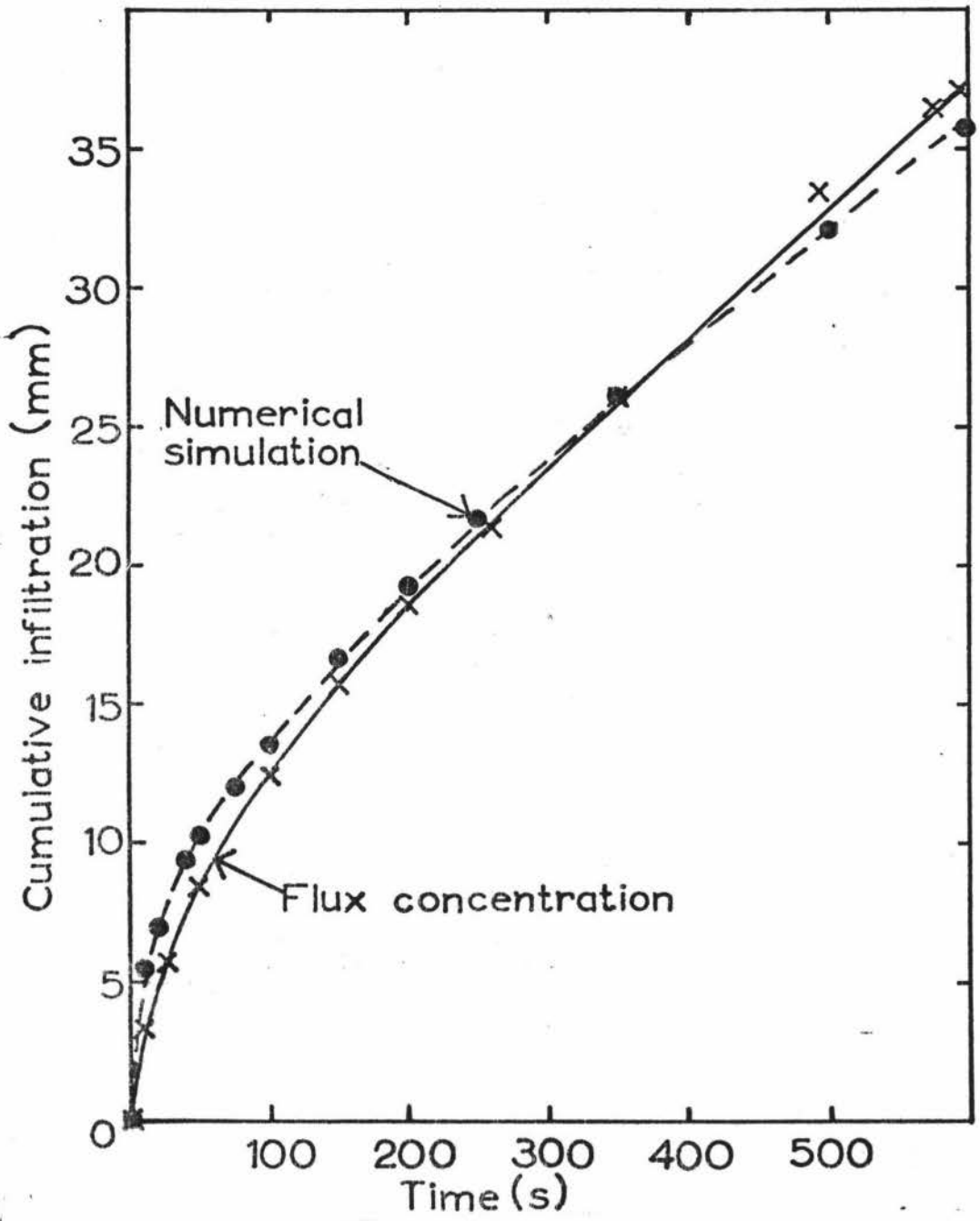

Fig.32 Cumulative infiltration against time for ponded (constant concentration) infiltration into the A horizon of Takapau sandy loam calculated with flux-concentration and numerical methods.

The recommended time for water to be available at the surface of the soil for infiltration with a border-dyke system for this soil is 70 minutes (Couling, pers. comm.). The end of the border nearest the intake will receive water for more than 70 minutes, and any high spots may receive water for less than 70 minutes. Infiltration was thus simulated for 40, 70 and 100 minutes i.e. 70±30 minutes, for initial pressure potentials of -10 m (Fig.33) and -154 m (Fig.34). Redistribution was then simulated with no evapotranspiration and also with a daily evapotranspiration rate of 5 mm day^{-1} (Figs.35,36, 37, 38, 39 and 40). The drainage rate with a constant daily evapotranspiration rate of 5 mm $day^{-1}$was the same after 3 days as that at 10 days with no evapotranspiration (Fig.41). The drainage rate in the field would probably lie somewhere between these two extremes.

The amount of water being lost to drainage during and following infiltration is quite substantial (Tables 4,5). If the soil is irrigated when the pressure potential reaches -10 m, then by using the border-dyke system greater than 50% of the water applied may be lost from the root zone of the soil (0.45 m). This value is similar to that found experimentally by Couling (pers. comm.) for the same rooting depth. If the soil is irrigated when the soil has dried out to a pressure potential of -154 m, then the amount lost to drainage following irrigation is less than 50% (Table 5).

These simulations indicate that if this soil is irrigated using the border-dyke method about 50% of the water applied would be lost from the root zone (top 0.45 m) to drainage. This would not only be a wasteful use of a scarce resource, but could lead to pollution of the aquifer under this area (Burden, 1979) with nitrates and other agricultural chemicals. Thus, a sprinkler system, where the application rate is less than the saturated hydraulic conductivity of the surface

Table 4: Simulated cumulative infiltration (I), drainage (DT) and percentage of cumulative infiltration occurring as drainage, during simulated ponded infiltration and redistribution of water in Takapau sandy loam, when the soil had an initial pressure potential of -10 m.

Infiltration			Redistribution			
Duration (minutes)	I (mm)	DI (mm)	ET=0, t= 10 days D (mm)	DT/I (%)	ET=5 mm day^{-1}, t=3 days D (mm)	DT/I (%)
40	96	0	39	41	25	26
70	154	19	78	63	64	54
100	211	76	78	73	64	66

DI is the cumulative drainage that occurs during infiltration
D is the cumulative drainage that occurs during redistribution
DT=DI+D, and is the total cumulative drainage (mm)
ET is the evapotranspiration rate
t is the time taken for the drainage rate to become small

Table 5: Simulated cumulative infiltration (I), drainage (DT) and percentage of cumulative infiltration occurring as drainage, during simulated ponded infiltration and redistribution of water in Takapau sandy loam, when the soil had an initial pressure potential of -154 m

Infiltration			Redistribution			
Duration (minutes)	I (mm)	DI (mm)	ET=0, t = 10 days D (mm)	DT/I (%)	ET=5 mm day^{-1}, t=3 days D (mm)	DT/I (%)
40	109	0	4	4	0	0
70	167	0	60	36	46	28
100	224	40	78	53	64	46

DI is the cumulative drainage that occurs during infiltration
D is the cumulative drainage that occurs during redistribution
DT = DI +D, and is the total cumulative drainage (mm)
ET is the evapotranspiration rate
t is the time taken for the drainage rate to become small

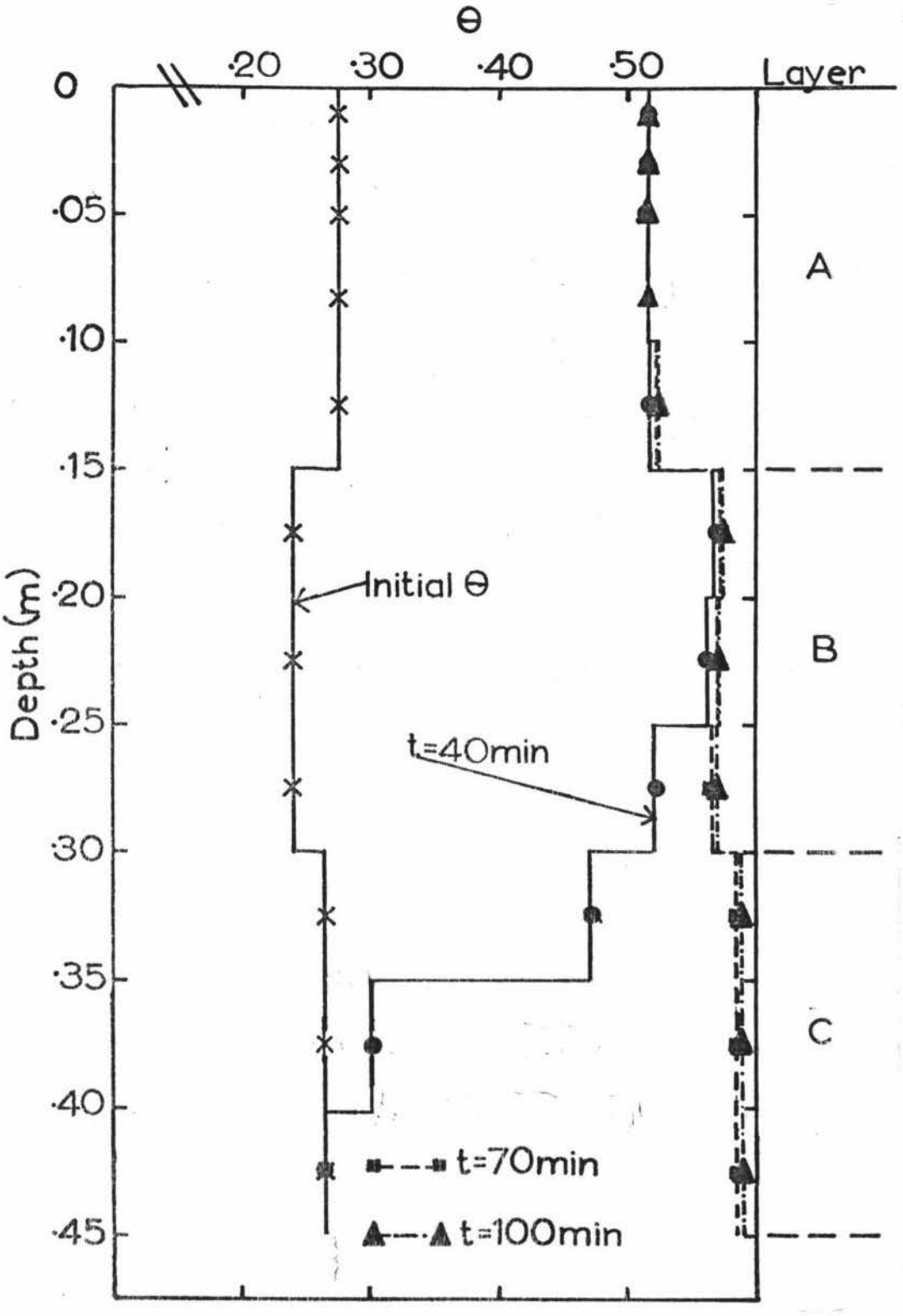

Fig.33 Volumetric water content (θ) profiles at various times (t), during simulated ponded infiltration of water into Takapau sandy loam, which had an initial θ corresponding to a pressure potential of -10 m.

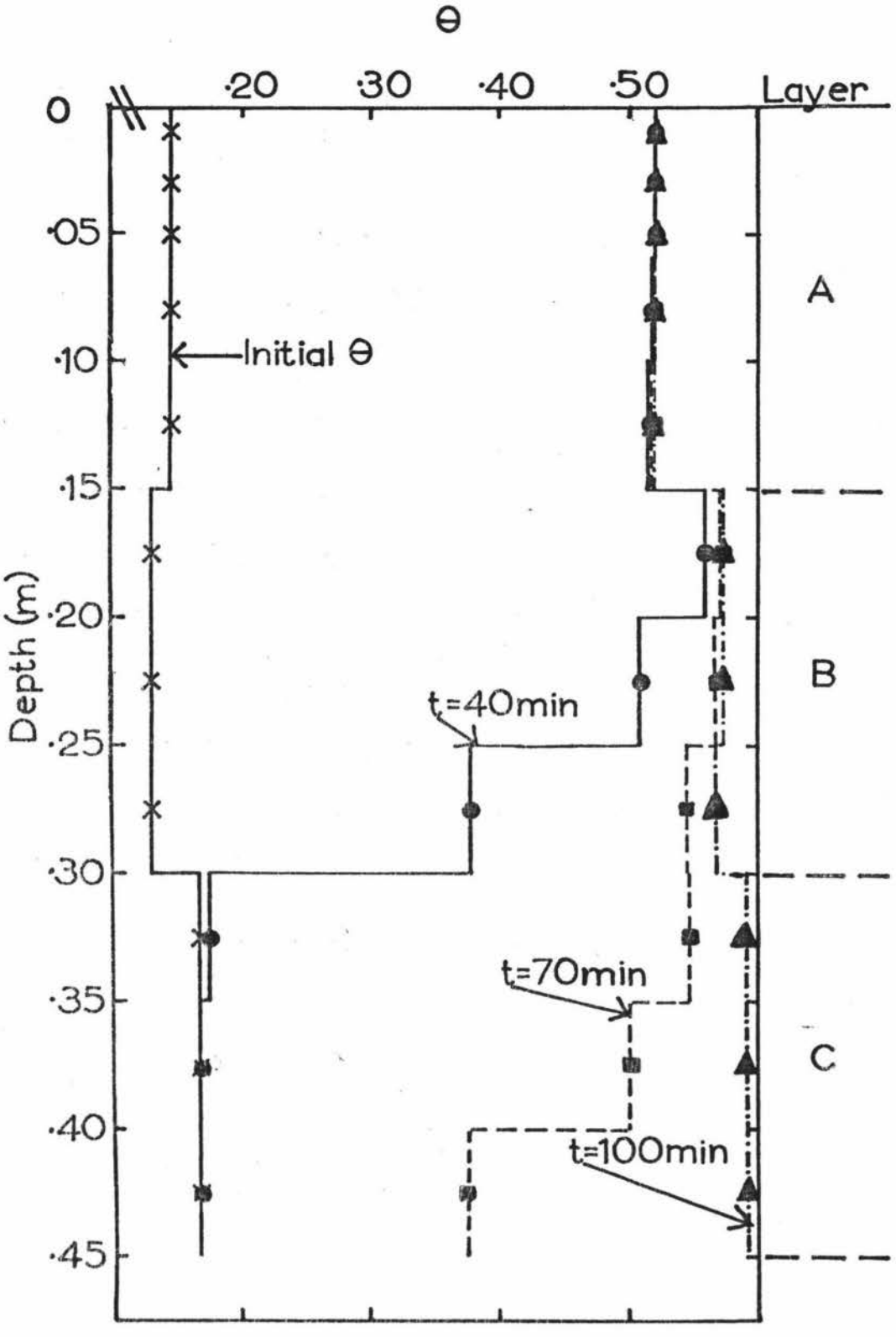

Fig.34 Volumetric water content profiles at various times (t), during simulated ponded infiltration of water into Takapau sandy loam, which had an initial θ corresponding to a pressure potential of -154 m.

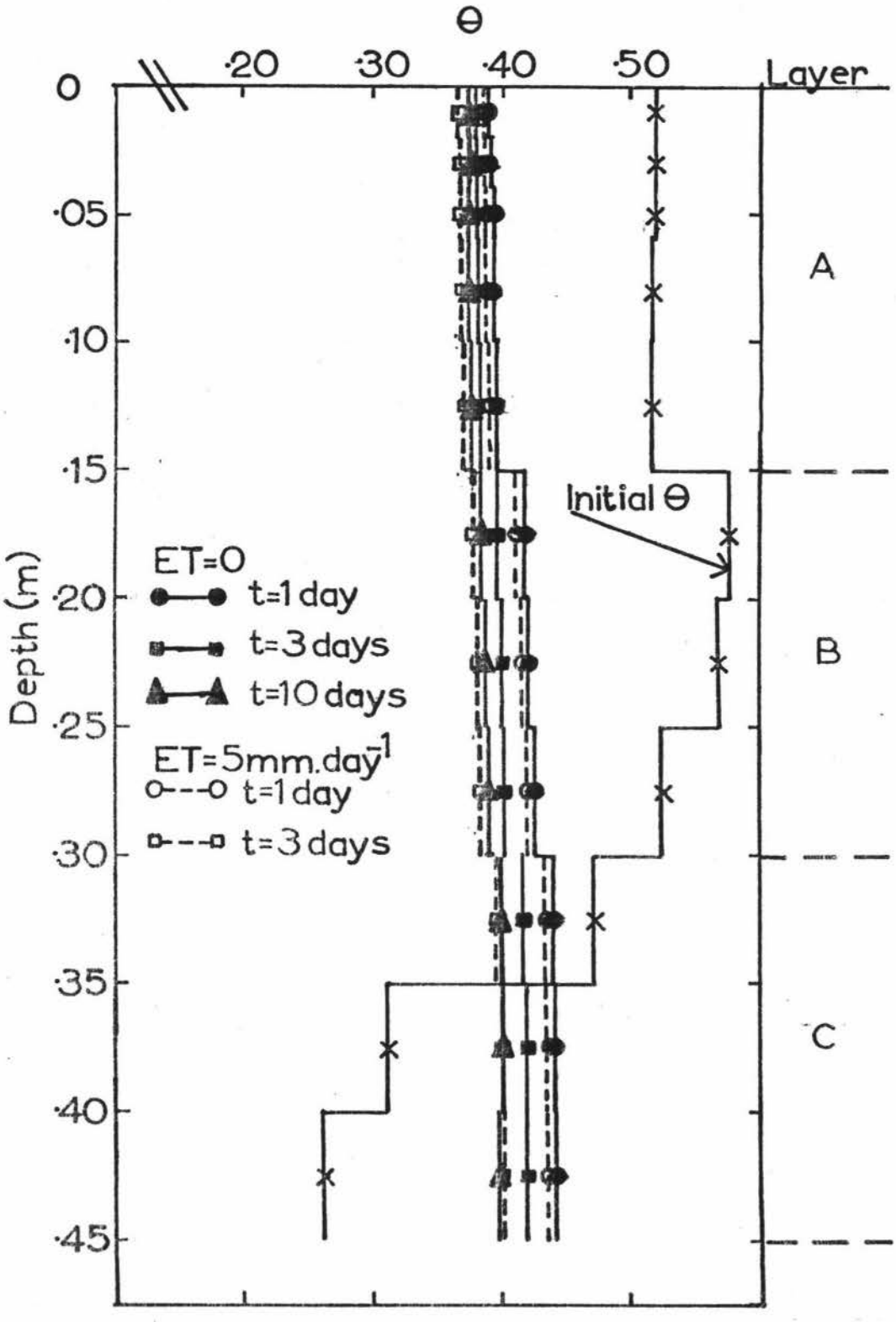

Fig 35. Simulated redistribution of water within the soil profile of Takapau sandy loam, with no evapotranspiration (ET) and with ET=5 mm day^{-1}. The initial θ profile was that obtained following simulated ponded infiltration of water into this soil, initially at a pressure potential of -10 m, for 40 minutes.

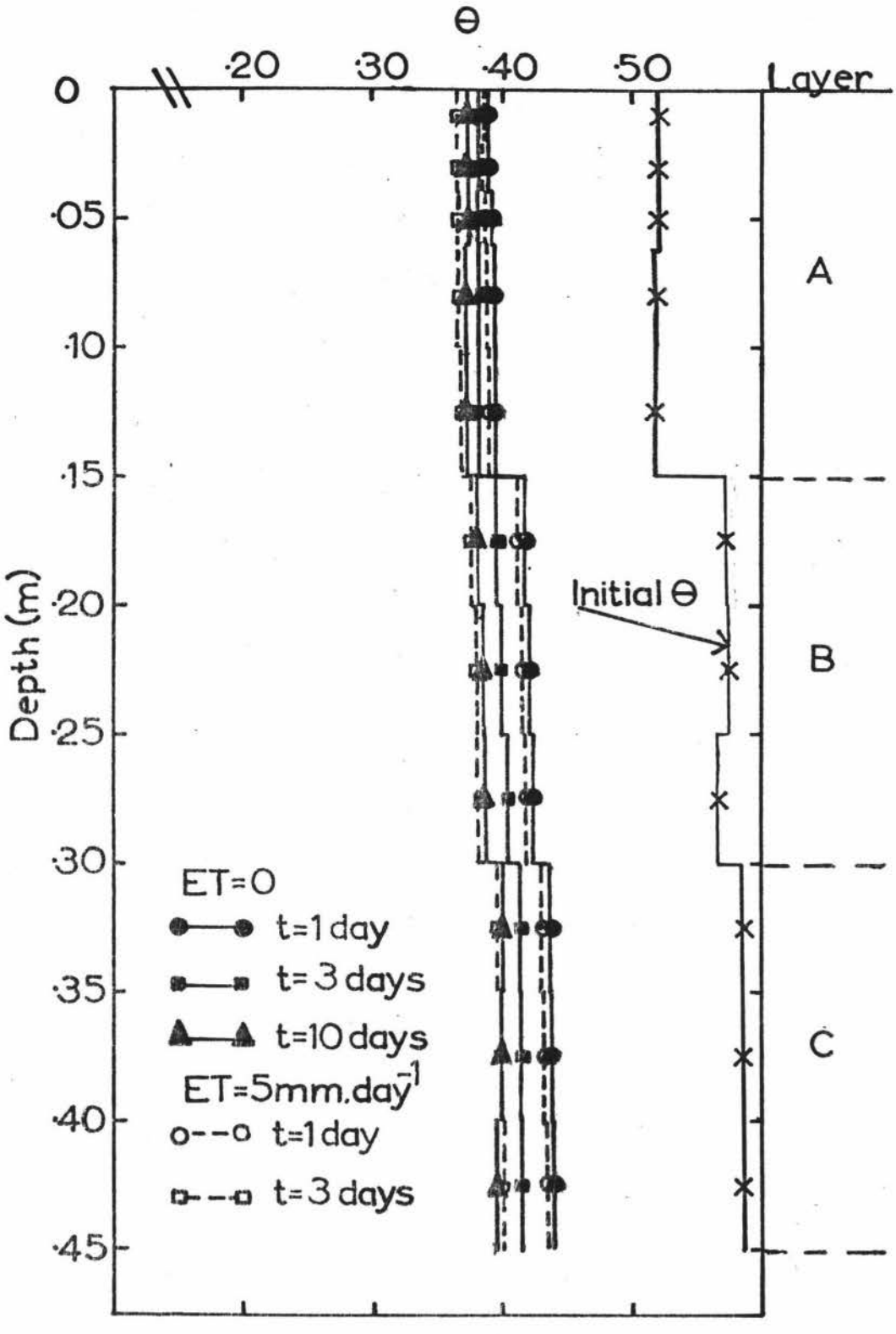

Fig.36 Simulated redistribution of water within the soil profile of Takapau sandy loam with no evapotranspiration (ET) and with ET=5 mm day^{-1}. The initial θ profile was that obtained following simulated ponded infiltration of water into this soil, initially at a pressure potential of -10 m, for 70 minutes.

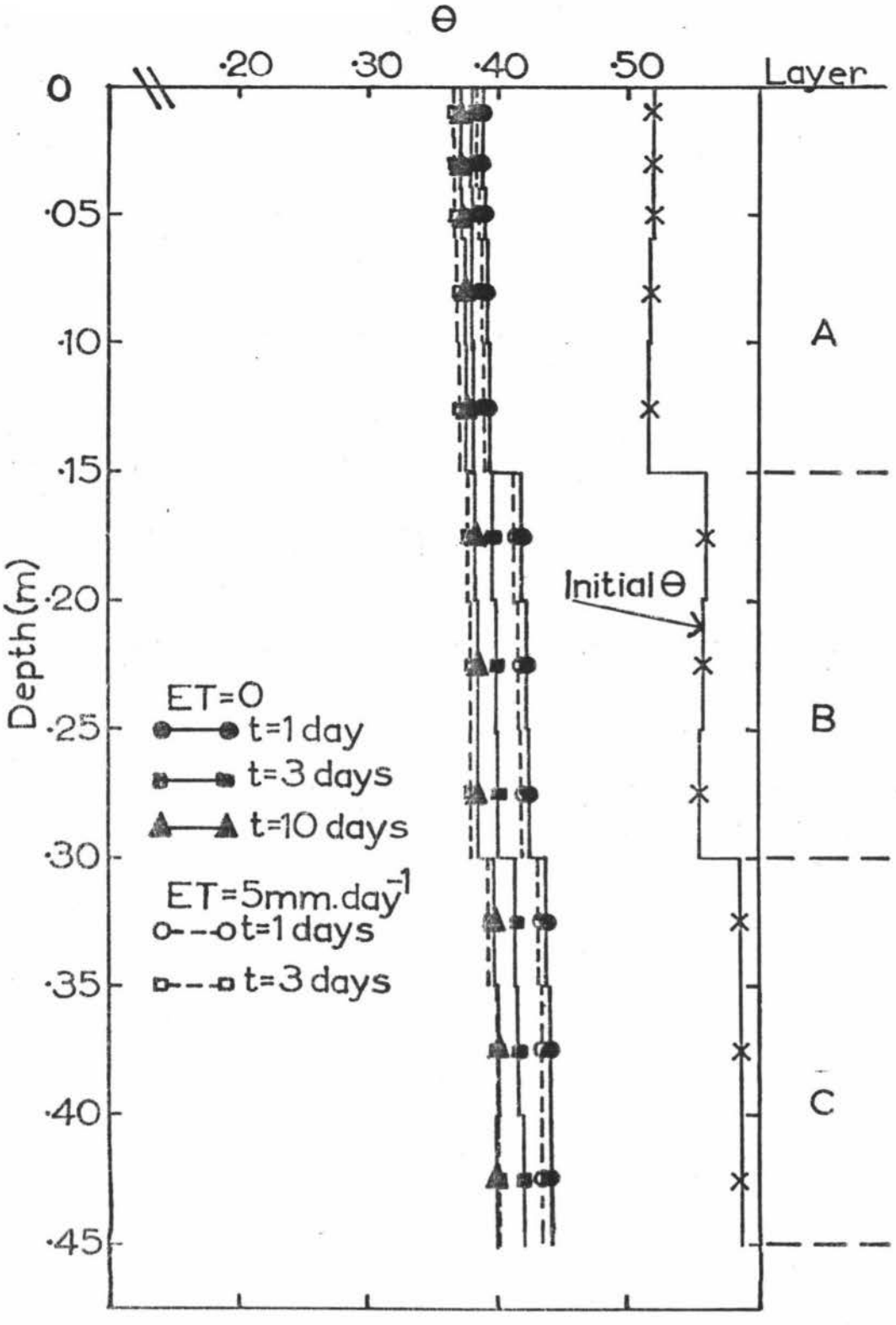

Fig.37 Simulated redistribution of water within the soil profile of Takapau sandy loam with no evapotranspiration (ET) and with ET=5 mm day^{-1}. The initial θ profile was that obtained following simulated ponded infiltration of water into this soil, initially at a pressure potential of -10 m, for 100 minutes.

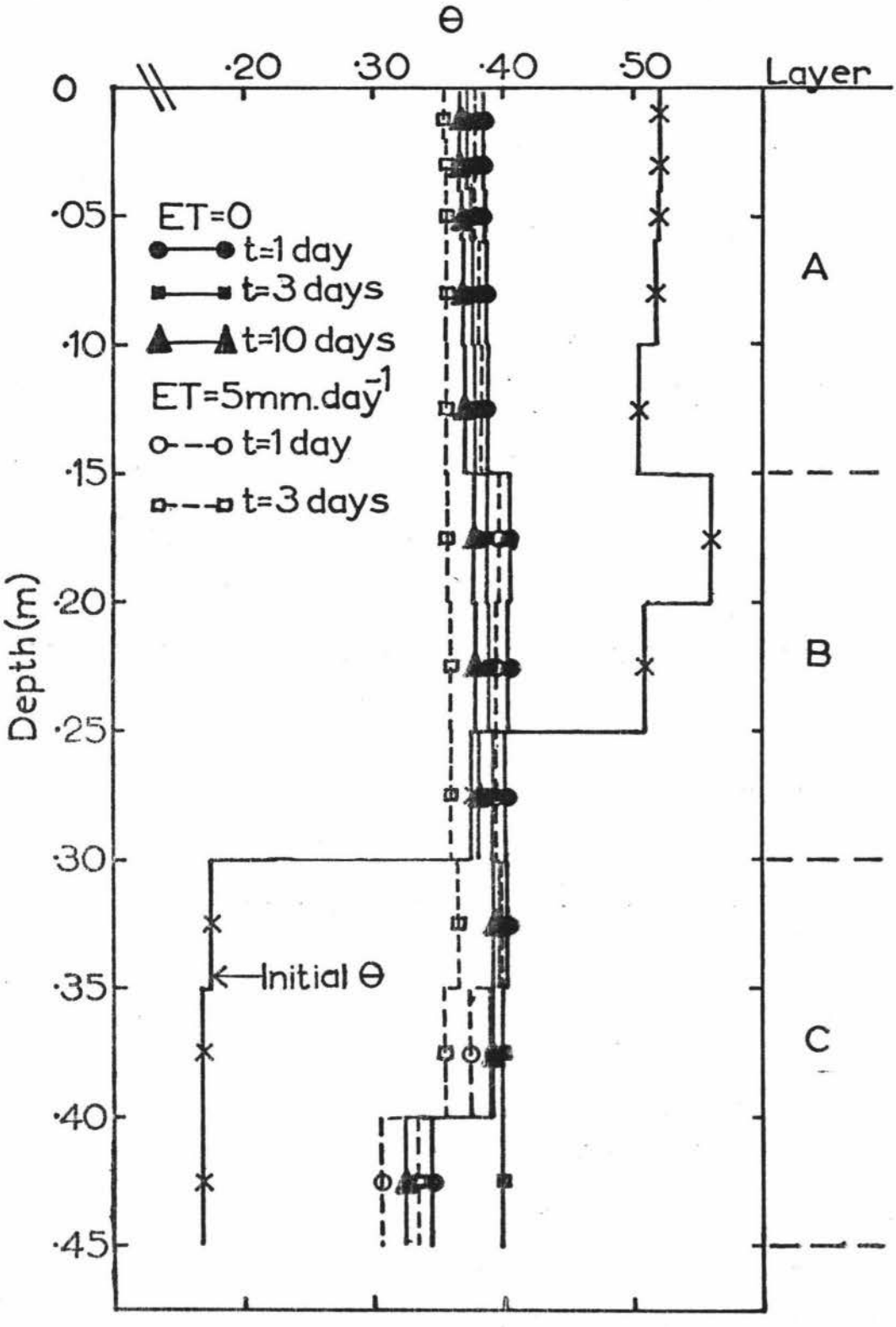

Fig.38 Simulated redistribution of water within the soil profile of Takapau sandy loam with no evapotranspiration (ET) and with ET=5 mm day^{-1}. The initial θ profile was that obtained following simulated ponded infiltration of water into this soil, initially at a pressure potential of -154, for 40 minutes.

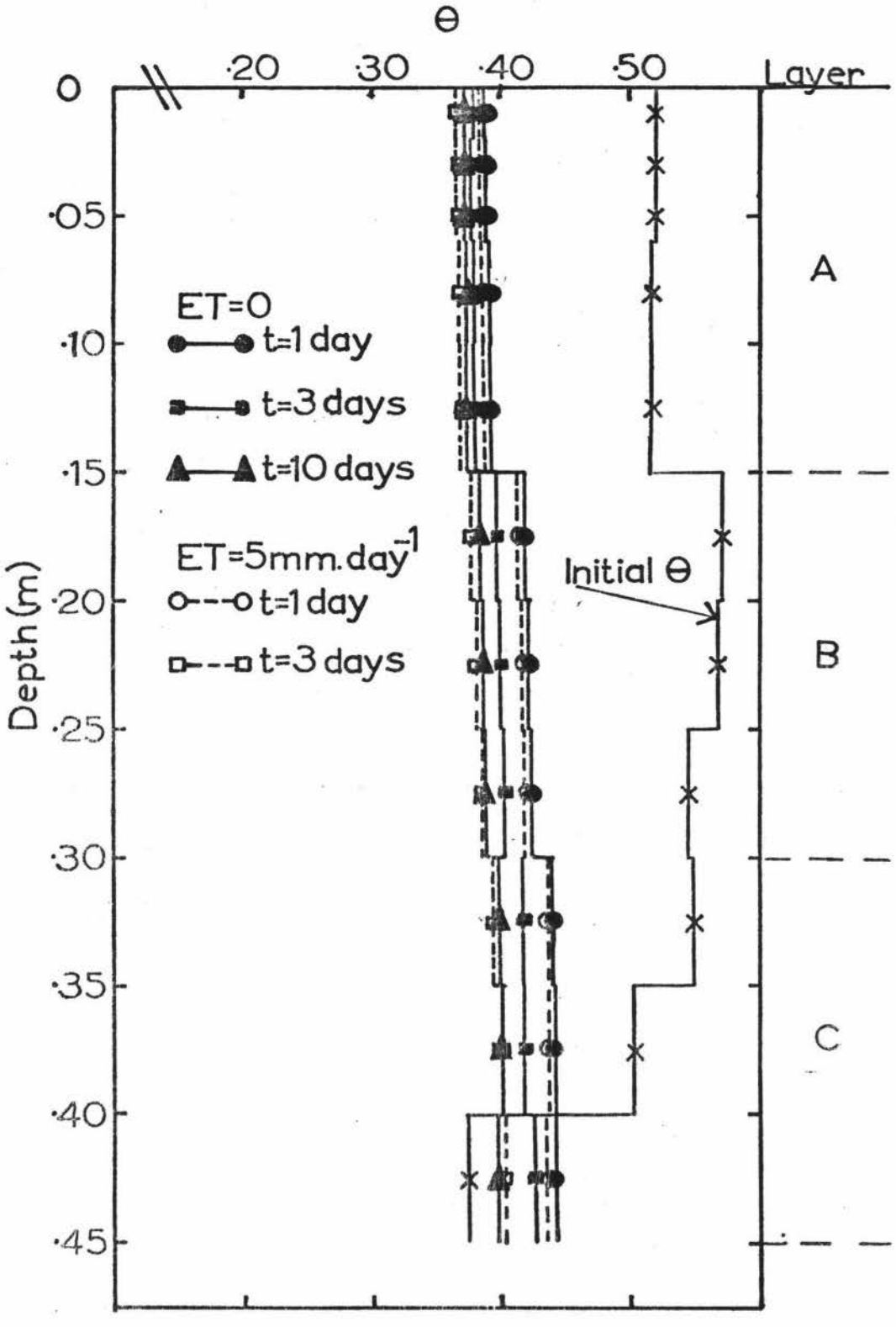

Fig.39 Simulated redistribution of water within the soil profile of Takapau sandy loam with no evapotranspiration (ET) and with ET=5 mm day^{-1}. The initial θ profile was that obtained following simulated ponded infiltration of water into this soil, initially at a pressure potential of -154 m, for 70 minutes.

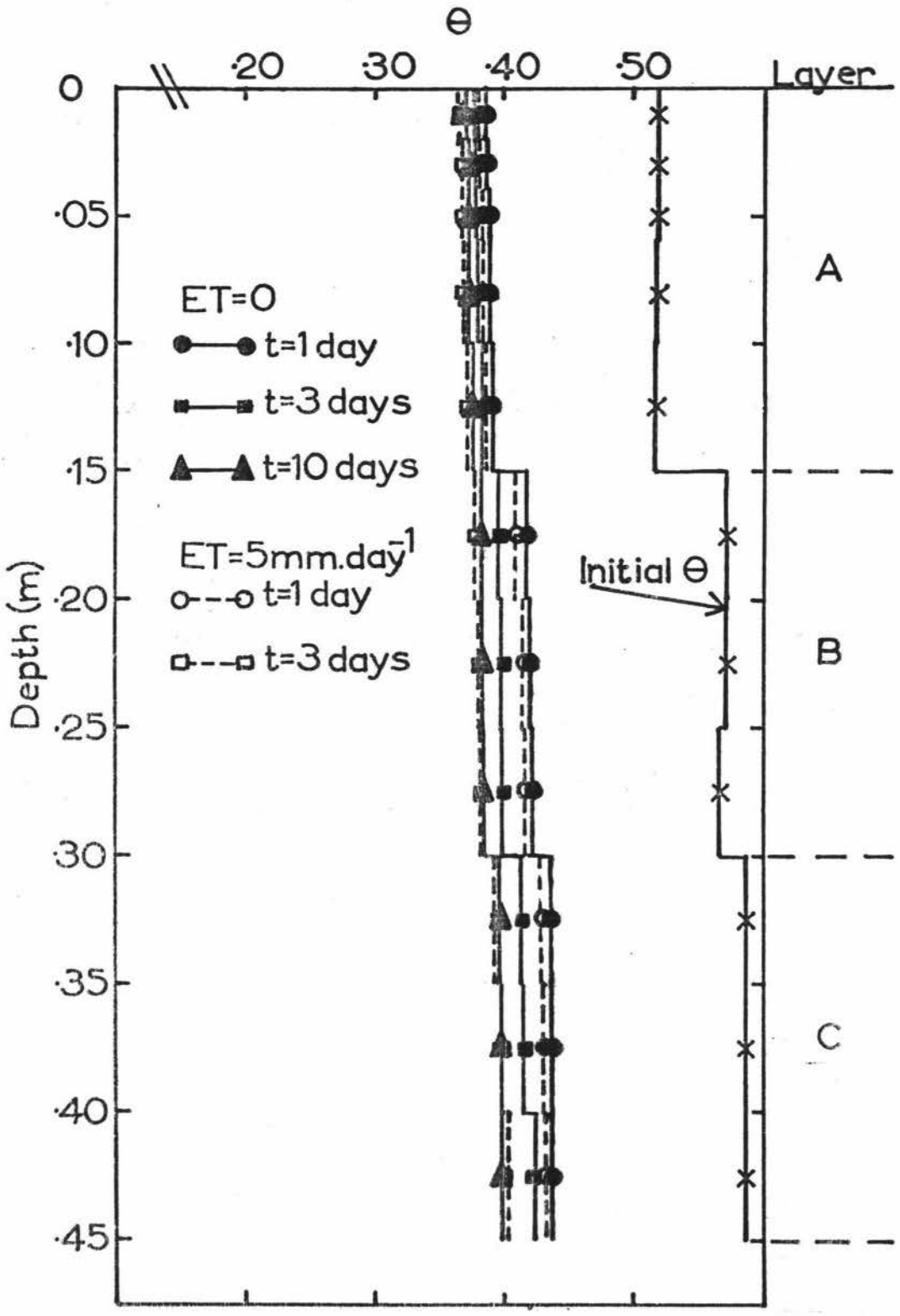

Fig.40 Simulated redistribution of water within the soil profile of Takapau sandy loam with no evapotranspiration (ET) and with ET=5 mm day^{-1}. The initial θ was that obtained following simulated ponded infiltration of water into this soil, initially at a pressure potential of -154 m, for 100 minutes.

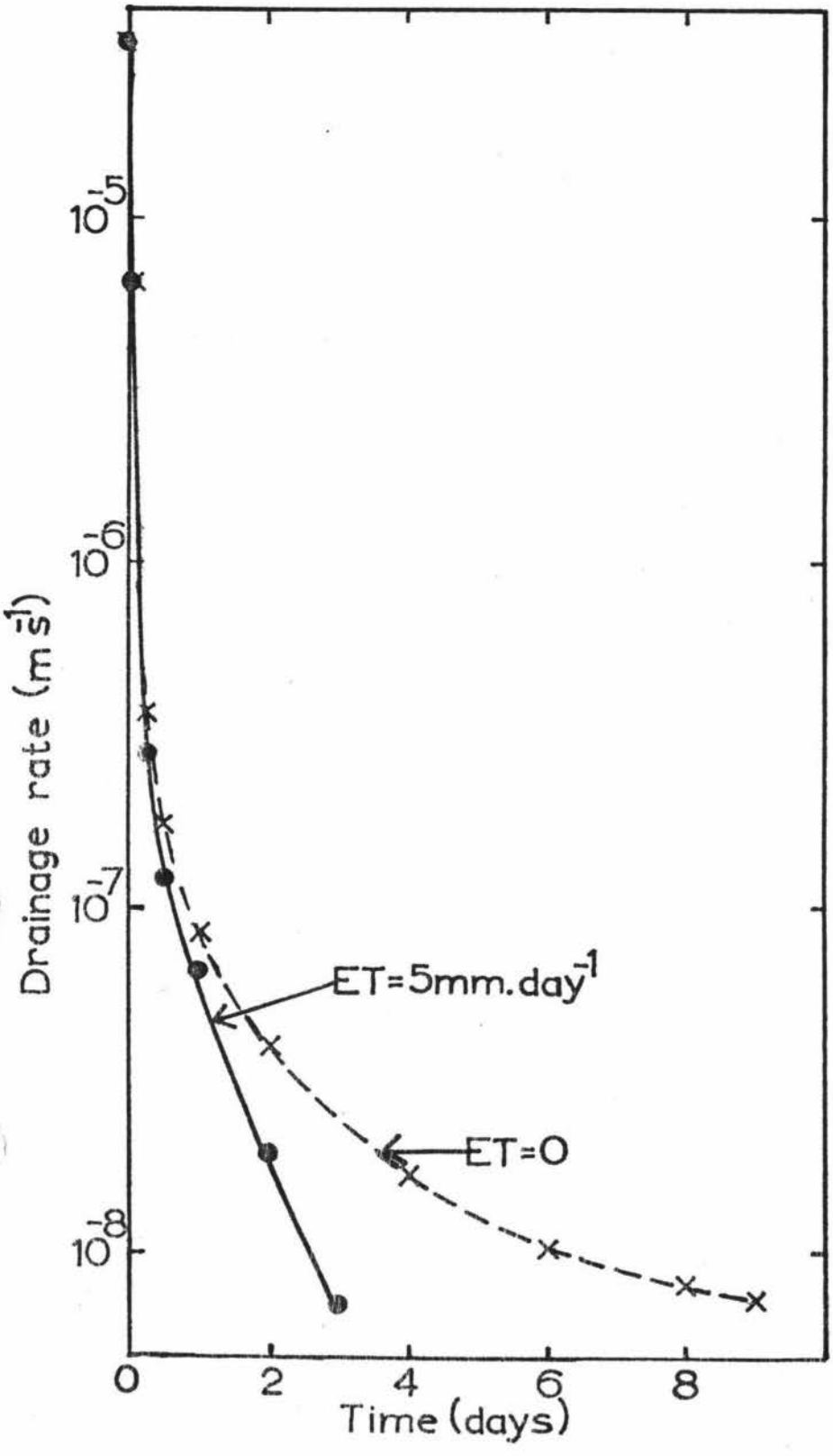

Fig.41 Simulated drainage rate against time for Takapau sandy loam, with no evapotranspiration (ET) and a constant daily rate, following simulated ponded infiltration into this, initially at a pressure potential of -10 m, for 100 minutes.

(100 mm hr^{-1}), would be preferable for irrigating this soil.

3.4 Pakowhai Silt Loam

Pakowhai silt loam is a soil consisting of many layers* of alluvial silt and sand underlain by a thick layer of pumiceous sand at approximately 1 m (Appendix I). The effect of this pumice layer on the drainage of this soil compared to the coarse layers in the Ngatarawa and Takapau sandy loams was of interest, as well as the hydraulic conductivity data.

Pakowhai silt loam has no stones or cemented layers to restrict the installation of the tensiometers, so pressure potentials were able to be measured down to a depth of 1.95 m (Figs. 42,43). During wetting this soil, like the Ngatarawa and Takapau sandy loams, could not be saturated. The tensiometers at depths of 1.36 m and 1.56 m in plot 017 indicated saturated conditions (Fig.42), but as the tensiometers above and below these, and those in the same horizon of plot 018, recorded negative pressure potentials, this may have been due to water reaching the tensiometer tip by moving down the side of the tensiometer access tube, or a soil fissure created during installation.

The pressure potential gradient during drainage was usually greater than or equal to zero, thus a large number of data points relating hydraulic conductivity and volumetric water content were obtained. Data on relationships between $\log_{10}k$ and θ from the duplicate plots for each layer agree quite well (Figs. 44,45,46,47). No hydraulic conductivity data were obtained for the A layer of plot 018 due to no tensiometer being placed at the bottom of the A layer. The poorest agreement is in the pumice layers (G,H and I), which is probably due to the shape of the volumetric water content/pressure potential relationship, as θ has a value of 0.656 for pressure potentials from -0.01 m to -0.20 m (Fig.49b).

---

* Layers are referred to instead of horizons, as horizon designations were not given in the soil description (Appendix I).

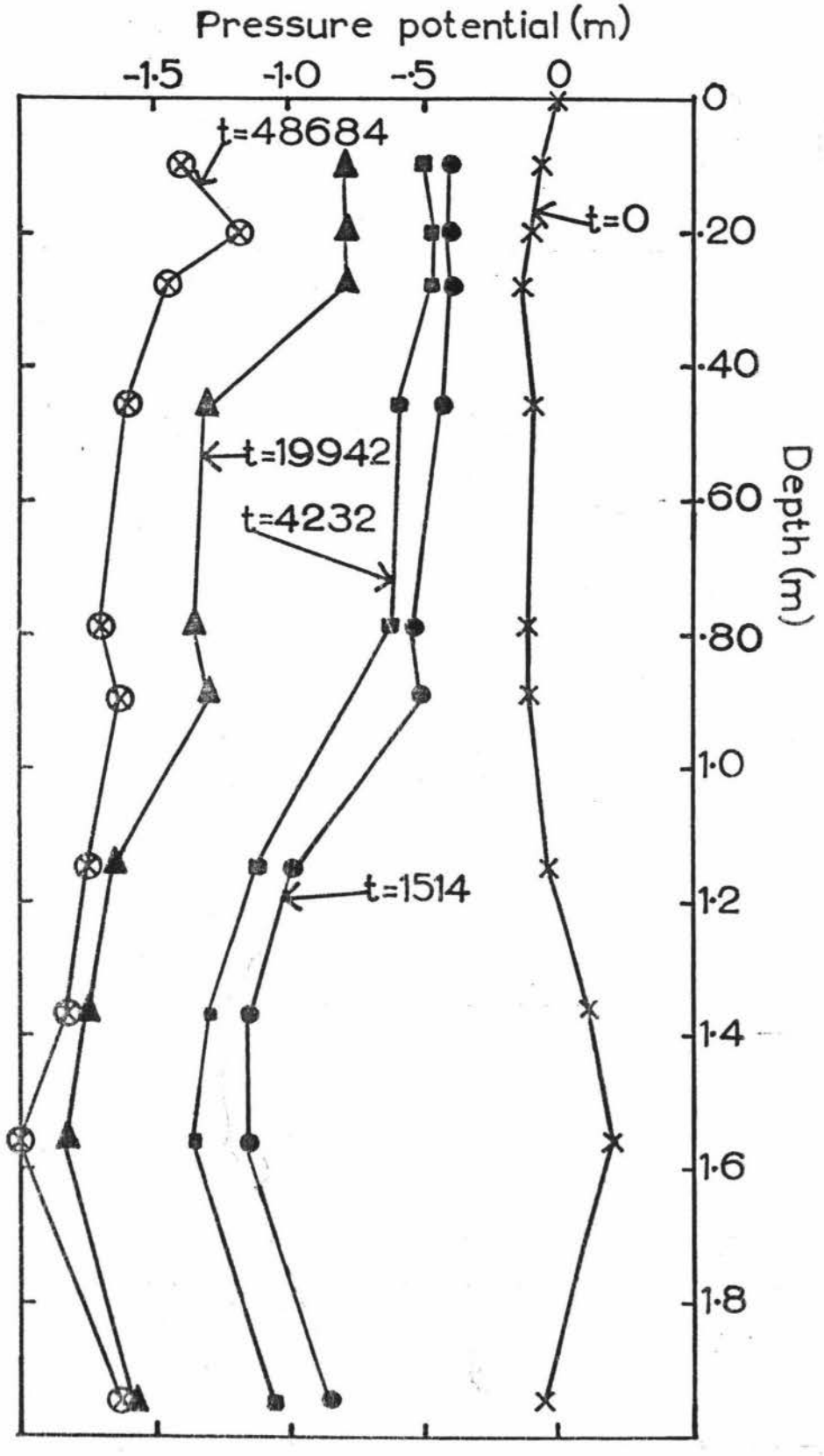

Fig.42 Pressure potential profiles at various times, t (minutes) during drainage of plot 017 of Pakowhai silt loam.

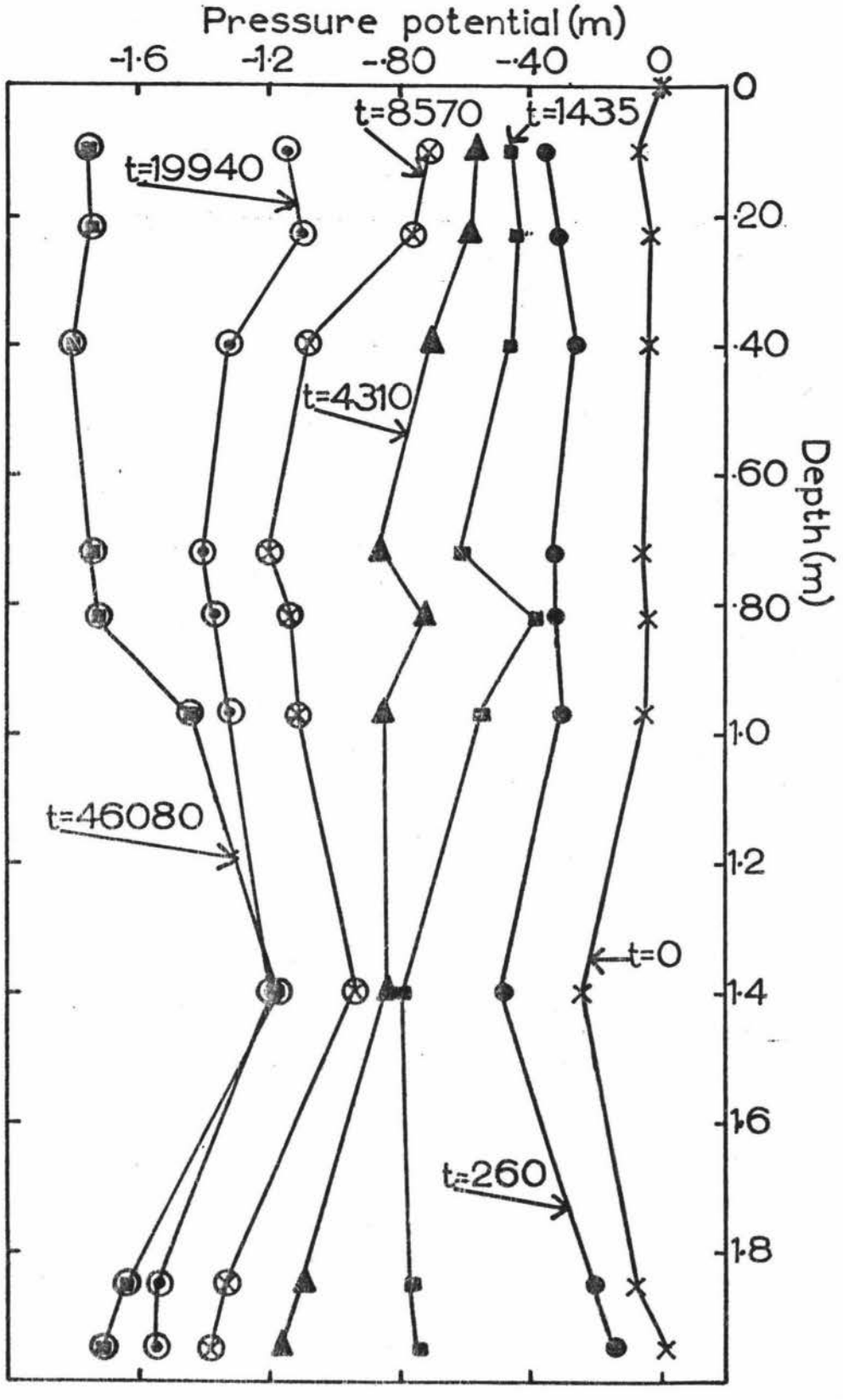

Fig.43 Pressure potential profiles at various times, t (minutes) during drainage of plot 018 of Pakowhai silt loam.

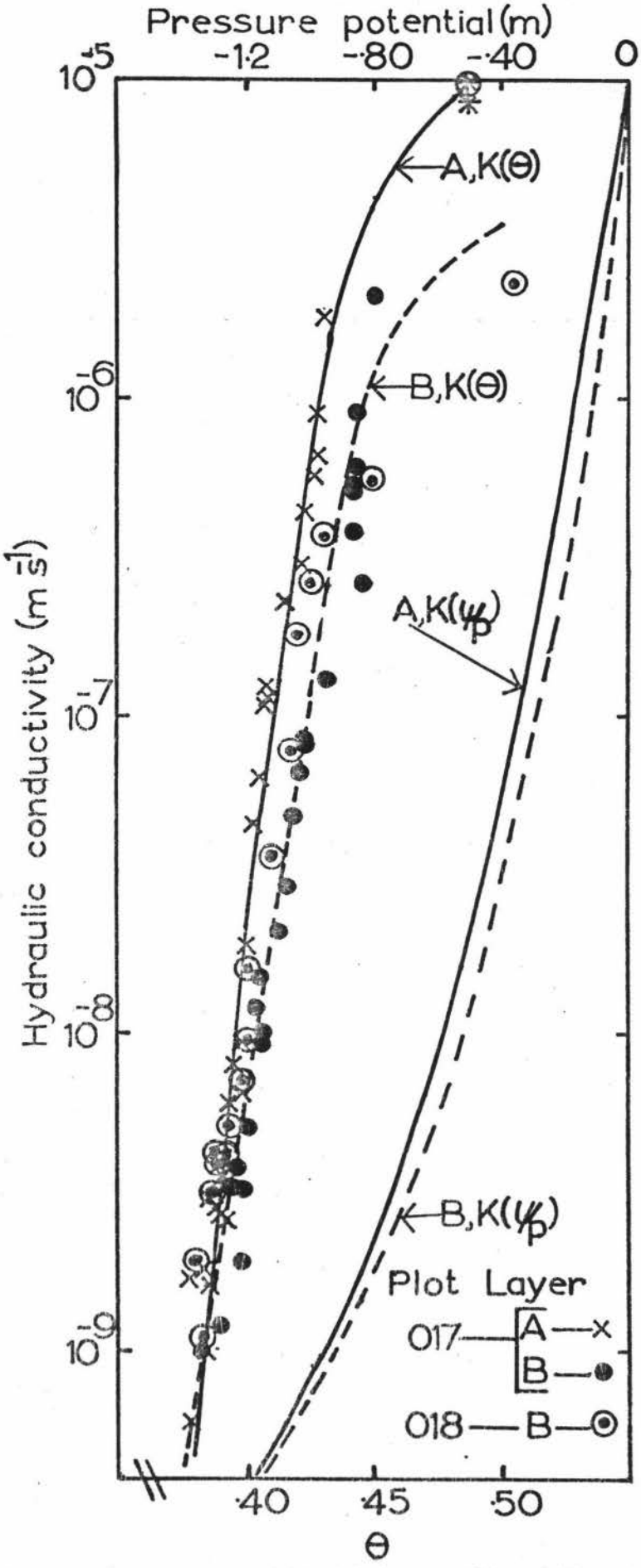

Fig.44 Hydraulic conductivity against volumetric water content (k(Θ)), and pressure potential (k (ψ_p)), for the A and B layers of Pakowhai silt loam. The final infiltration rate (✱ and ⊛) are also plotted.

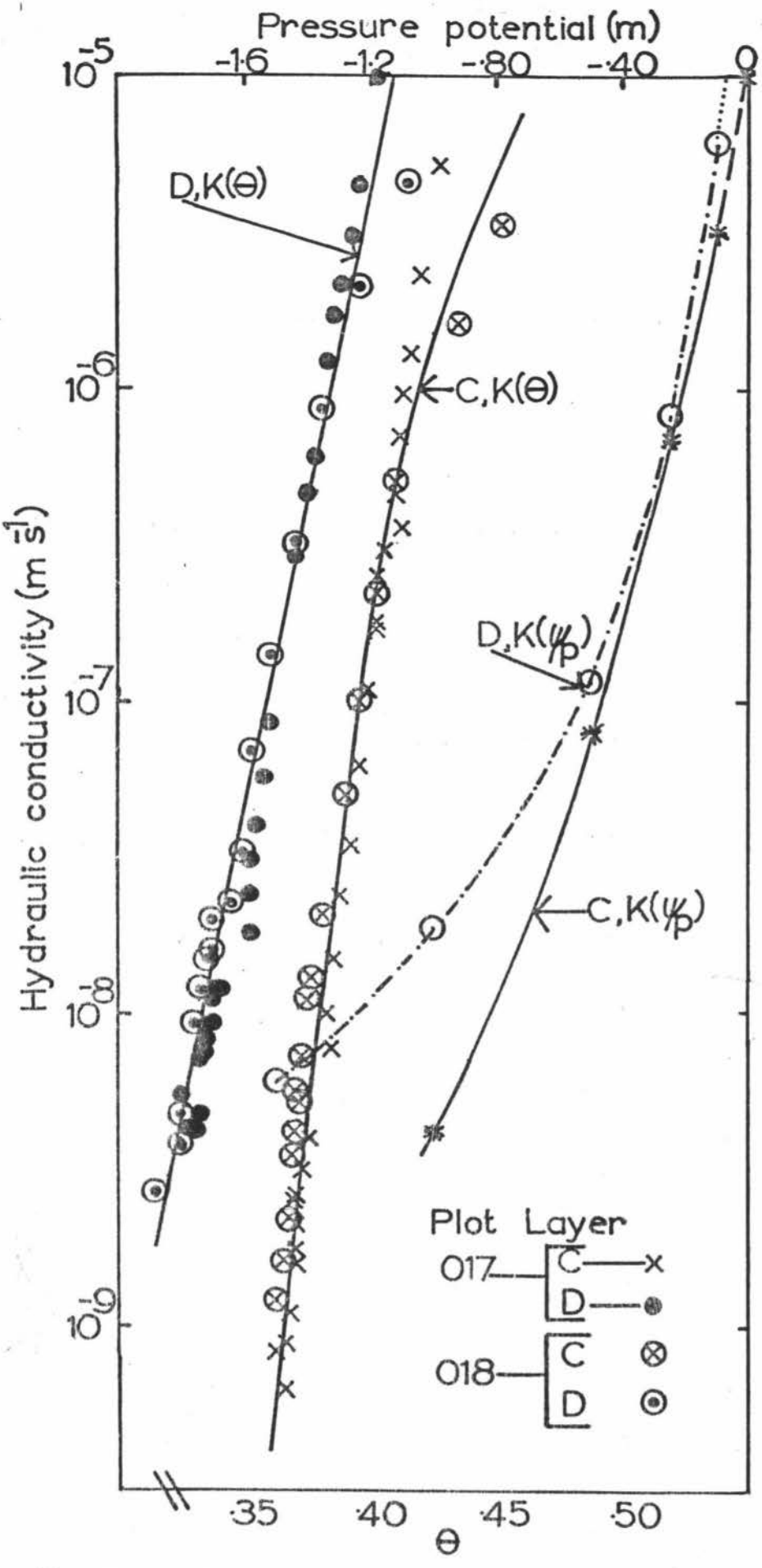

Fig.45 Hydraulic conductivity against volumetric water content ($k(\theta)$), and pressure potential ($k(\psi_p)$), for the C and D layers of Pakowhai silt loam.

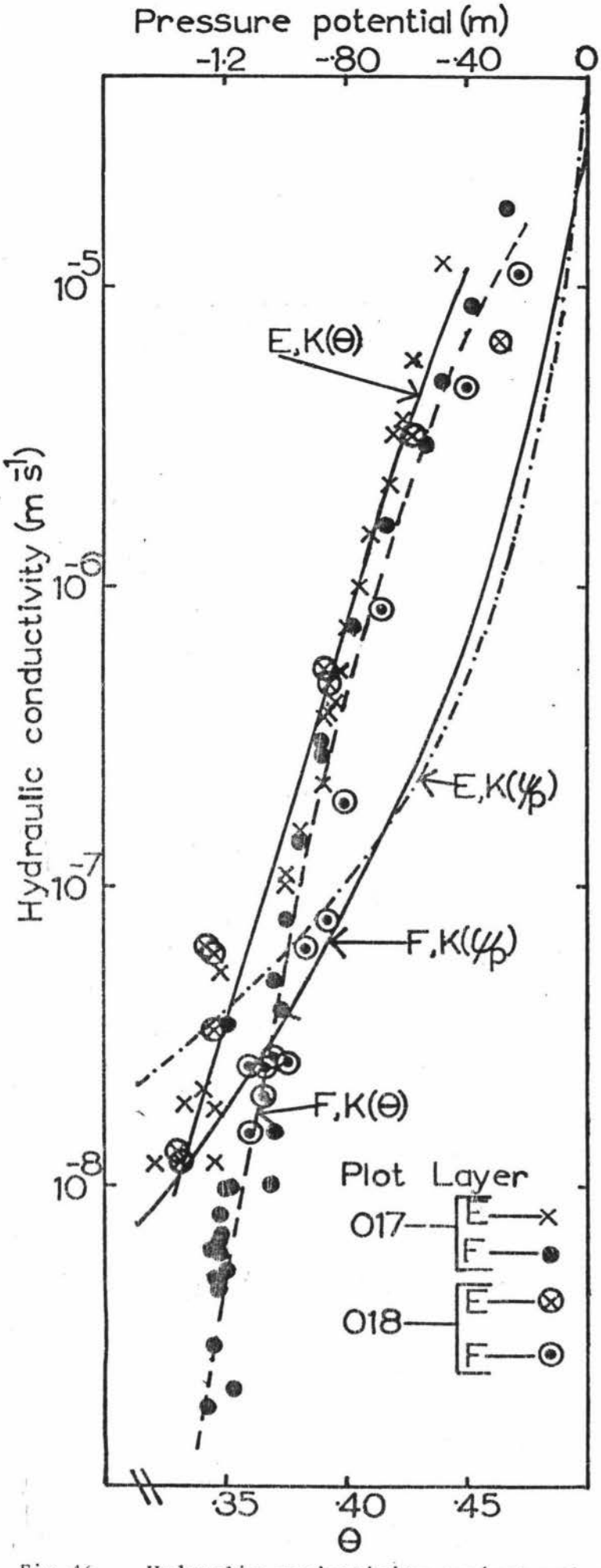

Fig.46 Hydraulic conductivity against volumetric water content ($k(\theta)$), and pressure potential ($k(\psi_p)$), for the E and F layers of Pakowhai silt loam.

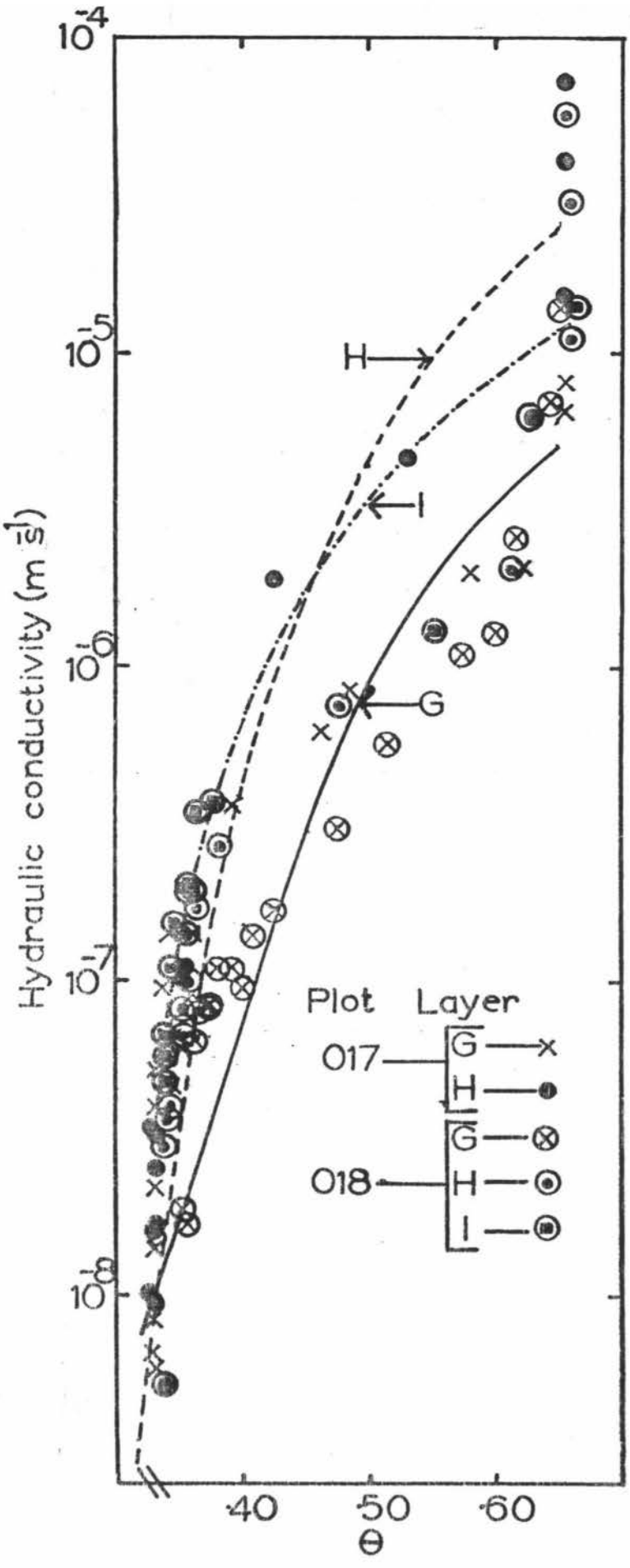

Fig.47 Hydraulic conductivity against volumetric water content for the G, H and I layers of Pakowhai silt loam. The lines drawn are quadratic regressions of $\log_{10}k$ on θ.

This causes quite a bit of scatter in the $\log_{10}k/\Theta$ data (Fig.47) of these layers. The D layer is considered to consist of one homogeneous soil material, based on earlier soil sampling, but actually consists of many thin bands of sandy loam and medium sand.

Gardner (1960) considered "field capacity" to occur when the drainage rate becomes small (1 mm day^{-1}, which is approximately $1x10^{-8}$m s^{-1}). Using the relationships between the volumetric water content and the pressure potential (Fig.49a,49b) and the $\log_{10}k/\Theta$ regressions, the relationships between $\log_{10}k$ and pressure potential were obtained (Figs.44,45,46,48). From these $\log_{10}k$/pressure potential data the pressure potentials when the hydraulic conductivity equalled $1x10^{-8}$ m s^{-1} were found and compared with the pressure potentials of the layers after 3 days of drainage (Table 6). The comparison is reasonably good for the A,B and C layers, but not as good for the lower layers where the pressure potentials were greater than the pressure potential when the hydraulic conductivity is equal to $1x10^{-8}$m s^{-1}. This indicates that these lower layers have not reached "field capacity". This is also indicated by the drainage rate from the soil above 1.95 m, which was 2 to 6 mm day^{-1} for the next 10 days, decreasing to 1 mm day^{-1} or less after this. Thus "field capacity" in this soil is not reached until after 14 days of drainage. The pressure potential in the soil decreased for up to 34 days after the start of drainage (Figs.42,43), but the amount of water lost after 14 days was small.

The AWC was calculated using values of "field capacity" after 3 days and 14 days of drainage and estimated using the volumetric water content when the pressure potential equalled -0.5 m, -1.0 m and -2.0 m (Table 7). The AWC measured, assuming the profile was at "field capacity" after 3 days of drainage, would overestimate the AWC by 20 to 25 mm, when compared with the AWC calculated when

Table 6: Pressure potentials (ψ_p) at which hydraulic conductivity is $1x10^{-8}$m s^{-1} compared with the pressure potentials found after 3 days of drainage for layers of Pakowhai silt loam

Layer	ψ_p, when k = $1x10^{-8}$m s^{-1}(m)	ψ_p after 3 days of drainage (m) Plot 017	Plot 018
A	-0.59	-0.49	-0.57
B	-0.53	-0.48	-0.60
C	-0.82	-0.59	-0.72
D	-1.24	-0.62	-0.86
E	less than -1.50	-0.52	-0.72
F	less than -2.00	-1.12	-0.85
G	less than -2.00	-1.31	-0.85
H	less than -2.00	-1.35	-1.11
I	less than -2.00	-1.06	-1.17

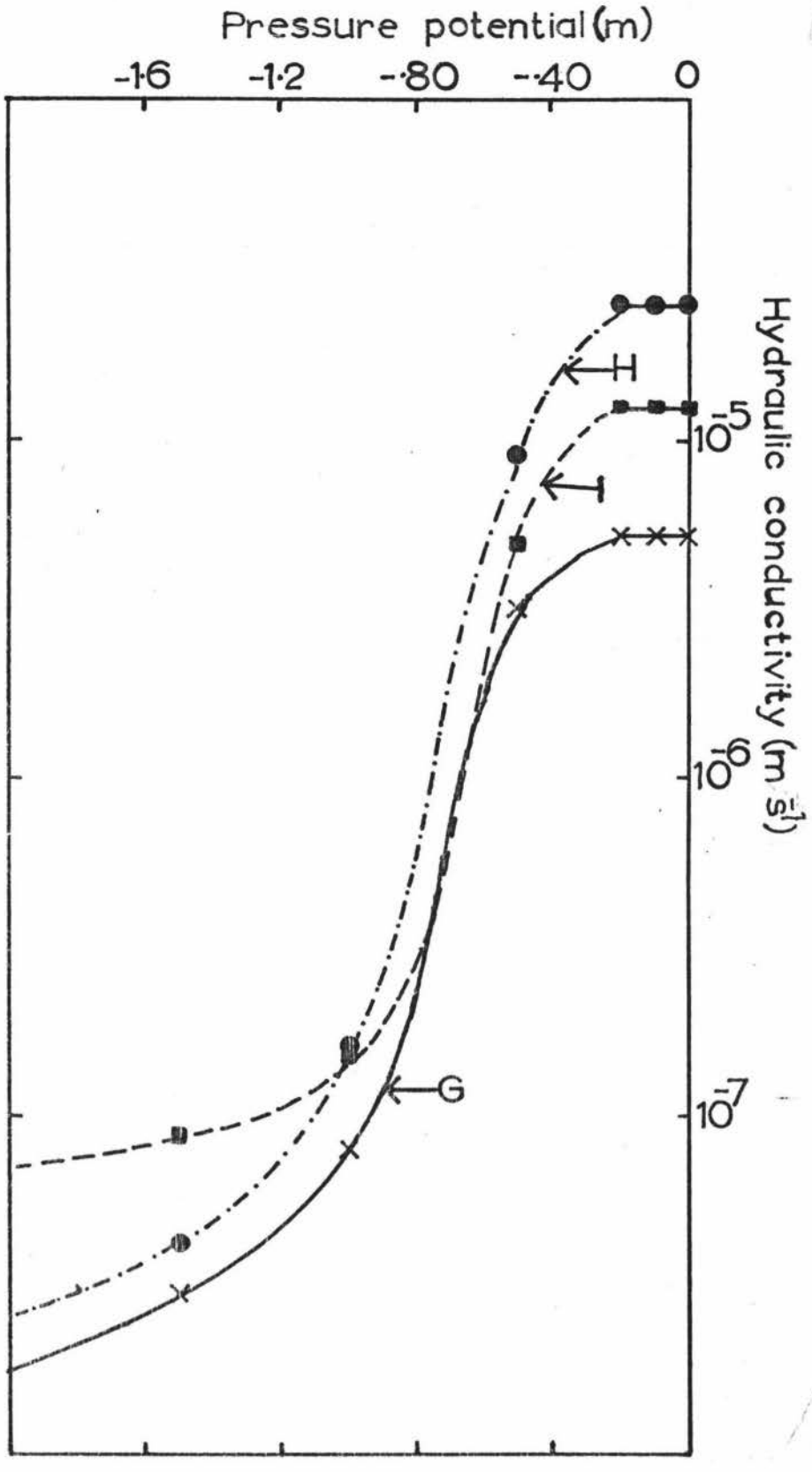

Fig.48 Hydraulic conductivity against pressure potential for the G, H and I layers of Pakowhai silt loam.

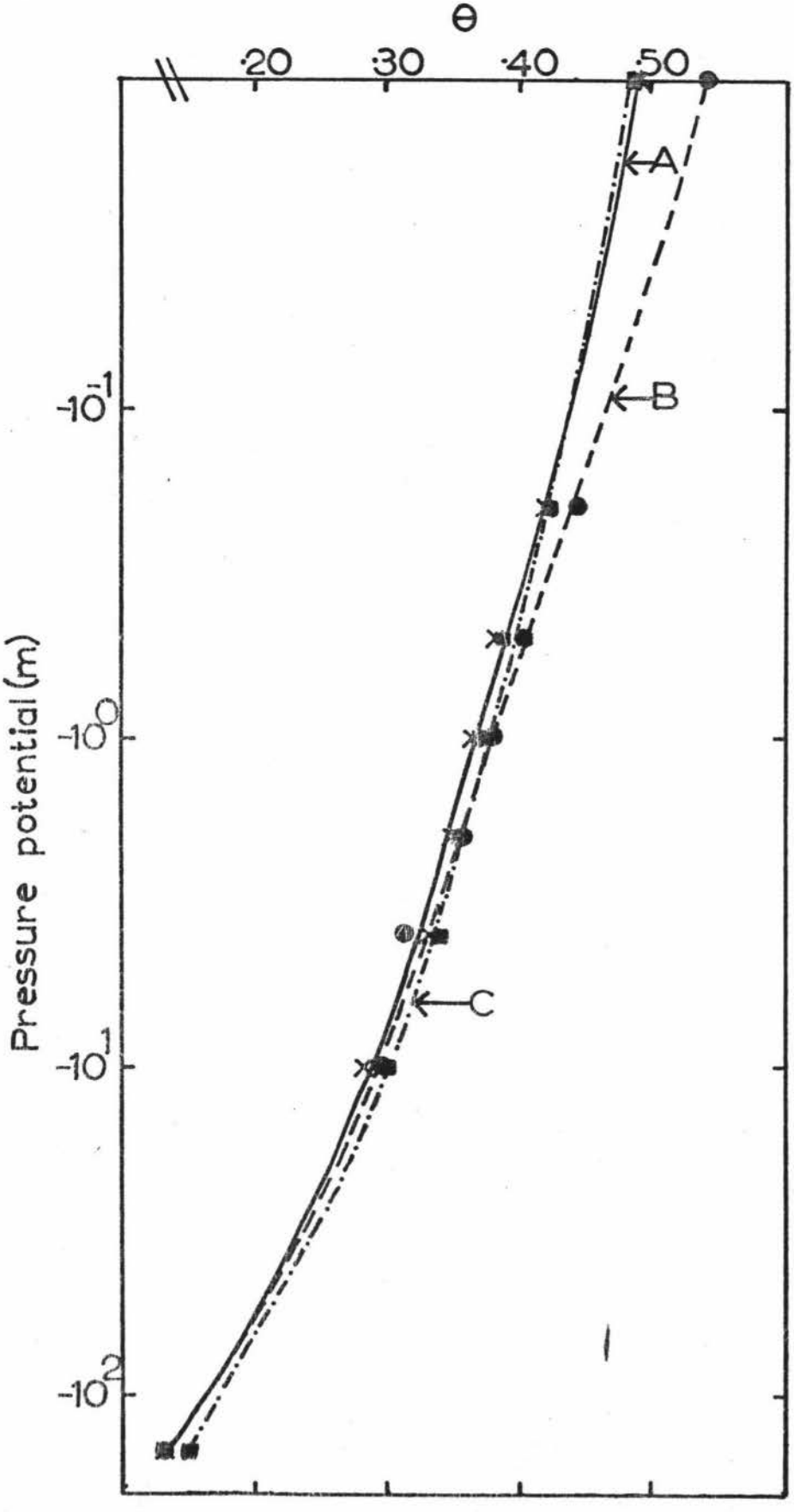

Fig.49a Volumetric water content against pressure potential for A(×), B(●) and C(■) layers of Pakowhai silt loam. The lines are fitted by eye.

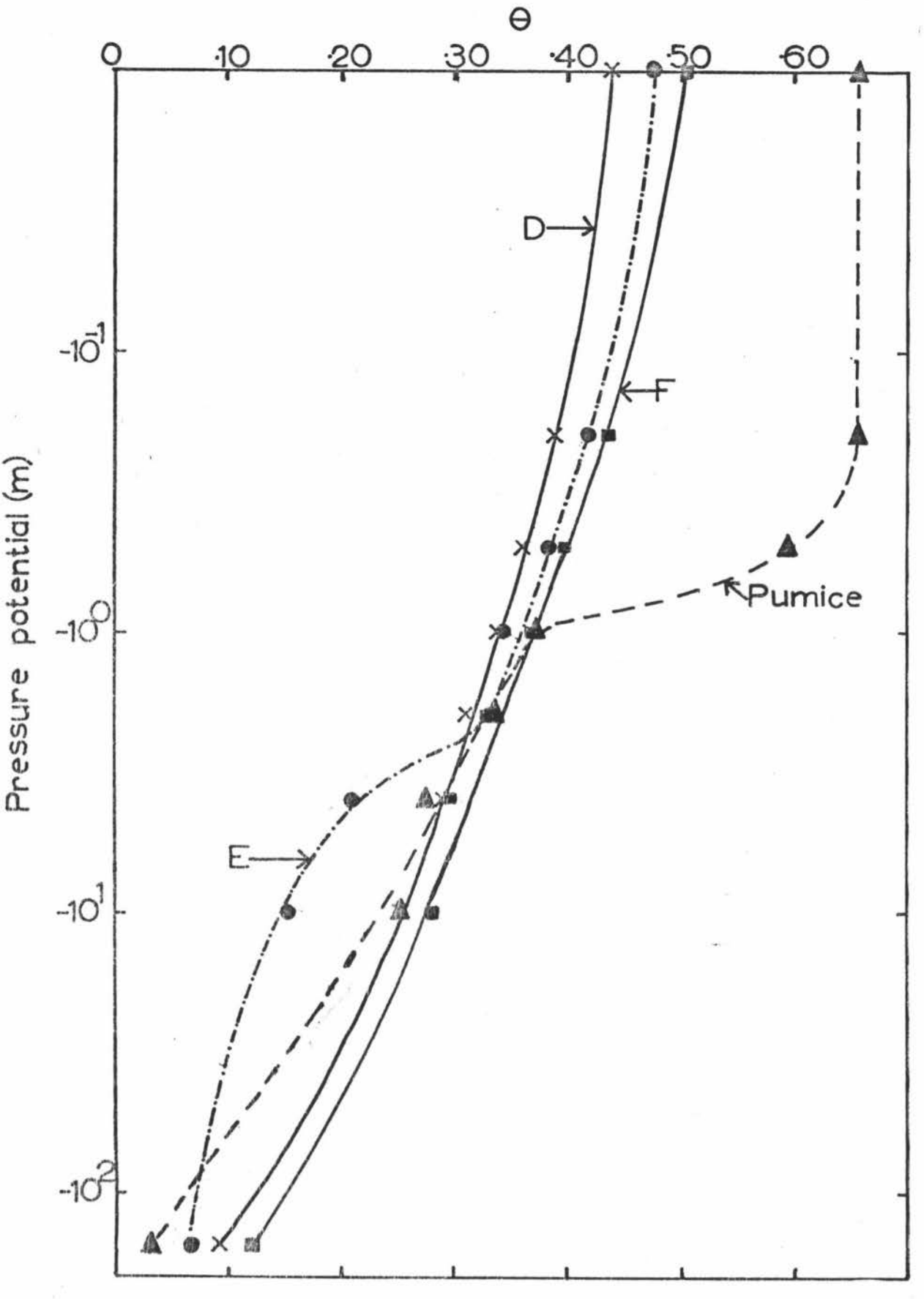

Fig.49b. Volumetric water content against pressure potential for D(X), E(●), F(■) and pumice (▲) (G,H and I) layers of Pakowhai silt loam. The lines are fitted by eye.

"field capacity" was taken after 14 days of drainage (AWC_E). The best estimate of AWC compared to AWC_E calculated assuming "field capacity" occurred at a specific pressure potential, was when the pressure potential was -1.0 m (Table 7). These AWC's were calculated for pasture with a rooting depth of approximately 1.1 m. Other crops may have greater or lesser rooting depths which will change the size of the AWC.

Although the AWC_E of this soil is large, (260 mm) a large proportion of this (170 mm) is held in the pressure potential range between -10 m and -154 m. Thus the RAWC of this soil is only 90 mm, similar to the Ngatarawa and Takapau sandy loams. For a similar amount of evapotranspiration from these three soils, pasture would become stressed and production reduced at the same time, but pasture on the Pakowhai silt loam would be able to survive for much longer without irrigation or rainfall.

The top 3 layers in this soil have pressure potentials greater than -0.5 m for 1 to 3 days after drainage started. The macro-porosity is only about 10 to 15% by volume (Fig.50), with only 3-4% by volume blind pores. Aeration problems are indicated in this soil by the mottling which occurs in these layers (Appendix I). The slow drainage would appear to be due to the small hydraulic conductivity of these layers at high pressure potentials (Figs.44,45) rather than water perching on an impermeable layer. Thus a drainage system (tile and moles) may not alleviate the aeration problem, although the cracking caused by the mole plough would probably help.

3.4.1 Computer Simulations

The moderately-slow final infiltration rate (Table 10), and the depth of soil would appear to make this soil suitable for irrigation using the border-dyke method. The computer simulation model was used to

Table 7: Comparison of available water capacity (AWC) calculated using experimental and laboratory estimates of "field capacity", for Pakowhai silt loam. Also the equivalent depth of water held between pressure potentials of -10 m and -154 m

AWC (mm) calculated using "field capacity" as:	Plot	
	017 *	018*
3 days of drainage	303	269
14 days of drainage AWC_E	277	248
Θ at a pressure potential of -0.5 m	308	278
Θ at a pressure potential of -1.0 m	281	263
Θ at a pressure potential of -2.0 m	254	230
Equivalent depth of water held between pressure potentials of -10 m and -154 m (mm)	195	150

* Rooting depth taken as 1.0 m

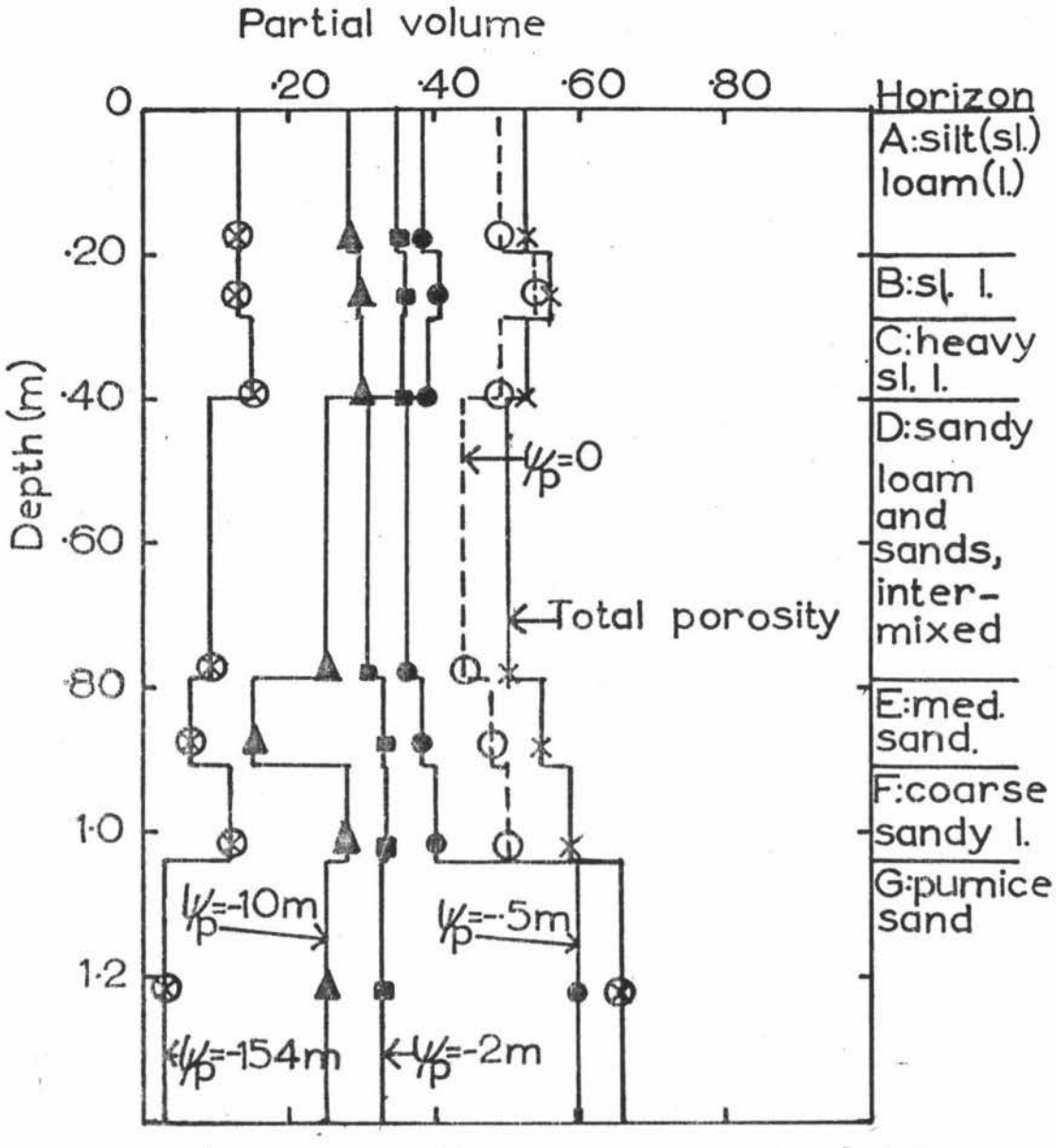

Fig.50 Partial volume of the soil occupied by water at various pressure potentials, the total porosity, depth and texture of each soil layer of Pakowhai silt loam.

predict the likely infiltration and redistribution patterns under border-dyke irrigation. Drainage from a similar pressure potential profile to that found in the plots after wetting was simulated. Simulated pressure potential profiles at various times compared well with experimental results (Fig.51), as did the simulated cumulative drainage compared to the experimental cumulative drainage (Fig.52). These simulations were only for the top metre of soil, as most of the water withdrawn by pasture will be from there.

Infiltration was simulated for durations of 90 minutes, 120 minutes and 150 minutes i.e. 120±30 minutes, for initial pressure potentials of -10 m and -154 m (Figs. 53,54). Redistribution following infiltration with no evapotranspiration and a constant daily evapotranspiration of 5 mm day^{-1}, is shown in Figures 55,56,57,58, 59 and 60. These data indicate that only 120 minute and 150 minute infiltrations wet the soil to 1 m when the initial pressure potential was -10 m, and that only the 150 minute infiltration would wet the soil to 1 m if the soil had an initial pressure potential of -154 m. The amount of the simulated irrigation water that went to drainage is small, less than 23% (Tables 8,9). This suggests that this soil would be very suitable for border-dyke irrigation. If the soil was irrigated when the pressure potential reached -10 m, the duration of infiltration should be 120 minutes. This soil allows a more flexible management policy in that, with its large AWC, if water cannot be supplied when the RAWC is exhausted, pasture would still be able to survive until water is available.

Table 8: Simulated cumulative infiltration (I), drainage (DT) and percentage of cumulative infiltration occurring as drainage, during simulated ponded infiltration and redistribution of water in Pakowhai silt loam, when the soil had an initial pressure potential of -10 m

Infiltration			Redistribution			
Duration (minutes)	I (mm)	DI (mm)	ET=0, t=10 days D (mm)	DT/I (%)	ET=5 mm day^{-1}, t = 5 days D (mm)	DT/I (%)
90	85	0	0	0	0	0
120	104	0	9	9	9	9
150	124	0	28	23	22	18

DI is the cumulative drainage that occurs during infiltration
D is the cumulative drainage that occurs during redistribution
DT = DI + D, and is the total cumulative drainage (mm)
ET is the evapotranspiration rate
t is the time taken for the drainage rate to become small during redistribution following infiltration for a duration of 150 minutes

Table 9: Simulated cumulative infiltration (I), drainage (DT) and percentage of cumulative infiltration occurring as drainage, during simulated ponded infiltration and redistribution of water in Pakowhai silt loam, when the soil had an initial pressure potential of -154 m

Infiltration			Redistribution			
Duration (minutes)	I (mm)	DI (mm)	ET=0, t= 5 days D (mm)	DT/I (%)	ET=5 mm day^{-1}, t=3 days D (mm)	DT/I (%)
90	104	0	0	0	0	0
120	128	0	0	0	0	0
150	140	0	0	0	0	0

DI is the cumulative drainage that occurs during infiltration (mm)
D is the cumulative drainage that occurs during redistribution (mm)
DT = DI + D, and is the total cumulative drainage (mm)
ET is the evapotranspiration rate
t is the time taken for redistribution to be completed

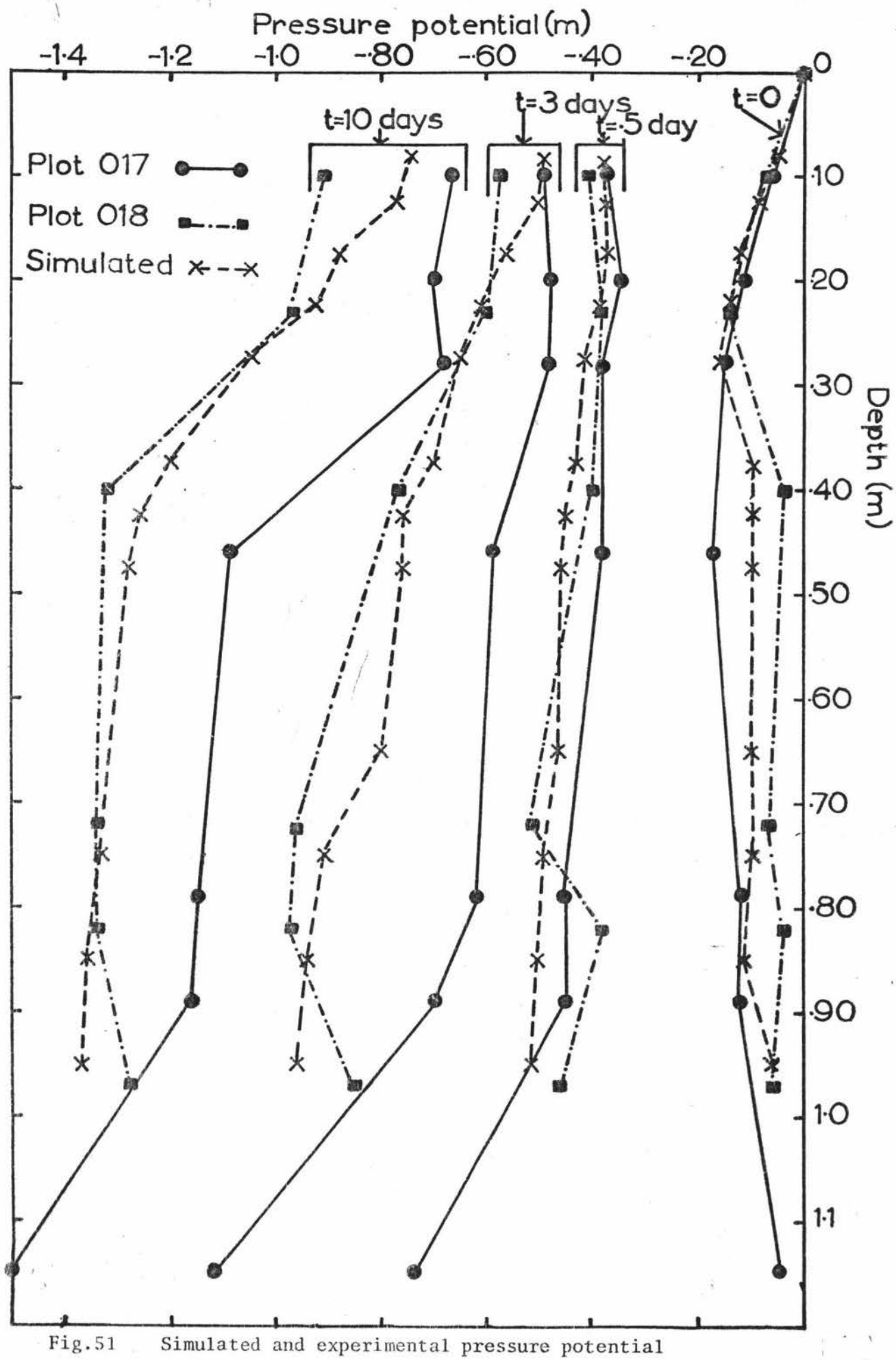

Fig.51 Simulated and experimental pressure potential profiles at various times (t), during drainage of a thoroughly wetted soil profile of Pakowhai silt loam.

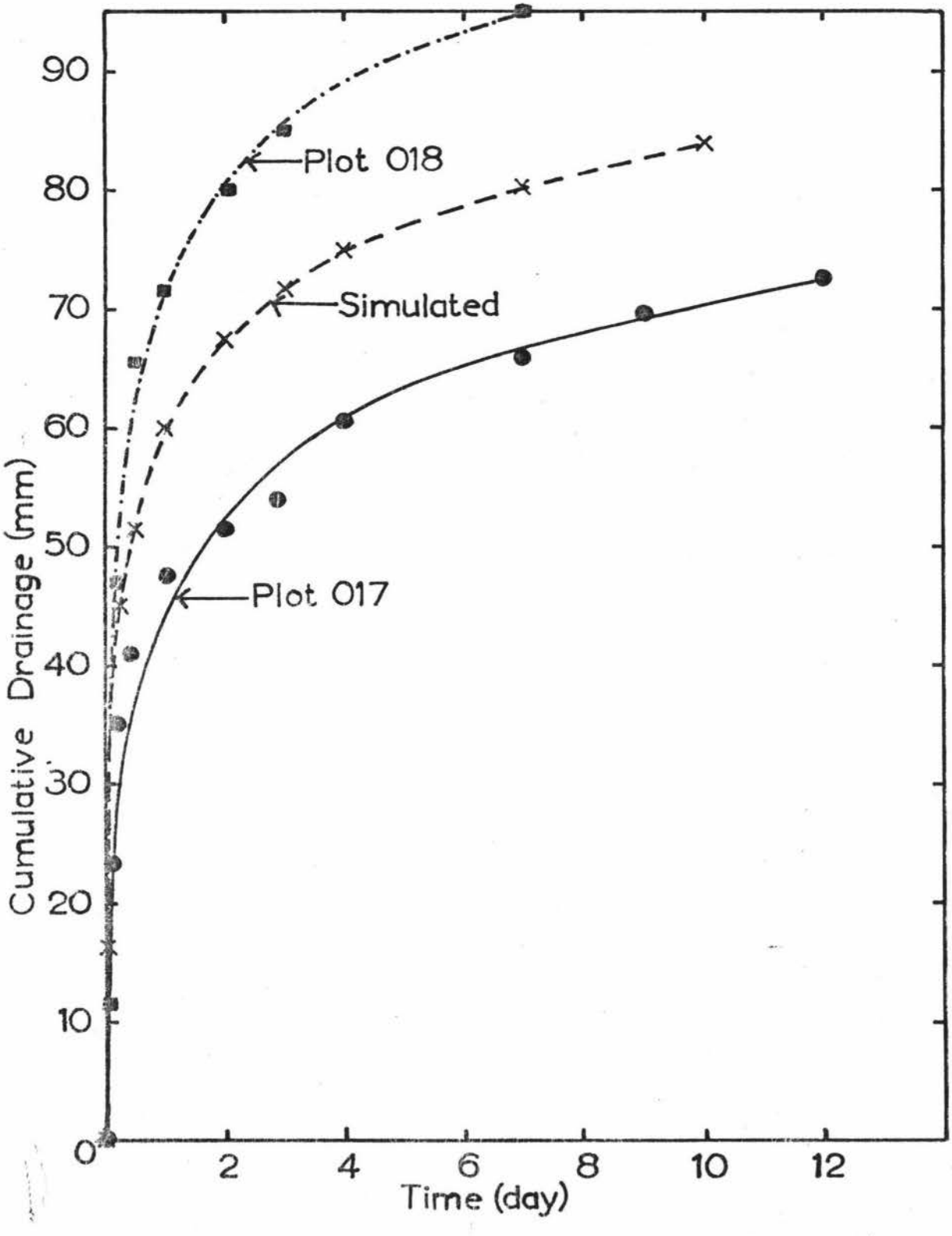

Fig.52 Simulated and experimental cumulative drainage against time from the top 1 m of Pakowhai silt loam.

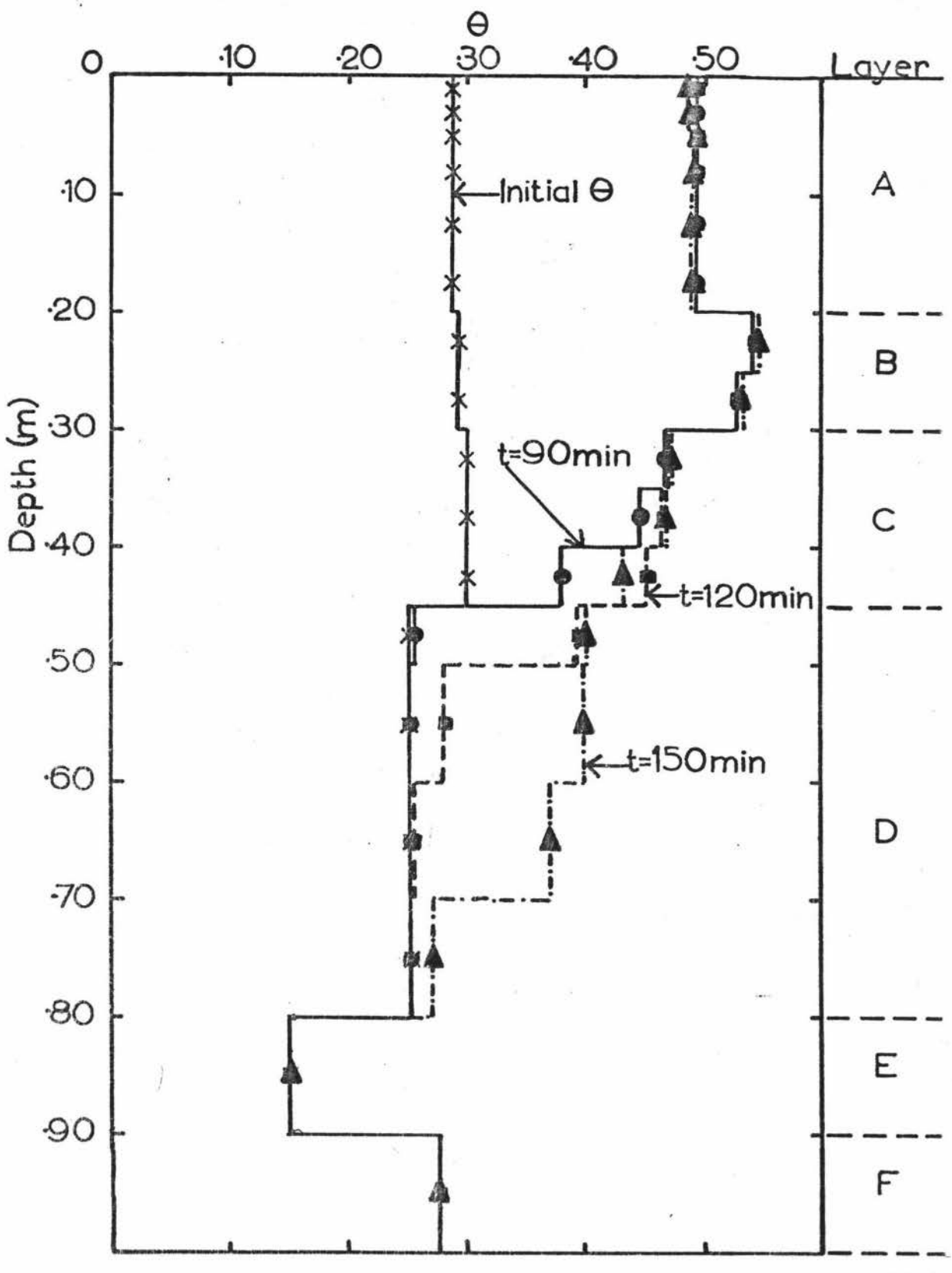

Fig.53 Volumetric water content (θ) profiles at various times (t) during simulated ponded infiltration of water into Pakowhai silt loam, which had an initial θ corresponding to a pressure potential of -10 m.

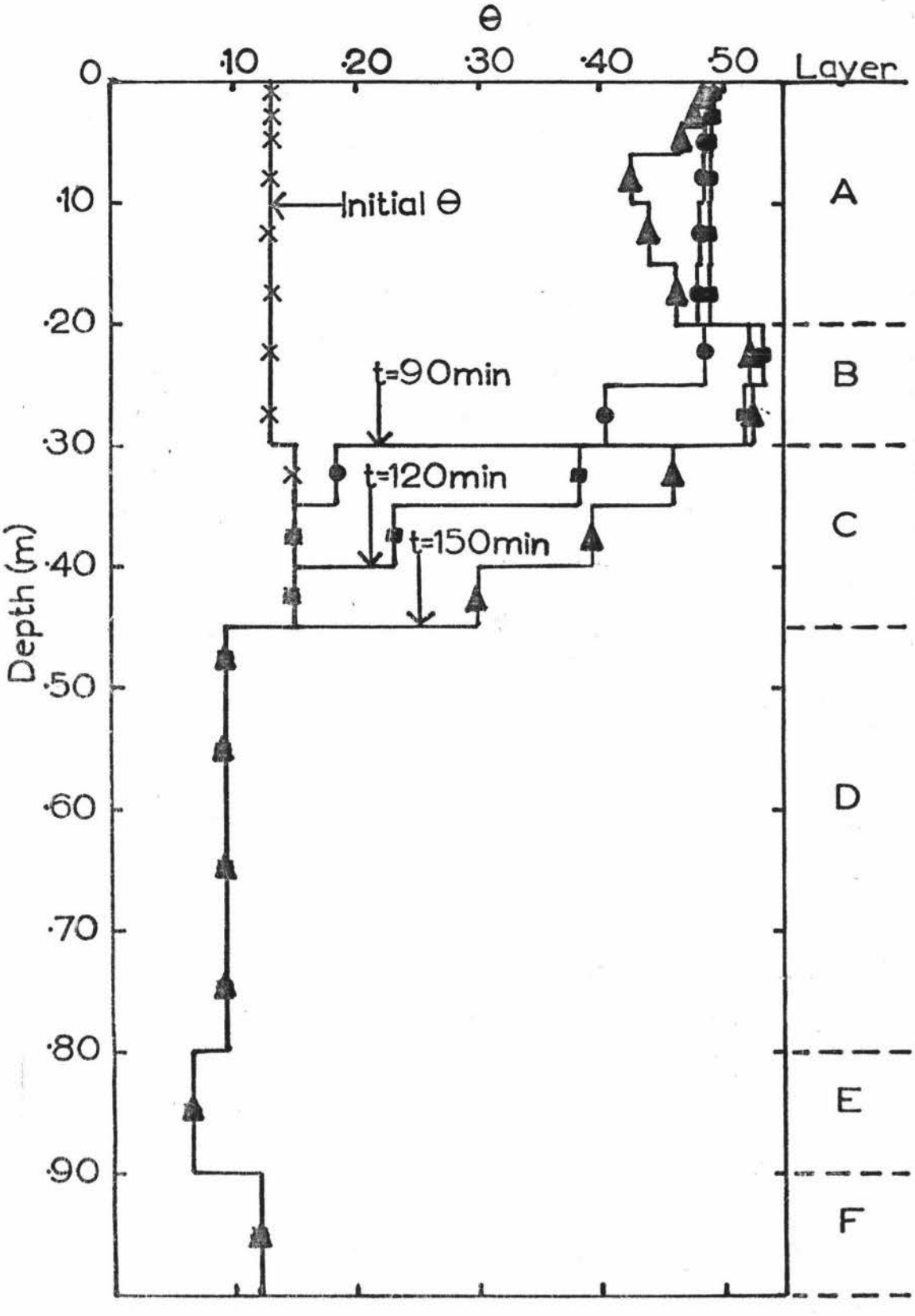

Fig.54 Volumetric water content (θ) profiles at various times (t) during simulated ponded infiltration of water into Pakowhai silt loam, which had an initial θ corresponding to a pressure potential of -154 m.

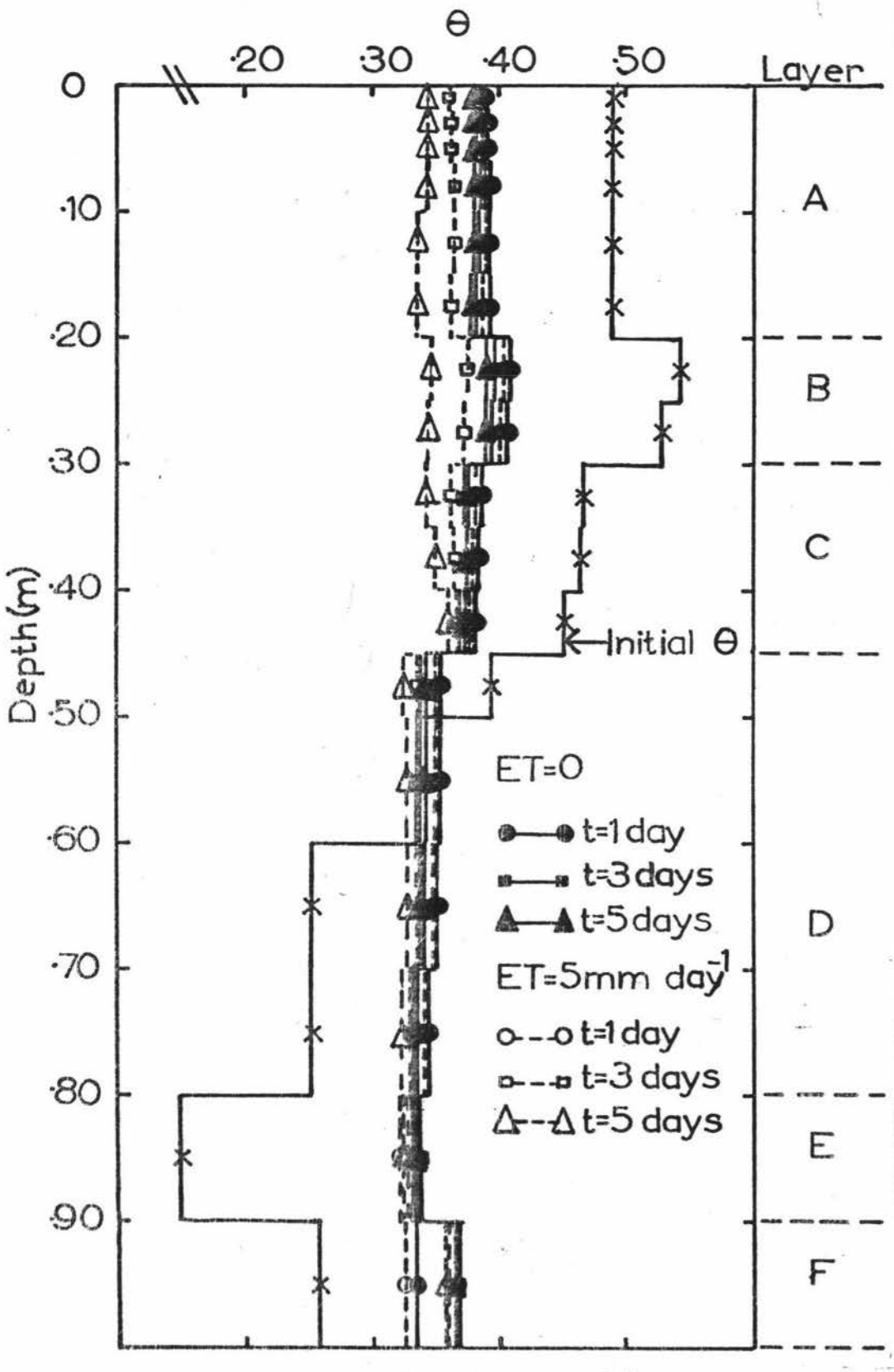

Fig. 55 Simulated redistribution of water, with no evapotranspiration (ET) and with ET=5 mm day^{-1} for Pakowhai silt loam. The intial θ profile was obtained following simulated ponded infiltration of water into this soil, initially at a pressure potential of -10 m, for 90 minutes.

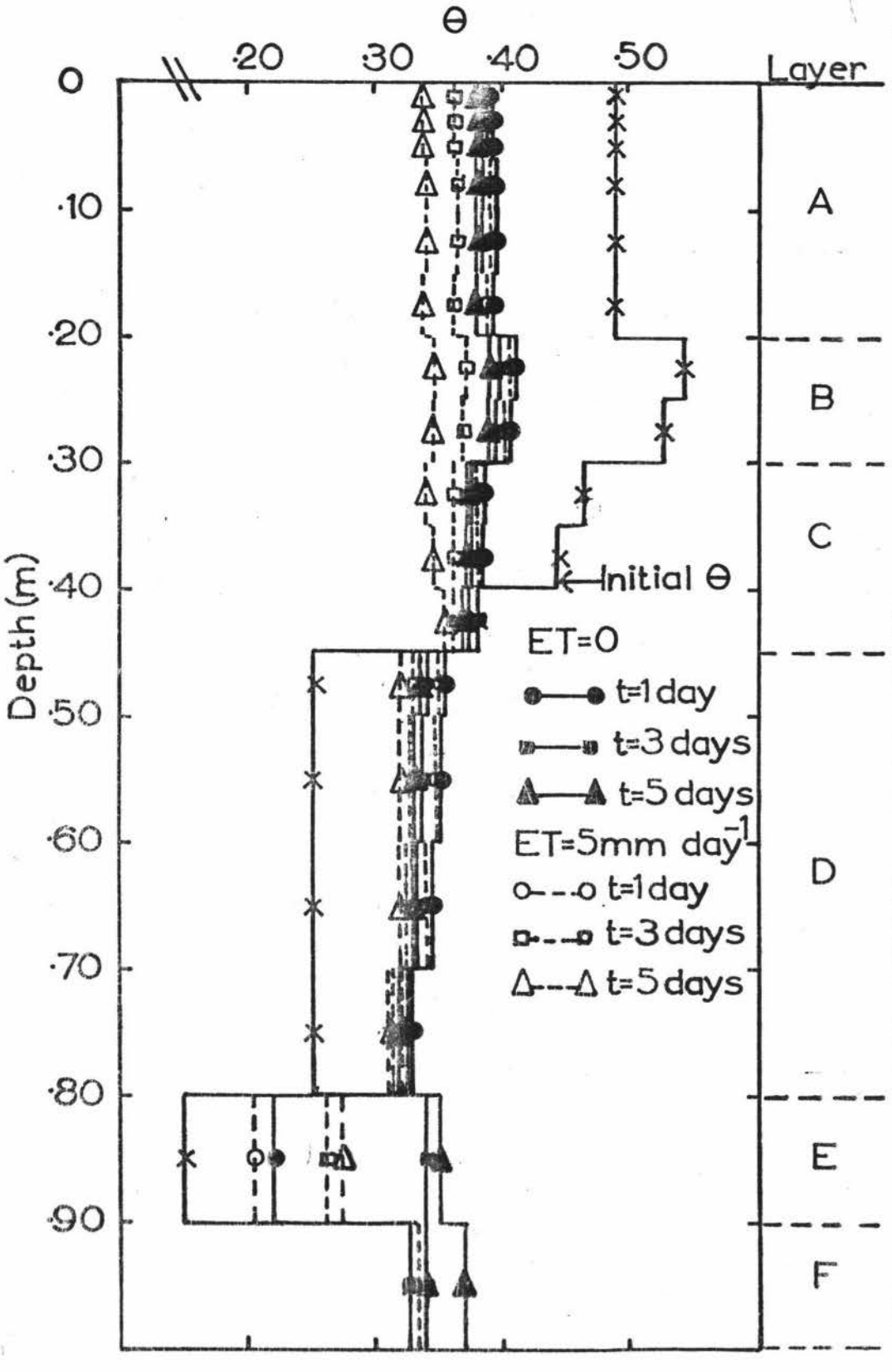

Fig.56 Simulated redistribution of water with no evapotranspiration (ET) and with ET=5 mm day^{-1} for Pakowhai silt loam. The initial θ profile was obtained following simulated ponded infiltration of water into this soil, initially at a pressure potential of -10 m, for 120 minutes.

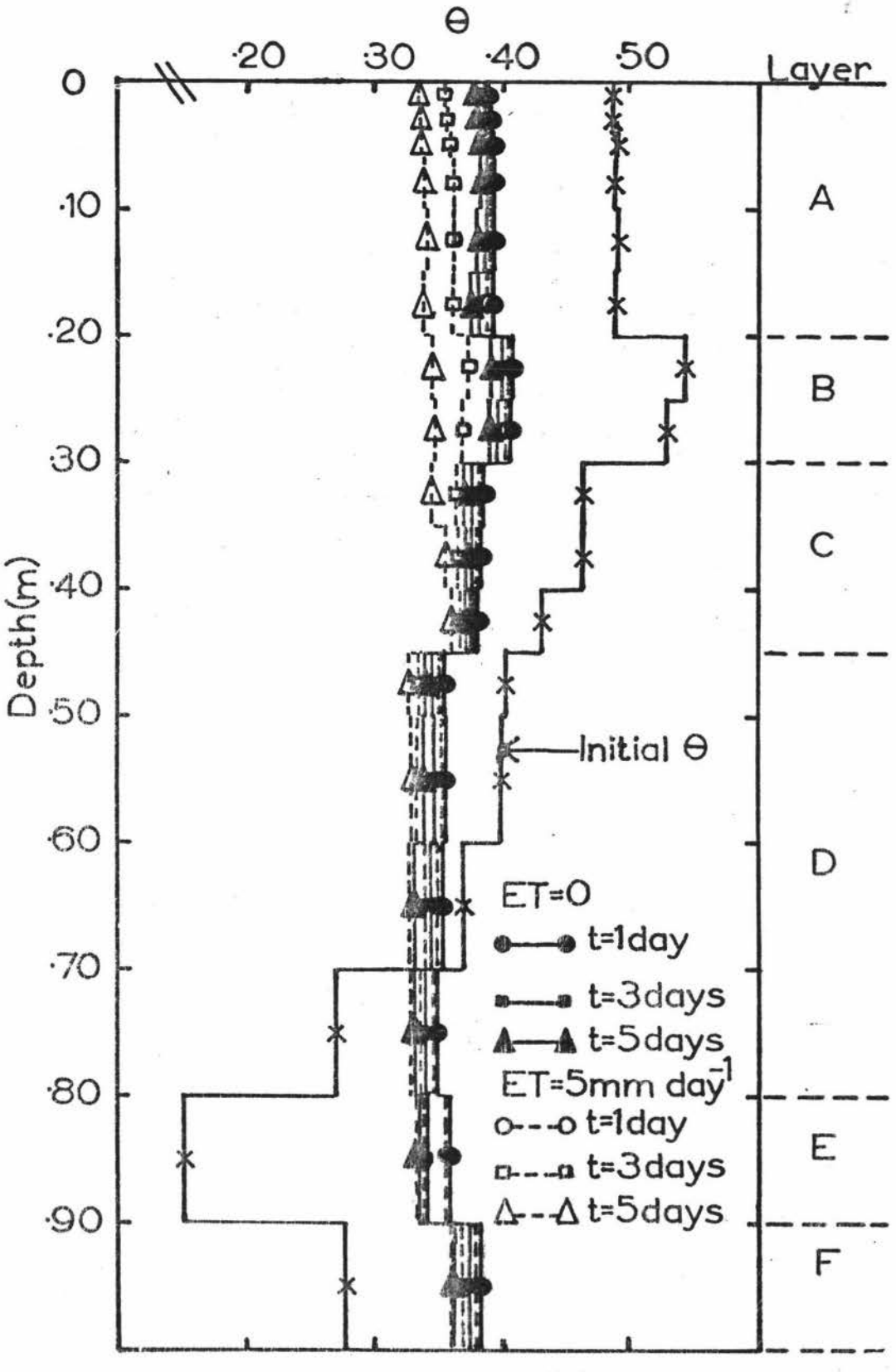

Fig.57 Simulated redistribution of water with no evapotranspiration (ET) and with ET=5 mm day^{-1} for Pakowhai silt loam. The initial Θ profile was obtained following simulated ponded infiltration of water into this soil, initially at a pressure potential of -10 m, for 150 minutes.

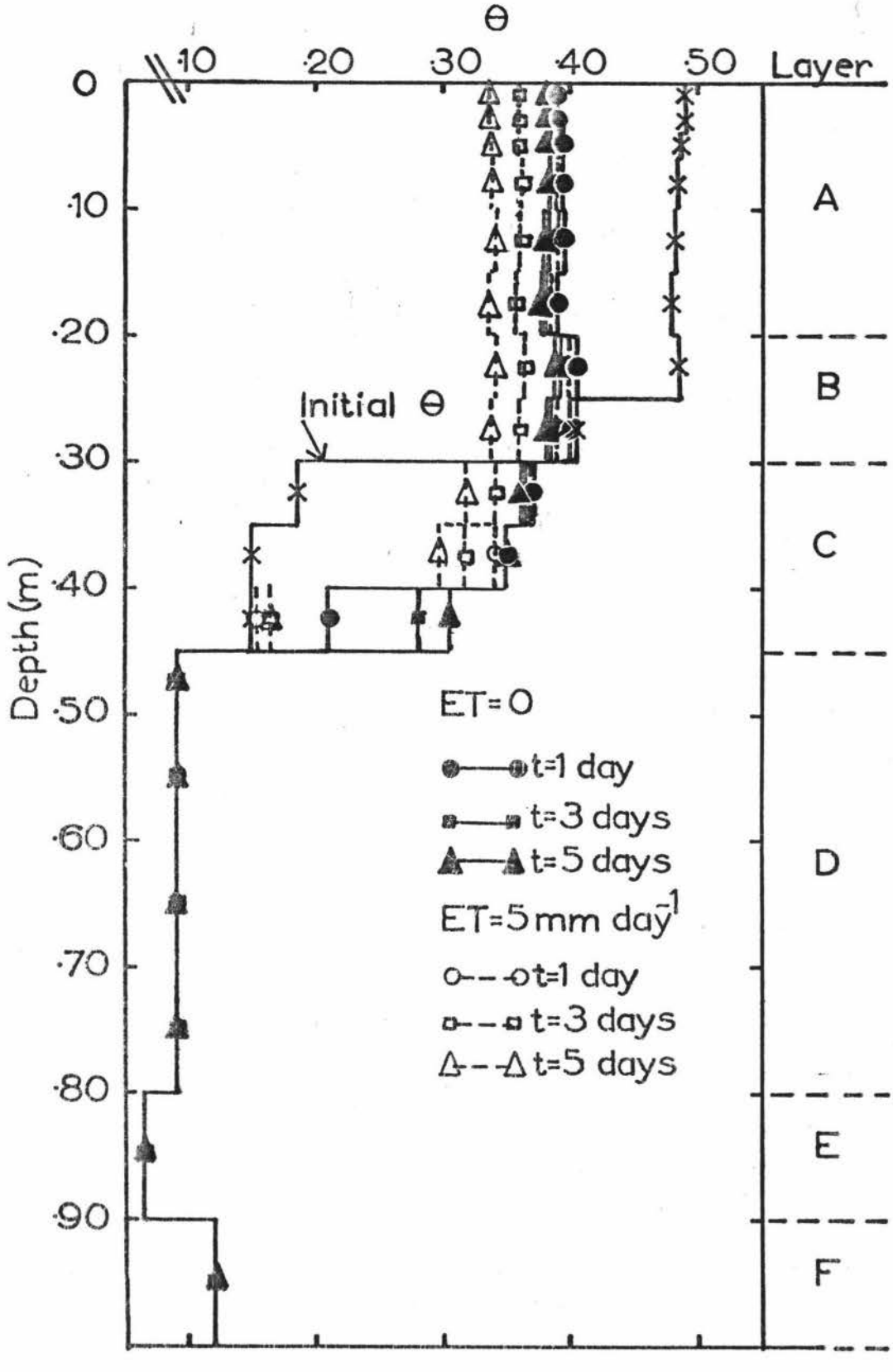

Fig.58 Simulated redistribution of water, with no evapotranspiration (ET) and with ET=5 mm day^{-1} for Pakowhai silt loam. The initial θ profile was obtained following simulated ponded infiltration of water into this soil, initially at a pressure potential of -154 m, for 90 minutes.

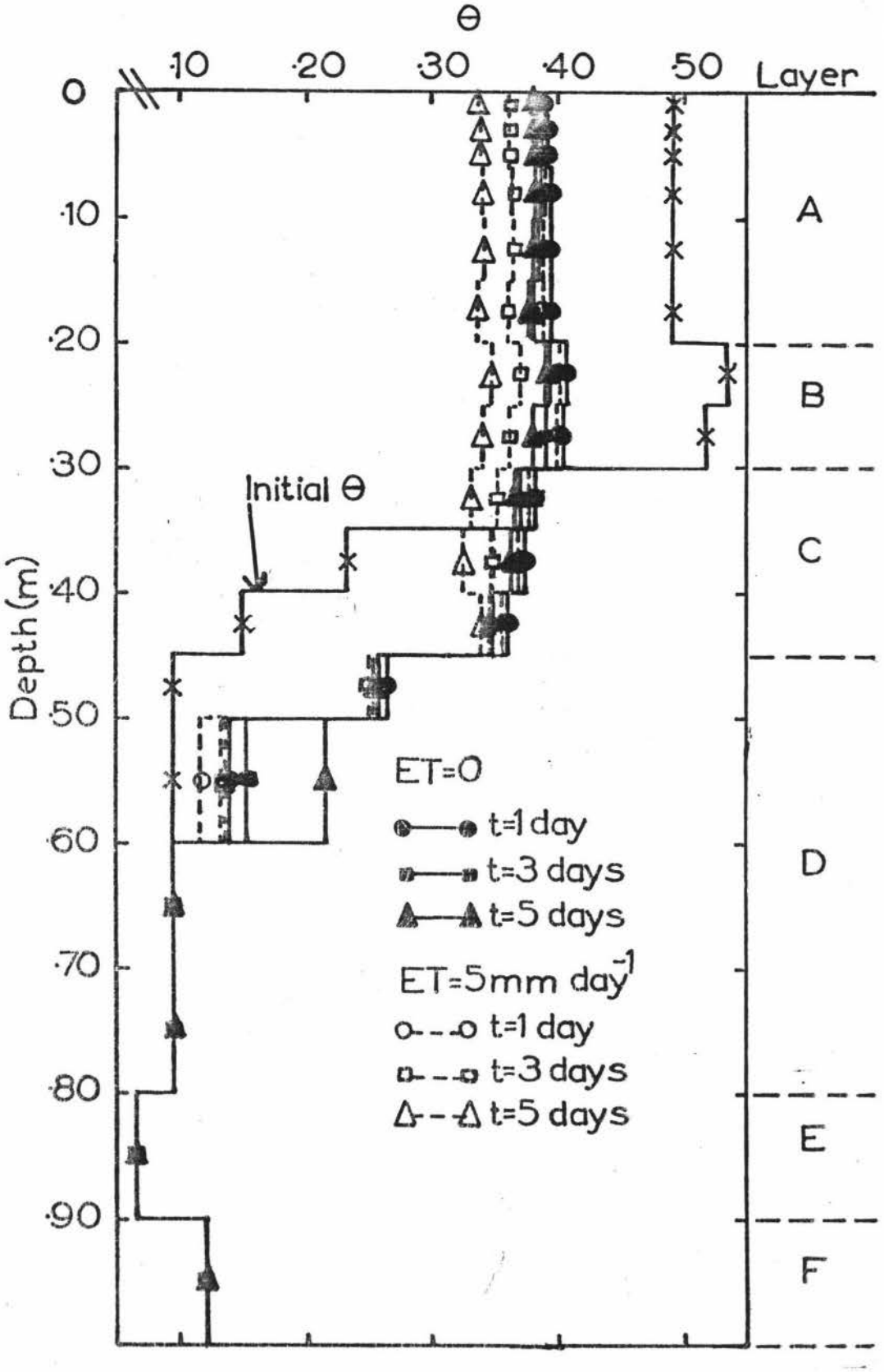

Fig.59 Simulated redistribution of water with no evapotranspiration (ET) and with ET=5 mm day^{-1} for Pakowhai silt loam. The initial θ profile was obtained following simulated ponded infiltration of water into this soil, initially at a pressure potential of -154 m, for 120 minutes.

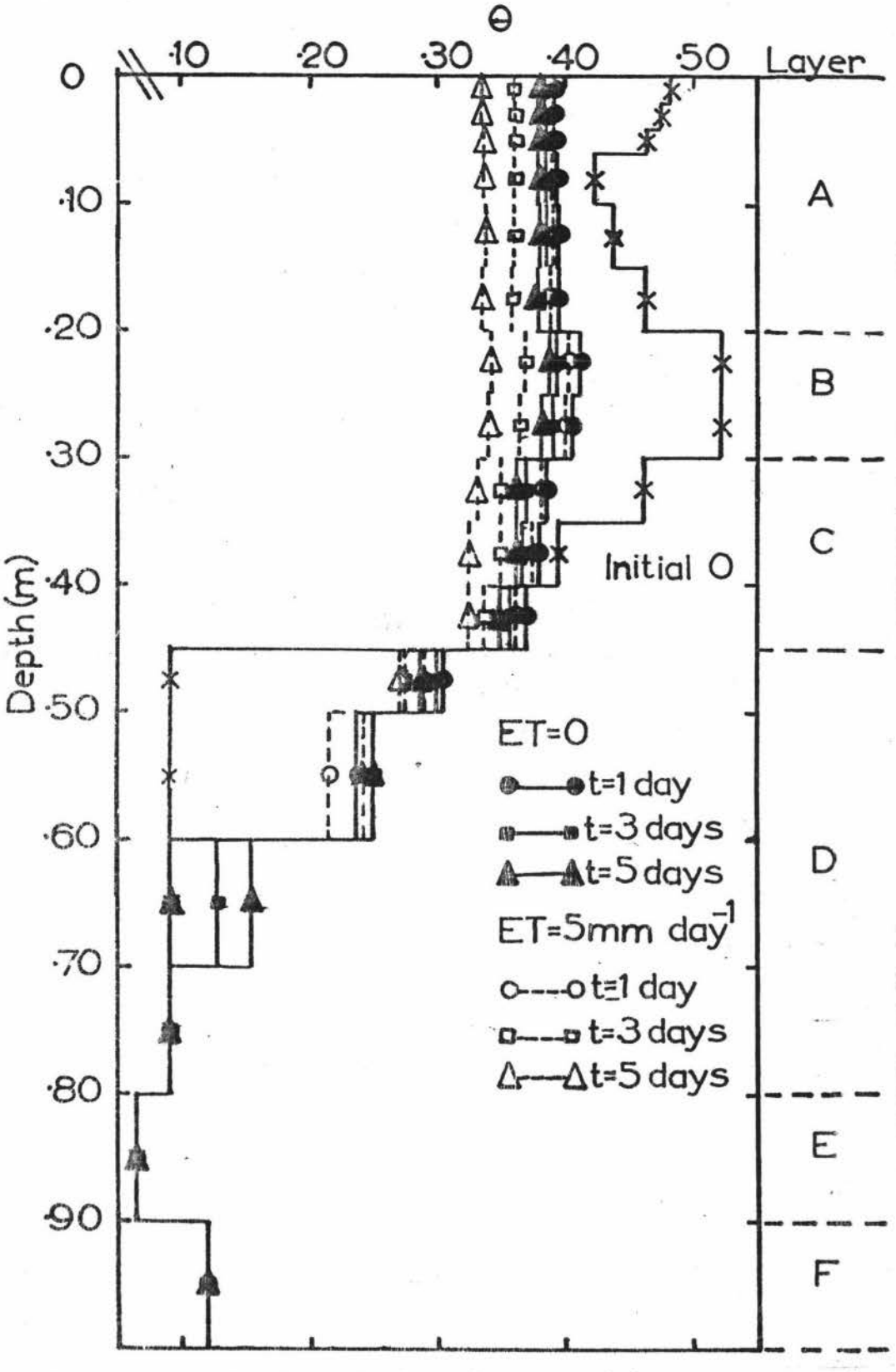

Fig.60 Simulated redistribution of water, with no evapotranspiration (ET) and with ET=5 mm day^{-1} for Pakowhai silt loam. The initial Θ profile was obtained following simulated ponded infiltration of water into this soil, initially at a pressure potential of -154 m, for 150 minutes.

4 SUMMARY AND CONCLUSIONS

4.1 The Instantaneous Profile Method

Using the instantaneous profile method, some of the hydraulic properties of the four soils in this study were measured. Reliable hydraulic conductivity data were obtained for only two soils, Takapau sandy loam and Pakowhai silt loam. The drainage behaviour of the other two soils, Poporangi sandy loam and Ngatarawa sandy loam can be described respectively by equations (35) and (36):

$$\psi_p(z) = z - Z_w, \quad Z \leqslant Z_w \qquad \text{--- (35)}$$

$$\psi_p(z) = \psi_c - Z_c + z \qquad \text{--- (36)}$$

for $z \leqslant Z_c$

where the terms used are defined in Chapter 3.

Equation (35) gives the pressure potential profile for Poporangi sandy loam during drainage and at "field capacity", and equation (36) gives the pressure potential profile for Ngatarawa sandy loam at "field capacity".

The instantaneous profile method allowed the water storage characteristics of the soils in this study to be measured, as well as hydraulic conductivity and drainage. The storage characteristics of these soils are summarised in Table 10.

A number of limitations of the instantaneous profile method were found during this study. Firstly hydraulic conductivity near saturation could not be obtained for the lower horizons, as the upper horizon was less permeable. This is not a serious problem, as these layers will not become saturated in the field. Secondly, lateral flow restricted the range of measurement, as data were rejected if $|\partial\psi_t/\partial z|$ was less than 0.3. However, steps can be taken to avoid this problem. Nagpal and de Vries (1976) stopped horizontal flow by isolating the plot from the surrounding soil with plastic sheets, and were able to extend the range of hydraulic conductivity data. This technique would be a useful modification in many situations.

Table 10: A summary of some of the soil water properties of the soils in this study

Soil	Rooting depth	Time taken to reach "field capacity" (days)	Pressure potential at "field capacity" (m)	AWC (mm)	RAWC (mm)	Final infiltration rate ($m\ s^{-1} \times 10^{-6}$)
Poporangi sandy loam	0.45	10	-0.5	88	58	3.3
Ngatarawa sandy loam	0.70	1	-0.5	160	85	3.3 to 9
Takapau sandy loam	0.72	10	-1.0	170	95	10 to 30
Pakowhai silt loam	1.10	14	-1.0	260	90	8.5 to 10

AWC is the available water capacity, which is the equivalent depth of water held in the root zone of the soil between "field capacity" and a pressure potential of -154 m

RAWC is the readily available water capacity, which is the equivalent depth of water held in the root zone of the soil between "field capacity" and a pressure potential of -10 m

The final infiltration rate is the final steady state infiltration measured for these soils during wetting. It would approximate the saturated hydraulic conductivity of the A horizon of the Ngatarawa and Takapau sandy loams, but the restriction to infiltration in the Pakowhai silt loam and Poporangi sandy loam is deeper in the soil profile, and so this approximation is no longer valid.

4.2 Storage Characteristics

This study has confirmed that "field capacity" is a dynamic soil property, as the time taken to reach "field capacity" and the pressure potential which best estimates "field capacity" is different for each of these soils (Table 10). Thus, the best method for measuring the "field capacity" of a soil is to measure it in the field.

The available water capacity (AWC), which is the amount of water held by the soil in the root zone between "field capacity" and a pressure potential of -154 m, of each of these soils was different (Table 10). Yet, the readily available water capacity (RAWC), which is the amount of water held in the root zone between "field capacity" and a pressure potential of -10 m, is similar for three of the four soils (Table 10) i.e. Takapau sandy loam, Ngatarawa sandy loam, and Pakowhai silt loam. Irrigation should be scheduled to occur when the RAWC of a soil is depleted, to prevent moisture stress. RAWC is often estimated by 50% of AWC (Griffiths, 1975b), but as the data in Table 10 show, the RAWC of one soil would have been overestimated and another underestimated by this approximation. Thus, it is better to measure RAWC directly rather than to irrigate when an arbitrary fraction of the AWC has been used.

4.3 Horizon Homogeneity

The assumption that each pedologically distinct horizon or layer has uniform physical properties would seem reasonably justifiable from the data in this study. Hydraulic conductivity data from duplicate plots compared well, except for the A horizon of the Ngatarawa sandy loam. The poor comparison between data of the A horizons of the Ngatarawa sandy loam was due to the difference in the retentivity data of the A horizon from the two plots. The retentivity data from both

plots for the other horizons of this soil, and all horizons of the other soils, compared well. Also, the draining volumetric water content at a pressure potential of -0.5 m obtained from the hysteresis experiments (Appendix II), compare well with those obtained earlier (Table 12, Appendix II). There is a marked variability in the depths of the horizons and the thickness of them between the plots e.g. the D layer of the Ngatarawa sandy loam was present in one plot but not in the other. However, this variability did not appear to affect the physical properties of the layers or horizons.

4.4 Irrigation Methods

A border-dyke system of irrigation would not be an efficient method for irrigating three of the soils in this study (Poporangi sandy loam, Ngatarawa sandy loam, and Takapau sandy loam) but would be a suitable method to use on Pakowhai silt loam. Reasons for this will be summarised below.

4.4.1 Poporangi sandy loam

Poporangi sandy loam has a restricted rooting depth of 0.45 m, due to a duripan occurring at this depth. Thus, any excess water from over-irrigation would perch above this duripan, and take several days to drain away. As this soil has an RAWC of only 58 mm, it may be difficult to prevent over-irrigation using a border-dyke system. Although the final infiltration rate is slow, due to the duripan, initial infiltration is rapid as the top horizons are similar to Takapau sandy loam, so application of only 58 mm of water would be difficult. A drainage system would help to lower the perched water table faster, alleviating any water-logging problems, particularly if heavy unexpected rainfall should occur following irrigation. Thus, for Poporangi sandy loam an irrigation system that could apply uniformly 58 mm, such as a sprinkler system, would be best.

4.4.2 Ngatarawa Sandy Loam

Ngatarawa sandy loam has a coarse layer at about 0.5 m. This layer ceases draining at a pressure potential of about -0.4 m, but when it is wet to pressure potentials greater than this, drainage water can be conducted through it at a moderate rate. The RAWC for this soil is 85 mm, which is a moderate amount. As this soil has only a moderate final infiltration rate (Table 10) it could possibly be irrigated with a border-dyke system. Any excess water infiltrated at the intake end of the border will be lost to drainage. Thus, a method where 85 mm of water could be applied uniformly to the soil would be more efficient, e.g. a sprinkler system.

4.4.3 Takapau Sandy Loam

Takapau sandy loam has a rapid final infiltration rate and a moderate RAWC of 95 mm. It is the least suitable soil for irrigation using the border-dyke system because any excess water is rapidly lost to drainage. If the recommended duration time of infiltration was used, the simulation results indicate that about 50% of the applied water would be lost to drainage from the top 0.45 m. Another method of irrigating this soil should be used that could apply the water uniformly. The rate at which this is applied must be less than the saturated hydraulic conductivity of the A horizon of the soil. Otherwise, a poor horizontal distribution of water within the soil can occur (Appendix IV).

4.4.4 Pakowhai Silt Loam

Pakowhai silt loam, because of its depth, moderate final infiltration rate and moderate RAWC, is very suitable for irrigation using the border-dyke method. This was confirmed by the simulation results which showed that even with an infiltration duration of 150 minutes

little of the applied water was lost to drainage from the top 1 m of soil.

4.5 Groundwater Quality

The Ngatarawa plains lie over the recharge area of the aquifer from which water is drawn for Hastings and Napier cities (Burden, 1979). This study indicates that if the soils in this area were irrigated using the border-dyke method, from three of the four major soil types an increased flux of water into the aquifer would result. This could lead to an increase in the nitrate levels of water in the aquifer, which could be detrimental to the health of people drinking this water.

4.6 Computer Simulation Model

The model for soil water dynamics used in this study was able to adequately simulate the drainage behaviour of Takapau sandy loam and Pakowhai silt loam. This model could be used to simulate most soil water dynamic problems and would be a useful tool for predicting what effect changes in management practices might have on the soil moisture regime. The model would be useful, as shown here, in the planning stage of an irrigation project to predict which soil types would be best irrigated using sprinkler or border-dyke methods. This model is not envisaged as being used for soil water status studies e.g. scheduling irrigation, as it is costly to run and simpler water-balance models are more appropriate. The flux-concentration relation, though only briefly used in this study, would appear to have great potential for use for describing infiltration in soil water studies where it is the major concern e.g. catchment studies, moisture regimes and irrigation.

REFERENCES

Baker, F.G., Veneman, P.L.M., and Bouma, J. 1974. Limitations of the instantaneous profile method for field measurement of unsaturated hydraulic conductivity. Soil Sci. Soc. Amer. Proc. *38:* 885-888.

Bhuiyan, S.I., Hiler, E.A., van Bavel, C.H.M. and Aston, A.R. 1971. Dynamic simulation of vertical infiltration into unsaturated soils. Water Resources Research *7(6):* 1597-1606.

Brandt, A., Brester, E., Diner, N., Ben-Asher, I., Heller, J. and Goldberg, D. 1971. Infiltration from a trickle source: I. Mathematic model. Soil Sci. Soc. Amer. Proc. *35:* 675-682.

Buckingham, E. 1907. Studies on the movement of soil moisture. U.S.D.A. Bur. Soils Bull. *38.* U.S.D.A., Washington, D.C.

Burden, R.J. 1979. Groundwater quality, Heretaunga Plains. Proceedings of Annual Symposium, N.Z. Hydrology Society.

Childs, E.C. and George, N.C. 1948. Soil geometry and soil-water equilibrium. Disc. Faraday Soc., *3:* 78-85.

Clothier, B.E., Scotter, D.R. and Kerr, J.P. 1977. Water-retention in soil underlain by a coarse-textured layer. Theory and field application. Soil Science *123(6):* 392-399.

Cook, F.J. 1976. The effect of irrigation on the drainage behaviour of the Tokomaru silt loam in relation to the soil's physical properties. Dip. Ag. Sci. Dissertation, Massey University.

Dane, J.H. and Wierenga, P.J. 1975. Effect of hysteresis on the prediction of infiltration, redistribution, and drainage of water in a layered soil. J. of Hydrology *25:* 229-242.

Davidson, J.M., Stone, L.R., Nielsen, D.R., La Rue, M.E. 1969. Field measurement and use of soil-water properties. Water Resources Research *5:* 1312-1321.

de Wit, C.T., and van Keulen, H. 1972. Simulation of Transport Processes in Soils. Centre for Agricultural Publishing and Documentation (PUDOC) Wageningen, Netherlands.

Everett, D.H. 1955. A general approach to hysteresis, 4. An alternative formulation of the domain model. Trans. Faraday Soc. *51:* 1551-1557.

Fluhler, H., Ardakani, M.S., Stolzy, L.H., 1976. Error propagation in determining hydraulic conductives from successive water content and pressure potential profiles. Soil Sci.Soc.Amer. J. *40:* 830-836.

Fugazi, K. 1973. CSMP73: Continuous System Modelling Program for the B6700. University of California, Davis, Computer Centre.

Gradwell, M.W. 1971. C. Methods for physical analysis of soils. New Zealand Soil Bureau Scientific Report *10C*.

Griffiths, E. 1975a. Appendix VI. Ngatarawa Irrigation Scheme Feasibility Report. Ministry of Works and Development, Water and Soil Division.

Griffiths, E. 1975b. Classification of land for irrigation in New Zealand. N.Z. Soil Bureau Scientific Report 22.

Guymon, G.L. 1974. Digital computers and drainage problem analysis. Part III. Finite element method. *In* Drainage for Agriculture (Agronomy No.17 Ed. van Schilfgaadre, J.). Madison, Wisconsin, U.S.A. American Soc. of Agronomy. pp 587-602.

Hagan, R.M. and Stewart, J.I. 1972. Water deficits-irrigation design and programming. J. of Irrigation and Drainage Division, Amer. Soc. Civil Engs. IR2.

Haines, W.B. 1930. Studies in the physical properties of soil: V. The hysteresis effect in capillary properties and the modes of moisture associated therewith. J. Agric. Sci. *20:* 97-116.

Hanks, R.J. and Bowers, S.A. 1962. Numerical solution of the moisture flow equation for infiltration into layered soils. Soil Sci. Soc. Amer. Proc. *26:* 530-534.

Hillel, D., Krentos, V.D., Styianou, Y. 1972. Procedure and test of an internal drainage method for measuring soil hydraulic characteristics *in situ.* Soil Science *114:* 395-400.

Hillel, D. 1977. Computer Simulation of Soil-Water Dynamics: A Compendium of Recent Work. Ottawa, I.D.R.C. Canada. 214 p.

Hsiao, T.C. 1973. Annual Review of Plant Physiology, *24:* 519 p.

IBM Corporation, 1969. System/360 Continuous System Modelling Program (360-A-CX-16X). Users Manual, H20-0367-2 Techn. Publ. Dept., White Plains, U.S.A.

Klute, A. 1952. A numerical method for solving the flow equation for water in unsaturated materials. Soil Science *73:* 105-116.

Knight, J.H. and Philip, J.R. 1974. On solving the unsaturated flow equation: 2. Critique of Parlange's method. Soil Sci. *116(6):* 407-416.

Maclean, A.H. and Yager, T.U. 1972. Available water capacities of Zambian soils in relation to pressure plate measurements and particle size analysis. Soil Science *113:* 23-29.

Milne, E.W. 1960. Numerical Solution of Differential Equations. McGraw-Hill, New York.

Ministry of Works and Development 1975. Ngatarawa irrigation scheme feasibility report. Ministry of Works and Development, Water and Soil Division, Napier district.

Mualem, Y. 1974. A conceptual model of hysteresis. Water Resources Research *10(3):* 514-520.

Nagpal, N.K., and de Vries, J. 1976. An evaluation of the instantaneous profile method for *in situ* determination of hydrologic properties of layered soil. Canadian J. Soil Sci. *56:* 453-461.

Neuman, S.P., Feddes, R.A., Brester, E. 1975. Finite element analysis of 2-D flow in soils considering water uptake by roots. I. Theory. Soil Sci. Soc. Amer. Proc. *39(2):* 224-230.

Nielsen, D.R., Jackson, R.D., Cary, J.W., Evans, D.D. 1972. Soil Water. American Soc. of Agronomy and Soil Sci. Soc. Amer. 175 p.

Nimah, M.N. and Hanks, R.J. 1973. Model for estimating soil water, plant, and atmospheric interrelations: I. Description and sensitivity. Soil Sci. Soc. Amer. Proc. *37:* 522-527.

Parlange, J.Y. 1971a. Theory of water movement in soils. 1. One-dimensional absorption. Soil Sci. *111:* 134-137.

_____ 1971b. Theory of water movement in soils. 2. One-dimensional infiltration. *Ibida:* 170-174.

_____1971c. Theory of water movement in soils. 3. Two and three dimensional absorption. Soil Sci. *112:* 313-317.

_____ 1972a. Theory of water movement in soils. 4. Two and three dimensional steady infiltration. Soil Sci. *113:* 96-101.

_____ 1972b. Theory of water movement in soils. 5. Multi-dimensional unsteady infiltration. *Ibida:* 156-161.

_____ 1972c. Theory of water movement in soils. 8. One-dimensional infiltration with constant flux at the surface. Soil Sci. *114(1):* 1-4.

Philip, J.R. 1957a. The theory of infiltration 1. The infiltration equation and its solution. Soil Sci. *83:* 345-357.

_____ 1957b. The theory of infiltration. 2. The profile at infinity. *Ibida:* 435-448.

_____ 1957c. The theory of infiltration. 4. Sorptivity and algebraic infiltration equations. Soil Sci. *84:* 257-264.

_____ 1957d. The theory of infiltration. 5. Influence of initial moisture content. Soil Sci. *84:* 329-340.

_____1969. Theory of infiltration. Advances in Hydroscience *5:* 215-296.

_____1973. On solving the unsaturated flow equation: 1. The flux-concentration relation. Soil Sci. *116(3):* 328-335.

Philip, J.R. and de Vries, D.A. 1957. Moisture movement in porous materials under temperature gradients. Amer. Geophys. Union, Trans. *38:* 222-232.

Philip, J.R., Knight, J.H. 1974. On solving the unsaturated flow equation. 3. New quasi-analytical technique. Soil Sci. *117(1):* 1-13.

Pulovassilis, A. 1962. Hysteresis of pore water. An application of the concept of independent domains. Soil Sci. *93:* 405-412.

Rose, C.W., Stern, W.R., and Drummond, J.E. 1965. Determination of hydraulic conductivity as a function of depth and water content for soil *in situ.* Australian J. Soil Research. *3:* 1-9.

Rich, C.I. 1971. "Glossary of Soil Science Terms". Soil Science Society of America, Madison.

Richards, L.A. 1931. Capillary conduction of liquids through porous mediums. Physics *1:* 318-333.

Rubin, J. 1968. Theoretical analysis of two-dimensional transient flow of water in unsaturated and partly unsaturated soils. Soil Sci. Soc. Amer. Proc. *32:* 607-615.

Scotter, D.R. 1975. Field capacity and available soil water. Proc. Soil and Plant Water Symposium, Palmerston North, New Zealand. 3-11.

Selim, H.M. and Kirkham, Don 1973. Unsteady two-dimensional flow of water in unsaturated soils above an impervious barrier. Soil Sci.Soc.Amer. Proc. *37(4):* 489-495.

Stroosnijder, L., van Keulen, H. and Vachaud, G. 1972. Water movement in layered soils. 2. Experimental confirmation of a simulation model. Neth J. Agric. Sci. *20:* 67-72.

van Keulen, H. and van Beek, C.G.E.M. 1971. Water movement in layered soils - A simulation model. Neth. J. Agric. Sci. *19:* 138-153.

van der Ploeg, R.R. and Benecke, P. 1974. Unsteady, unsaturated, n-dimensional moisture flow in soil: A computer simulation program. Soil Sci. Soc. Amer. Proc. *38:* 881-885.

Watson, K.K. 1966. An instantaneous profile method for determining the hydraulic conductivity of unsaturated porous materials. Water Resources Research *2:* 709-715.

Wilcox, J.C. 1959. Rate of soil drainage following an irrigation. I. Nature of soil drainage curves. Can. J. Soil Sci. *39:* 107-119.

APPENDIX I : SOIL PROFILE DESCRIPTIONS

The profile descriptions of the soils in this study were provided by Mr E. Griffiths and Mr B.R. Purdie from Soil Bureau, Havelock North. To identify which of these two pedologists had provided the description, their initials e.g. E.G. or B.R.P., follows the soil description.

Ngatara Sandy Loam

Pit 007

Depth (m)	Description
0-0.21	very dark greyish brown (10YR 3/2) medium sandy loam, friable, very weak nutty structure, many roots, few pieces of Taupo pumice at base, indistinct boundary;
0.21-0.28	dark brown (10YR 4/3) with many worm casts of 10YR 3/2, medium sandy loam with few pieces of Taupo pumice, friable, single grain to massive, many roots, indistinct boundary;
0.28-0.45	dark brown (10YR 4/3) with few worm casts, medium sandy loam, friable, single grain to massive, many roots, indistinct boundary;
0.45-0.53	dark yellowish brown (10YR 4/4), medium sandy loam, friable, massive, many roots, indistinct boundary;
0.53-0.75	dark yellowish brown (10YR 4/4) looks more yellow than above, medium sandy loam (heavier than above) few gravels, friable to firm, very weak nutty structure, many roots, sharp boundary;
0.75-*on*	brown (7.5YR 4/4), gravels and stones with sand, firm slightly cemented sand with pressure faces in between stones.

E.G.

Pit 008

Depth (m)	Description
0-0.20	very dark greyish brown (10YR 3/2) medium sandy loam, friable, very weak nutty to single grain structure, many roots, indistinct boundary;
0.20-0.27	dark brown (10YR 4/3) with many worm casts of 10YR 3/2, medium sandy loam, friable, single grain to massive structure, many roots, indistinct boundary;
0.27-0.36	dark brown (10YR 4/3) medium sandy loam (heavier than above), friable, massive structure, many roots, indistinct boundary;
0.36-0.50	dark brown (10YR 4/3) gravelly sandy loam, friable with loose gravels, massive, many roots, indistinct boundary;
0.50-0.65	brown (7.5YR 4/4) gravelly sandy loam (more gravels than above), friable, massive, many roots, indistinct boundary;
0.65-1.10	mixed colours brown (7.5YR 4/2) to dark reddish brown (5YR 3/3), with many faint mottles, brown (10YR 5/3), strong brown (10YR 5/6) and dark red (2.5YR 3/6), gravels and stones with sand, tightly packed with pressure faces in between stones and sand very weakly cemented, roots rare;
1.10-*on*	gravels continuing.

Notes: Depth to first gravels variable around pit from 0.27 m to 0.45 m. The mottled and weakly cemented gravels continuous around pit but highly variable below that.

E.G.

Poporangi Sandy Loam

Pit 011

Depth (m)	Description
0.0.19	A_1 10YR 3/2 fine sandy loam, friable, weak fine nut and medium nut structure, many worm casts and borings filled with material from layers below, many fine roots, indistinct, wavy, worm mixed boundary;
0.19-0.28	B_2 10YR 3/3, sandy loam (more silt than horizon above) friable, weak fine nut structure, but overall "structure" dominated by many worm borings, casts and some borings filled with soil from layers above and below, many fine roots, diffuse boundary;
0.28-0.44	B_{31} 10YR 3/3, top to 10YR 5/4 bottom, few iron-manganese concretions to 8 mm diameter, 5YR 2.5/1 centre to 5YR 4/4 outer edge, fine sandy loam, firm structure, few fine pores, few roots, diffuse boundary;
0.44-0.52	B_{32} 2.5Y 6/4, sandy loam, firm with few iron-manganese concretions to 4 mm diameter, massive structure, few medium and fine pores, very few worms, very few roots, distinct wavy boundary;
0.52-0.72	B pan, thickness varies over width of pit (0.8 m) from 0 to 0.20 m. Thin massive platy layers within this horizon, 10YR 6/3, very hard, remainder 10YR 5/3 very firm, massive, few medium and fine pores, no roots, distinct wavy boundary;
0.72-0.98	$2C_1$ 10YR 4/4 and 10YR 6/4 along some fractures, gritty sandy loam, very firm, slightly cemented, few medium pores, few greywacke grit and pebbles (4 mm to 20 mm), gravelly sandy loam from 0.93 m to 0.98 m, distinct wavy boundary;

0.98-*on*	$2C_2$ 10YR 3/3 sandy gravels (with some silt), pebbles less than 0.25 m in diameter, loose. B.R.P.

Pit 020

Depth (m)	Description
0-0.15	dark brown (8.75 YR 3/2) medium sandy loam, friable, pseudo fine nut to single grain structure;
0.15-0.25	dark brown (7.5YR 4/4) with many 10YR 3/2 worm casts and few 10YR 5/4 worm casts, medium sandy loam, few Taupo pumice lapillae, friable,single grain structure;
0.25-0.32	yellowish brown (10YR 5/4) with faint 10YR 5/6 and 7.5YR 5/6 mottles, medium sandy loam, friable, massive to single grain structure;
0.32-0.38	light olive brown (1.2Y 5/4) with many 7.5Y 5/6 mottles, friable, massive to single grain structure;
0.38-0.381	cutan, wavy horizontal vein, brown (10YR 4/3), heavy silt loam;
0.381-0.42	pale brown 10YR 6/3 with large (5-8 mm) hard mottles 10YR 5/6 and 2.5Y 5/6 in colour, heavy sandy loam, firm, massive with Fe and Mn concretions and stains;
0.42-0.421	cutan, wavy horizontal vein, very dark greyish brown (10YR 3/2), heavy silt loam;
0.421-0.49	no single colour, mass of variable yellowish brown (10YR 5/4), pale brown (10YR 6/3) with cutans of brown (10YR 4/3), hard, massive with brittle fractures; fragile in part and appears very hard and cemented in portions, others only slightly hard, upper part of pan;

0.49-0.495	cutan, wavy horizontal vein, 10 mm thick in parts, very dark greyish brown (10YR 3/2) in part and yellowish brown (10YR 4/4) in others, silty clay loam, firm, massive structure;
0.495-0.57	1st pan extremely hard platy top layer, 5 mm thick, pale brown (10YR 6/3) below pale brown (10YR 5/3), very hard massive structure, one stone found on top;
0.57-0.63	2nd pan extremely hard platy top layer, 3 mm thick, very pale brown (10YR 6/3) below this light yellowish brown (10YR 6/4) very hard, massive, few stones on top (texture sandy loam?);
0.63-0.87	3rd pan extremely hard platy top layer 3 mm thick, very pale brown (10YR 7/3) below this pale brown (10YR 5/3) very hard massive, many stones on top, sandy loam, 2 vertical veins 20-30 mm wide 0.18 m apart connecting the 3rd and 4th pans;
0.87-0.89	4th pan extremely hard platy layer very pale brown (10YR 7/9) (this is the thickest pan and is at 0.8 m at tube);
0.89-1.02	pale brown (10YR 6/3) with 10YR 6/2 and 10YR 4/4 mottles, sandy loam, with gravels, hard massive;
1.02-*on*	gravels.

Note: Pans around the pit vary in the depth to the top from 0.45 m to 0.52 m. The number of pans varies, at the tube 3 pans on the west face 2 pans.

E.G.

Takapau Sandy Loam

Pit 010

Depth (m)	Description
0-0.08	A_{1p} 10YR 3/2, medium sandy loam, friable, very weak medium nut structure, few pumice lapillae up to 4 mm, many fine roots, very weak positive fluoride reaction,* indistinct wavy boundary;
0.08-0.14	A_1 10YR 3/2 (looks paler than A_{1p}) medium sandy loam, friable, non-sticky, non-plastic, very weak fine nut structure, few pumice lapillae, few worm borings filled with material from B horizon, many fine roots, very weak positive fluoride reaction, distinct worm mixed wavy boundary;
0.14-0.30	B_{21} 10YR 3/4, fine sandy loam, very friable, non-sticky, non-plastic, single grain structure, many worm borings filled with material from A horizon, many fine roots, at 0.20 m fine pumice lapillae up to 10 mm in diameter, very weak positive fluoride reaction, diffuse boundary;
0.30-0.46	B_{22} 10YR 4/4 fine sandy loam, very friable, single grain structure, many fine roots, weak positive fluoride reaction, indistinct irregular boundary;
0.46-0.68	B_3 10YR 4/5 gravelly loamy sand, rounded greywacke gravels 5 mm to 140 mm in diameter, with loamy sand matrix, many fine roots, negative fluoride reaction, indistinct undulating boundary;

---

* Indicates the presence of amorphous clays i.e. allophane.

0.68-1.05	greywacke gravels with medium sand matrix, colour bands 10YR 4/3 and 10YR 4/6, no roots. B.R.P.

Pit 021

Depth (m)	Description
0-0.07	A_{1p} 10YR 3/2, medium sandy loam, very friable, very weak medium nut structure, many fine roots, diffuse boundary, few pumice lapillae up to 2 mm in diameter, few greywacke gravels, weak positive fluoride reaction, diffuse boundary;
0.07-0.15	A 10YR 3/2 (looks slightly darker than A_{1p}), medium sandy loam, friable, single grain structure, many fine roots, weak positive fluoride reaction, indistinct worm mixed wavy boundary;
0.15-0.35	B_2 10YR 3/3, light sandy loam, very friable, single grain structure, many fine roots, many worm burrows and casts filled with material from A horizon, moderate positive fluoride reaction, diffuse boundary;
0.35-0.47	B_{31} 10YR 3/3 to 10YR 4/3, light fine sandy loam, friable, many fine pores, single grain structure, few greywacke grit pieces (less than or equal to 2 mm diameter), many fine roots, weak positive fluoride reaction, indistinct wavy boundary;
0.47-0.74	B_{32} mixed size greywacke gravels (2 mm to 140 mm in diameter) with a matrix of 10YR 3/3 to 10YR 4/3, fine loamy sand, many fine roots, weak positive fluoride reaction, indistinct wavy boundary;
0.75-115+	C mixed size greywacke gravels as above, with a matrix of 10YR 4/1 to 10YR 4/3 mixed, gritty coarse sand with

irregular bands of medium sand (10YR 3/6), very few roots, negative fluoride reaction.

B.R.P.

Pakowhai Silt Loam

The following description is of the soil profile in a pit dug between the two plots. The horizons in relation to those in the plots is shown in Fig.61.

Depth (m)	Description
0-0.20	dark yellowish brown (10YR 4.5/4), silt loam (very silty), friable with few pores, very weak fine nutty structure with many worm casts, many roots, indistinct boundary;
0.20-0.29	yellowish brown (10YR 5/4) with many distinct mottles strong brown (7.5YR 5/8), red (2.5YR 5/6), and light brownish grey (10YR 6/2), silt loam, friable, very weak fine nutty structure, many roots, distinct boundary;
0.29-0.40	very dark grey (10YR 3/1) many prominent root stains and red (2.5YR 4/8) mottles, silt loam (heavier than above), friable and very porous, medium nutty structure, many roots, distinct boundary;
0.40-0.48	greyish brown (10YR 5/2) with many distinct mottles and root stains, strong brown (7.5YR 5/6), very fine sandy loam, friable, massive, many roots, distinct boundary;
0.48-0.58	greyish brown (2.5YR 5/2) with many distinct mottles, strong brown (7.5YR 5/6), light fine sandy loam, very friable, massive, few roots indistinct boundary;

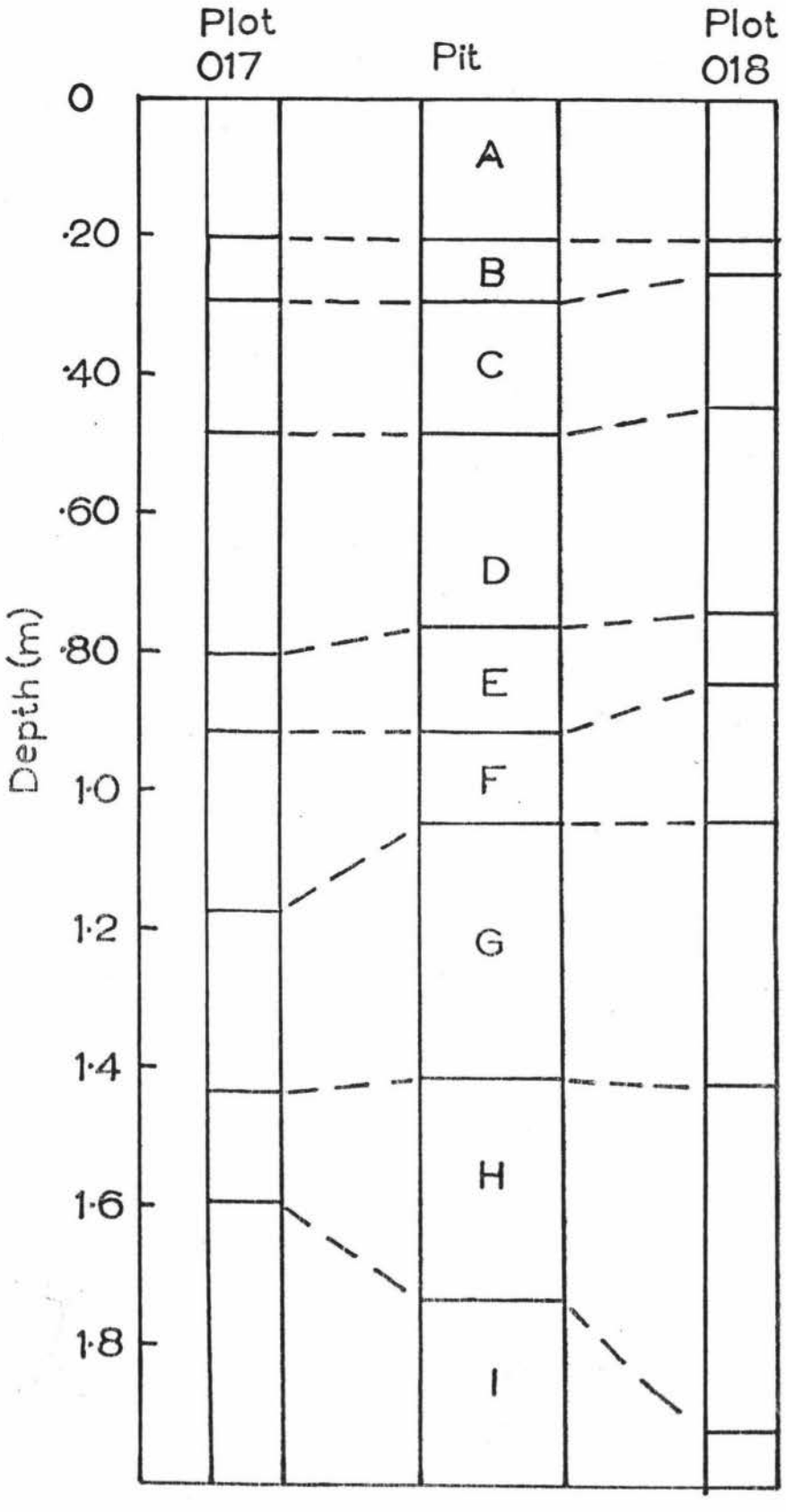

Fig.61 Comparison of the depth and thickness of each layer between the pit and the two plots, for Pakowhai silt loam.

0.58-0.68 light brownish grey (2.5Y 6/2) many faint mottles yellowish brown (10YR 5/6), medium sand, with pumice fragments, loose, single grain structure, few roots, distinct boundary;

0.68-0.76 olive grey (5Y 5/2) with many distinct mottles, strong brown (7.5YR 5/6), medium sandy loam, friable, massive structure, few roots, distinct boundary;

0.076-0.91 light brownish grey (2.5Y 6/2) many faint mottles strong brown (7.5YR 5/6) medium sand, loose, single grain structure, few roots, distinct boundary;

0.91-1.04 olive grey (5Y 4/2) many distinct mottles and root stains yellowish brown (10YR 5/6), medium to coarse sandy loam with many pumice fragments and charcoal in coarse sand size range, friable with many fine pores, massive to very weak nutty structure, roots rare, sharp boundary;

1.04-0.41 light brownish grey (2.5Y 6/2) pumice sand, loose single grain structure, distinct boundary;

1.41-1.45 light brownish grey (2.5Y 6/2) coarse pumice, gravel size, loose single grain structure;

1.45-1.70 light brownish grey (2.5Y 6/2) mixed layers of coarse and fine pumice, loose, single grain structure;

1.70-1.73 light brownish grey (2.5Y 6/2) with dusting, mottling yellowish brown (10Y 5/6);

1.73-240 Taupo pumice alluvium, interlayered, fine sand and coarse pumice.

E.G.

APPENDIX II : HYSTERESIS EXPERIMENTS

Hysteresis occurs in the relationship between volumetric water content and pressure potential i.e. the volumetric water content is not a unique function of the pressure potential, but depends to some extent on the previous wetting and drying history of the soil. Hysteresis can thus affect infiltration, redistribution and drainage of water in soil. If draining retentivity curves alone are used in the computer simulations of infiltration, the validity of these simulations could be questioned. Thus to determine the extent of hysteresis in the retentivity data of Takapau sandy loam and Pakowhai silt loam, "undisturbed" cores were taken and the following experiments performed.

Two cores were taken from each layer of the two soils using methods described by Cook (1976). Both cores were saturated. One core was then drained to a pressure potential of -10 m on a pressure plate, before being transferred to a Haines apparatus (Haines, 1930), where it was rewetted to a pressure potential of -0.5 m, at which point the volumetric water content was determined. The second core was drained from saturation on a Haines apparatus to a pressure potential of -0.5 m, and the volumetric water content determined. The data obtained from these and the volumetric water content at a pressure potential of -0.5 m determined in the earlier experiments (Chapter 2), are presented in Table 11. Agreement between the volumetric water content at a pressure potential of -0.5 m for draining soil is good for all layers of these two soils (Table 11).

The primary scanning curve (Dane and Wierenga, 1975), the relationship between volumetric water content and pressure potential, for wetting was obtained using three points:

(1) the volumetric water content at saturation (pressure potential equals zero)

Table 11: Comparison of volumetric water content at a pressure potential of -0.5 m reached by wetting (Θw) or draining (Θd) the soil i.e. hysteresis. The draining volumetric water content from earlier experiments is also given (Θdl)

Soil	Layer or Horizon	Θdl		Θd	Θw
Takapau sandy loam	A_1	0.420	0.450	0.420	0.378
	B_{21}	0.484	0.468	0.470	0.407
	B_{22}	0.54	0.476	0.486	0.454
Pakowhai silt loam	A	0.442		0.443	0.388
	B	0.383		0.386	0.350
	C	0.404		0.413	0.356
	D	0.361		0.359	0.340
	E	0.383		0.375	0.308
	F	0.399		0.381	0.369

(2) the volumetric water content at a pressure potential of -0.5 m from the wetting retentivity data

(3) the volumetric water content at a pressure potential of -10 m from the draining retentivity data.

Using these three points a wetting retentivity curve was drawn resembling the draining retentivity curve. From this wetting curve points of volumetric water content/pressure potential were obtained for use in the function tables of the computer model.

Various models for predicting scanning loops from the primary wetting and draining curves have been proposed (Everett, 1955; Poulovassilis, 1962; Mualem, 1974). These models all have pressure potential as the independent variable, whereas the computer simulation model (Chapter 2) has volumetric water content as the independent variable. Thus without a lot of modification to the computer model, these models for predicting scanning curves cannot be used. However, an empirical model for predicting scanning loops from the primary wetting and draining retentivity curves, which has volumetric water content as the independent variable, was proposed by Dane and Wierenga (1975). Their model was used in this study to simulate hysteresis, and the computer program used is given in Table 12.

The volumetric water content profiles calculated using the draining retentivity curves, wetting retentivity curves, and hysteresis model for simulated infiltration are compared in Fig.62. There is almost no difference between the volumetric water content profile obtained using the wetting retentivity curves, and the hysteresis model (Fig.62). There is a difference between the volumetric water content profiles obtained using the draining retentivity curves and the hysteresis model. For drainage and redistribution there was little difference found between volumetric water content profiles obtained using the draining retentivity curves and the hysteresis model.

Table 12: Hysteresis model computer program

```
      DO 9 I=1,5
      T(I)=1.
      IF(NF(I).LT.0.) T(I)=-1.
      IF((S(I)-T(I)).EQ.0.) GO TO 10
      WCMN(I)=THETA(I)
      PSW(I)=MPOT(I)
      MPD(I)=-AFGEN(SUTDA,THETA(I))
      MPW(I)=-AFGEN(SUTWA,THETA(I))
      C(I)=C(I)+1
      IF(MPD(I).EQ.MPW(I)) GO TO 10
      RAT(I)=(PSW(I)-MPW(I))/(MPD(I)-MPW(I))
      IF(T(I).LT.0.) RAT(I)=(PSW(I)-MPD(I))/(MPD(I)-MPW(I))
      GO TO 11
   10 IF (C(I).EQ.0.) GO TO 13
      RAT(I)=1.
   11 THETA(I)=VOLW(I)/TCOM(I)
      CURVE=(0.01*RAT(I))/(THETA(I)-WCMN(I)+0.01)
      IF(T(I).LT.0.) CURVE=1.+(0.01*RAT(I))/(THETA(I)-WCMN(I)-0.01)
      MPOT(I)=CURVE (-AFGEN(SUTDA,THETA(I)))+(1.-CURVE)*(-AFGEN(...
           SUTWA,THETA(I)))
      GO TO 12
   13 THETA(I)=VOLW(I)/TCOM(I)
      MPOT(I)=-AFGEN(SUTWA,THETA(I))
      IF(T(I).LT.0.)MPOT(I)=-AFGEN(SUTDA,THETA(I))
   12 S(I)=T(I)
    9 COND(I)= EXP(-249.12*THETA(I)**2+277.55*THETA(I)-87.32)
```

T(I), C(I), and S(I) are variables used for determining whether the process has changed i.e. from water moving into to out of the compartment.

NF(I) is the net flux density.

WCMN(I) is the water content at which the change in the process occurred.

PSW(I) is the pressure potential at which the change in the process occurred.

MPD(I) is the pressure potential on the draining retentivity curve corresponding to WCMN(I).

MPW is the pressure potential on the wetting retentivity curve corresponding to WCMN(I).

RAT(I) is a ratio necessary if WCMN(I) does not occur on a primary curve, (see Dane and Wierenga (1975)).

CURVE is the parameter used to determine the rate at which the pressure potential moves from one primary retentivity curve to the other.

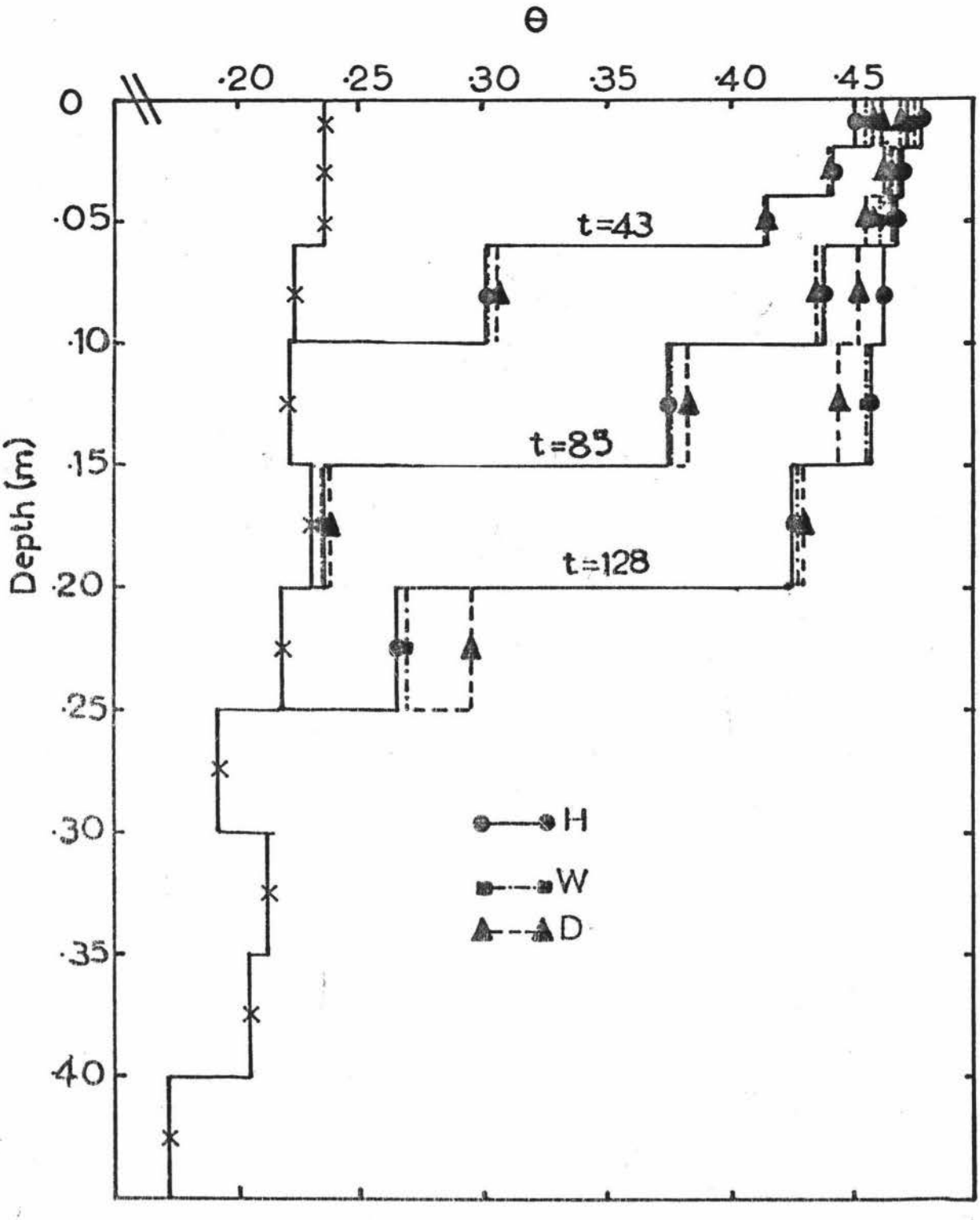

Fig.62 Comparison of the simulated volumetric water content profiles at various times, t (minutes), during infiltration of water in Takapau sandy loam, calculated using the hysteresis model (H), wetting (W) and draining (D) retentivity curves.

Thus it was concluded that little error would be introduced to the simulations if the wetting retentivity curves were used during simulated infiltration, and the draining retentivity curves used during redistribution and drainage. This procedure was used for the simulations described in the text, that is, the wetting retentivity curves were used for infiltration and the draining retentivity curves used for redistribution and drainage.

APPENDIX III : COMPUTER PROGRAM FOR SIMULATION OF SOIL WATER DYNAMICS

A listing of the computer program used in this study to simulate soil water dynamic behaviour is given in Table 13. This program is written in CSMP73 (Fugazi, 1973).

The program consists of three major sections, the initial, dynamic and terminal sections. The parameter statements (PARAM) are placed before the initial section. This allows the value of these to be changed in the terminal section. These parameters, and all other quantities in the program, are expressed in S.I. units.

Initial Section

The first statement in this section is NOSORT which indicates that the statements will be executed in the order given. The TIMER statement which is next consists of three parts: (a) the finishing time (FINTIM), (b) the integration time step (DELT), and (c) the time increments for printing output (OUTDEL).

The function tables of SUFYX (Y=D,W where D and W represent the drying and wetting retentivity curves respectively, and X = A,B,C,.... for the horizon or layer) consist of points on the volumetric water content pressure potential curves over the required range of volumetric water content. The function table for the flux density at the surface is RAINTB, which consists of points relating flux density and time.

The next three statements assign storage space in the computer's memory to the variable arrays. The EQUIVALENCE statement assigns the two variable names in the brackets to the same memory location i.e. the two variables have the same value. This is necessary as CSMP73 cannot integrate arrays, thus non-array variables must be used in the integral statements.

Table 13: CSMP73 Input List

```
*CSMP73 INPUT LIST *  25.003.000
0001    TITLE TAKAPAU SOIL WATER DYNAMIC SIMULATION
0002    PARAM SATCON=3.E-5
0003    PARAM B=7.272E-5
0004    PARAM A=1.818E-7
0005    PARAM R=1.
0006    INITIAL
0007    NOSORT
0008    TIMER FINTIM=1800.,DELT=1.,OUTDEL=1800.
0009    FUNCTION SUTDA=0.145,154.,0.165,100.,0.2,50.,0.233,25.,...
0010          0.275,10.,0.31,5.,0.342,2.5,0.386,1.,0.42,0.5,...
0011          0.455,0.25,0.488,0.1,0.52,0.,1.,-100.
0012    FUNCTION SUTDB=0.13,154.,0.14,100.,0.165,50.,0.193,25.,...
0013          0.24,10.,0.278,5.,0.325,2.5,0.4,1.,0.468,0.5,...
0014          0.517,0.25,0.55,0.1,0.575,0.,1.,-100.
0015    FUNCTION SUTDC=0.168,154.,0.18,100.,0.2,50.,0.225,25.,...
0016          0.262,10.,0.296,5.,0.337,2.5,0.41,1.,0.48,0.5,...
0017          0.536,0.25,0.571,0.1,0.592,0.,1.,-100.
0018    FUNCTION RAINTB=0.,0.,800000.,0.
0019    STORAG TCOM(11),ITHETA(11),COND(11),AVCOND(11),MPOT(11)
0020    /DIMENSION HPOT(11),FLUX(12),THETA(11),VOLW(11),IVOLW(11)
0021    /DIMENSION NFLUX(11),DEPTH(11),DIST(11)
0022    /EQUIVALENCE(V1,VOLW(1)),(V2,VOLW(2)),(V3,VOLW(3)),(V4,VOLW(4))
0023    /EQUIVALENCE(V5,VOLW(5)),(V6,VOLW(6)),(V7,VOLW(7)),(V8,VOLW(8))
0024    /EQUIVALENCE(V9,VOLW(9)),(V10,VOLW(10)),(V11,VOLW(11))
0025    /EQUIVALENCE(NF1,NFLUX(1)),(NF2,NFLUX(2)),(NF3,NFLUX(3))
0026    /EQUIVALENCE(NF4,NFLUX(4)),(NF5,NFLUX(5)),(NF6,NFLUX(6))
0027    /EQUIVALENCE(NF7,NFLUX(7)),(NF8,NFLUX(8)),(NF9,NFLUX(9))
0028    /EQUIVALENCE(NF10,NFLUX(10)),(NF11,NFLUX(11))
0029    FIXED I
0030    DO 1 I=1,3
0031    1 TCOM(I)=0.02
0032    TCOM(4)=0.04
0033    DO 3 I=5,11
0034    3 TCOM(I)=0.05
0035    ITHETA(1)=0.51966
0036    ITHETA(2)=0.51926
0037    ITHETA(3)=0.51877
0038    ITHETA(4)=0.51771
0039    ITHETA(5)=0.51528
0040    ITHETA(6)=0.56
0041    ITHETA(7)=0.50934
0042    ITHETA(8)=0.37702
0043    ITHETA(9)=0.17493
0044    ITHETA(10)=0.168
0045    ITHETA(11)=0.168
0046    DO 7 I=1,11
0047    NFLUX(I)=0
0048    7 IVOLW(I)=ITHETA(I)*TCOM(I)
0049    DEPTH(1)=0.5*TCOM(1)
0050    DIST(1)=DEPTH(1)
0051    DO 8 I=2,11
```

Table 13 (contin.)

```
0052    DEPTH(I)=DEPTH(I-1)+0.5*(TCOM(I)+TCOM(I-1))
0053    8 DIST(I)=0.5*(TCOM(I)+TCOM(I-1))
0054    IV1=IVOLW(1)
0055    IV2=IVOLW(2)
0056    IV3=IVOLW(3)
0057    IV4=IVOLW(4)
0058    IV5=IVOLW(5)
0059    IV6=IVOLW(6)
0060    IV7=IVOLW(7)
0061    IV8=IVOLW(8)
0062    IV9=IVOLW(9)
0063    IV10=IVOLW(10)
0064    IV11=IVOLW(11)
0065    NF1=0.
0066    NF2=0.
0067    NF3=0.
0068    NF4=0.
0069    NF5=0.
0070    NF6=0.
0071    NF7=0.
0072    NF8=0.
0073    NF9=0.
0074    NF10=0.
0075    NF11=0.
0076    DYNAMIC
0077    V1=INTGRL(IV1,NF1)
0078    V2=INTGRL(IV2,NF2)
0079    V3=INTGRL(IV3,NF3)
0080    V4=INTGRL(IV4,NF4)
0081    V5=INTGRL(IV5,NF5)
0082    V6=INTGRL(IV6,NF6)
0083    V7=INTGRL(IV7,NF7)
0084    V8=INTGRL(IV8,NF8)
0085    V9=INTGRL(IV9,NF9)
0086    V10=INTGRL(IV10,NF10)
0087    V11=INTGRL(IV11,NF11)
0088    NOSORT
0089    DO 9 I=1,5
0090    11THETA(I)=VOLW(I)/TCOM(I)
0091    MPOT(I)=-AFGEN(SUTDA,THETA(I))
0092    9 COND(I)=EXP(-249.12*THETA(I)**2+277.55*THETA(I)-87.32)
0093    DO 16 I=6,8
0094    29THETA(I)=VOLW(I)/TCOM(I)
0095    MPOT(I)=-AFGEN(SUTDB,THETA(I))
0096    16 COND(I)=EXP(-72.19*THETA(I)**2+112.78*THETA(I)-51.25)
0097    DO 20 I=9,11
0098    31THETA(I)=VOLW(I)/TCOM(I)
0099    MPOT(I)=-AFGEN(SUTDC,THETA(I))
0100    20 COND(I)=EXP(-104.25*THETA(I)**2+147.91*THETA(I)-61.23)
0101    DO 25 I=1,11
0102    25 HPOT(I)=MPOT(I)-DEPTH(I)
0103    FLUX(12)=COND(11)
0104    DO 15 I=2,11
0105    15 AVCOND(I)=(COND(1)*TCOM(I)+COND(I-1)*TCOM(I-1))/(TCOM(I)+TCOM(I-1))
0106    DO 14 I=2,11
0107    14 FLUX(I)=(HPOT(I-1)-HPOT(I))*AVCOND(I)/DIST(I)
0108    SINK=A*SIN(B*TIME)
```

Table 13 (contin.)

```
0109    SINK=SINK/0.4
0110    IF(SINK.LE.0.) SINK=0.
0111    S=SINK*0.4
0112    37 RAIN=AFGEN(RAINTB,TIME)*R
0113    INCAP=(0.-HPOT(1))*.5*(SATCON+COND(1))/DIST(1)
0114    IF (RAIN.GT.0.) GO TO 30
0115    FLUX(1)=0.
0116    GO TO 40
0117    30 INFILT=INCAP
0118    IF (RAIN.LT.INCAP)  INFILT=RAIN
0119    FLUX(1)=INFILT
0120    40 DO 41 I=1,10
0121    41 NFLUX(I)=FLUX(I)-FLUX(I+1)-SINK*TCOM(I)
0122    NFLUX(11)=FLUX(11)-FLUX(12)
0123    F12=FLUX(12)
0124    F1=FLUX(1)
0125    SORT
0126    CUMDRN=INTGRL(0.,F12)
0127    CUMINF=INTGRL(0.,F1)
0128    ET=INTGRL(0.,S)
0129    NOSORT
0130    CUMWTR=0.
0131    DO 42 I=1,11
0132    42 CUMWTR=CUMWTR+VOLW(I)
0133    T1=THETA(1)
0134    T2=THETA(2)
0135    T3=THETA(3)
0136    T4=THETA(4)
0137    T5=THETA(5)
0138    T6=THETA(6)
0139    T7=THETA(7)
0140    T8=THETA(8)
0141    T9=THETA(9)
0142    T10=THETA(10)
0143    T11=THETA(11)
0144    METHOD RECT
0145    PRINT CUMDRN,CUMINF,CUMWTR,F12,ET
0146    PRINT T1,T2,T3,T4,T5,T6,T7,T8,T9,T10,T11
0147    CONTIN
0148    TIMER FINTIM=86400.,DELT=10.,OUTDEL=21600.
0149    CONTIN
0150    TIMER  FINTIM=864000.,DELT=100.,OUTDEL=86400.
0151    END
0152    ENDJOB
```

The rest of this section involves assigning values to TCOM, DIST, and DEPTH, and assigning initial values to ITHETA (initial volumetric water content).

Dynamic Section

Integration of the net flux densities to give the volume of water (VOLW) in each compartment is the first part of this section. The integration method used is rectangular thus:

$$VOLW(I) = \int_{o}^{t^*} NFLUX(I)d\beta + IVOLW(I) = \sum_{i=1}^{m} NFLUX(I).\ \Delta t \ + \ IVOLW(I)$$

where $t^* = \sum_{i=1}^{m} \Delta t$, and IVOLW(I) is the initial volume of water in the ith compartment, and Δt = DELT. The volume of water in the ith compartment after each integration step is thus found, and hence THETA(I), MPOT(I) and COND(I) can then be calculated. MPOT(I) is calculated using an arbitrary function generator (AFGEN). AFGEN provides linear interpolation between the points in the function table. This part of the dynamic section calculates the value of the parameters needed for calculating the flux densities between the compartments.

The next part of the dynamic section calculates the flux densities between the compartments. An explanation of this is given in the text. The parameter R used with RAINTB allows for re-runs (see Terminal section) for different surface fluxes, without having to recompile the program for new RAINTB values. The cumulative infiltration, drainage and evapotranspiration, are calculated by integration of FLUX(1), FLUX(n+1) and S respectively. These and all other integrations must be in a sorted part of the program, hence the SORT statement.

Arrays cannot be printed in CSMP73, so each array element is assigned a variable name. The output required is obtained by using the PRINT statement. The statement METHOD RECT refers to the integration method which is rectangular.

Terminal Section

The use of a CONTIN statement, after the last statement in the dynamic section, means that the simulation will continue with the new conditions which are in the statements after CONTIN. In particular this allows the TIMER variables DELT and OUTDEL to be changed to save computer time (as the simulation flux densities change), and to avoid printing unwanted output. PARAM statements can also be changed. A more detailed description is given by Fugazi (1973).

If the dynamic section is followed by an END statement with no further statements,then the program stops. If the END statement is followed by TIMER or PARAM statements, then the simulation will be re-run using the new TIMER values and/or PARAM values, but in this case the initial section is also executed, so that the simulation starts with the same initial values as the first run.

APPENDIX IV : IRRIGATION OF TAKAPAU SANDY LOAM USING A "BIG GUN" IRRIGATOR

During irrigation of an area of Takapau sandy loam using a "Big Gun" irrigator (Fig.63), measurements of the amount of water applied to the surface of the soil and the change in the water content of the soil were made. It was then intended that, by simulating infiltration of water into this soil at the same initial water content and the same application rate, the simulated water content profile during wetting could be compared with that found experimentally. This could then be used to assess the ability of the computer model to predict infiltration, but due to reasons outlined below this was not possible.

Twelve containers of known surface area ($2.65 \times 10^{-3} m^2$) (Fig.63) were uniformly spread over an area 50 m by 50 m. Water was applied to the soil surface for 45 minutes, and the irrigator then stopped. The volume of water in each of the containers was measured and soil samples taken as follows. The irrigator was then restarted and this procedure repeated a further three times i.e. the total time of irrigation was 180 minutes.

Soil samples were taken at three different locations within the area. At each of these locations three samples were taken and bulked. The samples were taken in increments of 50 mm, down to 0.45 m. The gravimetric water content of these samples was determined and the volumetric water content calculated, using the bulk densities determined in earlier experiments.

Soil samples were taken before irrigation and the initial volumetric water content (θ_n) calculated. Using these and the other data, the amount of water that had infiltrated into the soil (I) to the time of sampling, was calculated as:

Fig.63 A photograph of the experimental site, showing the containers used for measuring the amount of water applied, and the "big gun" irrigator.

$$I = \int_0^{z_w} (\theta - \theta_n) dz \simeq \sum_{i=1}^{m} (\theta(i) - \theta_n(i)) \Delta z \qquad \text{--- (37)}$$

where z_w is the depth to the wetting front (m), θ is the volumetric water content at some depth z, $\theta_n(i)$ and $\theta(i)$ are initial and current volumetric water contents of the ith increment, Δz is the thickness of the depth increment (50 mm) and m is the number of increments.

When the amount of water applied is compared with that infiltrated (Fig.64) the agreement is very poor. A possible explanation for this poor agreement is as follows. The topography of this area is undulating with elevation differences of approximately 0.1 m occurring within distances of 0.5 m. Water from the "big gun" is applied to a point on the soil surface for only 20 seconds during each six minute circular sweep by the irrigator. In this 20 seconds, 3.5 mm of water is applied, which is a rate of approximately 1.8×10^{-4} m s^{-1}. This is six times greater than the infiltration rate measured for this soil (Table 10), so that water will pond on the surface of the soil during each 20 second application. Some of this ponded water will flow from the high spots to the low spots. Thus the high spots will infiltrate less water than was applied to the surface of them, while the low spots will infiltrate more water than was applied to the surface of them. Puddles in the low spots of this soil were observed during this experiment. Thus, the reasons given above would explain the scatter in the data from this experiment (Fig.64).

Application of water from the "big gun" at the rate described above, caused considerable disturbance to the soil surface. The soil surface was pitted by droplet impact and soil was "splashed" up the sides of, and into, the containers used to measure the amount of water applied. This disturbance of the soil surface is likely to cause a crust to be formed, which will lower the infiltration rate of the soil.

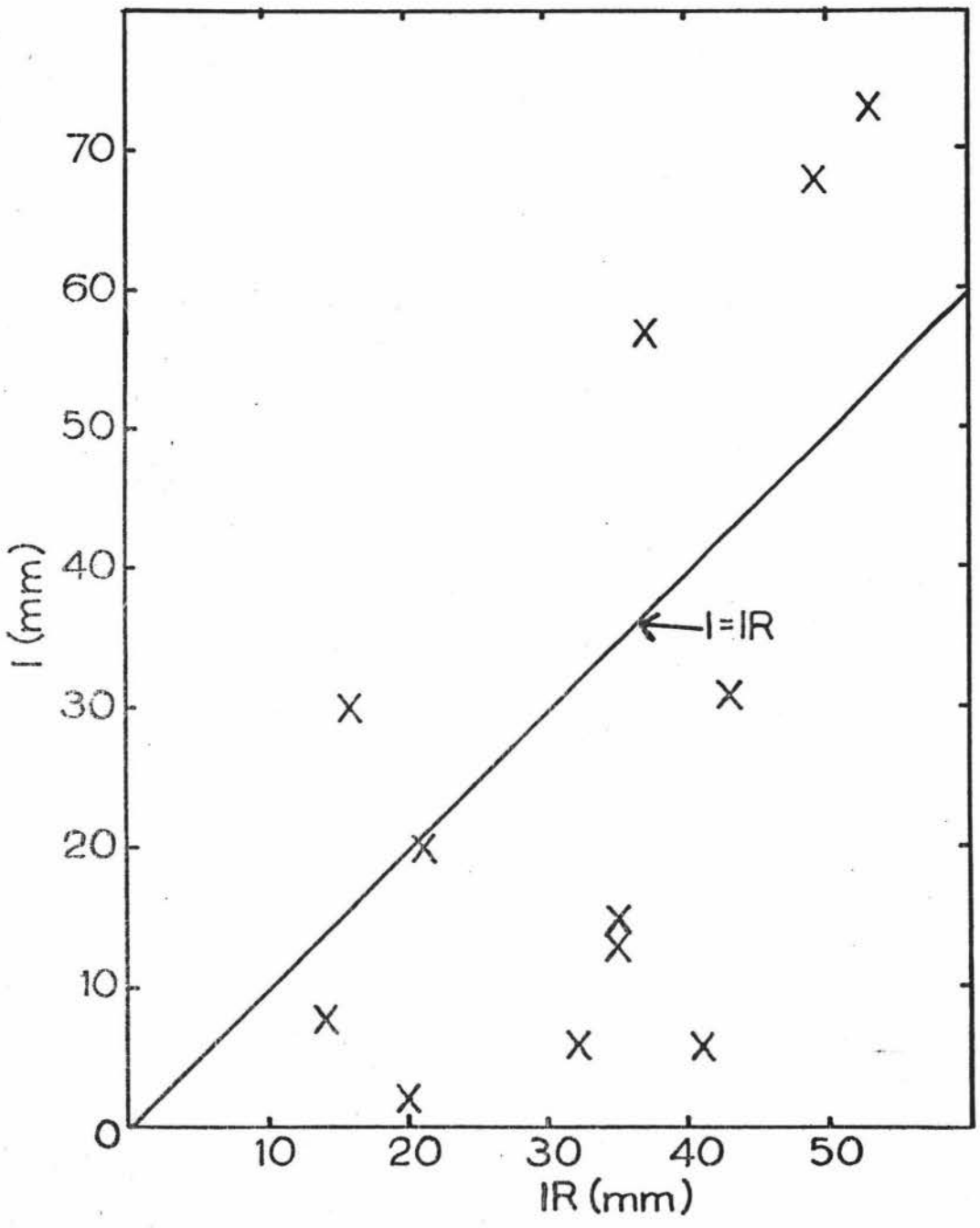

Fig.64 Cumulative amount of water infiltrated (I) into Takapau sandy loam, versus the cumulative amount of water applied to the soil surface (IR). The line I = IR is the expected relationship but does not fit these data.

This would cause the amount of water ponded on the soil surface to increase and exacerbate the "patchy" spacial distribution of water infiltrated into the soil.

If the rate of application of water to the soil surface was decreased, a more even spatial distribution of water infiltrated into the soil could be produced. This would reduce the amount of disturbance to the soil surface, reduce the amount of water lost to drainage from the low spots, and better utilise the same volume of water for pasture production. Thus, in irrigation of soils using a sprinkler system, unless the application rate is less than the saturated hydraulic conductivity of the A horizon, then the advantage of uniform infiltration of water into the soil by using sprinkler irrigation is lost.